

**UNIVERSIDADE DE SÃO PAULO**  
**CENTRO DE ENERGIA NUCLEAR NA AGRICULTURA**

**JOYCE RIBEIRO SANTOS RASERA**

**Evaluation of distribution, chemical speciation, and toxic effects of CuO  
and ZnO nanoparticles in *Daphnia magna* and *Danio rerio***

**Piracicaba**

**2021**



**JOYCE RIBEIRO SANTOS RASERA**

**Evaluation of distribution, chemical speciation, and toxic effects of CuO  
and ZnO nanoparticles in *Daphnia magna* and *Danio rerio***

**Revised version according the Resolution CoPGr 6018 at 2011**

**Thesis presented to Center for Nuclear Energy in  
Agriculture of the University of Sao Paulo as a  
requisite to the Doctoral Degree in Sciences**

**Concentration Area: Chemistry in Agriculture  
and Environment**

**Advisor: Prof. Hudson Wallace Pereira de  
Carvalho**

**Piracicaba**

**2021**

AUTORIZO A REPRODUÇÃO E DIVULGAÇÃO TOTAL OU PARCIAL DESTE TRABALHO, POR QUALQUER MEIO CONVENCIONAL OU ELETRÔNICO, PARA FINS DE ESTUDO E PESQUISA, DESDE QUE CITADA A FONTE.

Dados Internacionais de Catalogação na Publicação (CIP)

**Seção Técnica de Biblioteca - CENA/USP**

Rasera, J. R. S.

Avaliação da distribuição, especiação química, e efeitos tóxicos de nanopartículas de CuO e ZnO em *Daphnia magna* e *Danio rerio* / Evaluation of distribution, chemical speciation, and toxic effects of CuO and ZnO nanoparticles in *Daphnia magna* and *Danio rerio* / Joyce Ribeiro Santos Rasera; orientador Hudson Wallace Pereira de Carvalho. - - Versão revisada de acordo com a Resolução CoPGr 6018 de 2011. - - Piracicaba, 2021.

111 p.: il.

Tese (Doutorado – Programa de Pós-Graduação em Ciências. Área de Concentração: Química na Agricultura e no Ambiente) – Centro de Energia Nuclear na Agricultura da Universidade de São Paulo, Piracicaba, 2021.

1. Absorção de raios X 2. Biotransformação 3. Ecotoxicologia 4. Fluorescência de raios X 5. Monitoramento biológico 6. Nanopartículas 7. Qualidade da água 8. Toxicologia ambiental I. Título

CDU 574.64 : 620.3

**Elaborada por:**

Marília Ribeiro Garcia Henyei

CRB-8/3631

Resolução CFB N° 184 de 29 de setembro de 2017

To my son, Heitor, with love



## ACKNOWLEDGMENTS

To God for all the gifts received and for bestowing this achievement upon me.

To the University of São Paulo, Center for the Nuclear Energy in Agriculture (CENA) for all support and structure for carrying out this research.

To the whole structure of CNPEM for the support to perform many analyzes.

To CAPES - Coordination for the Improvement of Higher Education Personnel (CAPES), Finance Code 001 and CNPq (Process N<sup>o</sup>. 141014/2019-9) for the scholarship and all financial support.

To Professor Hudson W. P. de Carvalho (CENA) for the opportunity, trust, respect and patience during the course and preparation of this work.

To Professor Regina (CENA) for the suggestions and corrections in the articles and chapters of the thesis and mainly for the advice and conversations during these years.

To Professor Cornelis A. van Gestel (Vrije Universiteit, Holand), Arnalder Neto, DeJane S., Alves and Rafael G. de Lima for suggestions and corrections to the articles and chapters of the thesis.gv

To Professor Rosangela Marucci (UFLA) for the opportunity to participate in an article.

To my husband, Rodrigo Rasera, for the companions, respect, love and for all the emotional support during all these years. To my son, Heitor, already gives me an emotional support in this final stage of the course. I love you!

To my parents Maria Rita and Donaldo, for their love and support. To my brothers Donaldo and Alexandre, who ever far away were always been by my side. I love you!

To psychologist and therapist Farid for all emotional support and understanding at difficult times when I wanted to give up everything. Thank you so much for the conversations and advice. You and my husband are responsible for me getting to the end of the course.

The librarian Marilia (CENA), for the help in the thesis, the advice and conversations.

To the laboratory technicians Eduardo de Almeida, Luis Eduardo Fonseca, Cleusa Pereira Cabral, Glauco Arnald Tavares, for their technical support and respect during the course.

To Carlos Perez (LNLS) for all the support during the XRF beam time measurements.

To friends Gilda, Gleison, Fabiana, Renan, Leandro, Gabriela, Francine, Geovani, Susi, Nadia, Tatiana for the coexistence, advice and laughter.

To the laboratory colleagues, Sara, Gabriel, Rafael, Eduardo, Marcos, Bianca, Camila, Lidiane, João Paulo for respect and good coexistence.

To baby-sistter Larissa Zago, for taking care of my son to finish this job.

I thank everyone who in some way contributed directly and indirectly for doing this work.





“Experience is not what happens to a man; This is what a man does with what happens to him”

**Aldous Huxley**



## ABSTRACT

RASERA, J. R. S. **Evaluation of distribution, chemical speciation, and toxic effects of CuO and ZnO nanoparticles in *Daphnia magna* and *Danio rerio***. 2021. 111 p. Tese (Doutorado em Ciências) – Centro de Energia Nuclear na Agricultura, Universidade de São Paulo, Piracicaba, 2021.

The use of products with nanoparticles has been growing in recent years. Currently, there is the application of nutrients in nanoparticulate form in agriculture. With this growth, it is important to safely expand their use and assess the environmental risk caused by them, as discharges may occur near water flows. In this work, the toxicity, distribution, concentration and chemical speciation of CuO and ZnO nanoparticles in ecotoxicology model organisms, *Daphnia magna* and *Danio rerio* were evaluated. Copper and zinc were chosen due to their agronomic importance. In this study, higher toxicity was determined in CuSO<sub>4</sub> and in smaller nanoparticles of CuO, for both organisms. For ZnO, the toxicity depended on the particle size and the presence of surfactant, also higher for smaller nanoparticles. The chemical speciation analysis showed that there was biotransformation of CuO (25 nm) and CuSO<sub>4</sub> into Cu<sub>3</sub>(PO<sub>4</sub>)<sub>2</sub> in *D. magna*; however there was no transformation in *D. rerio*. The distribution of copper and zinc was similar for organisms, with the highest concentration occurring in the intestinal and gastrointestinal systems for *D. magna* and *D. rerio*, respectively. In this study, there was no ZnO clearance in *D. magna* observed for 24 h.

**Keywords:** *Daphnia magna*. *Danio rerio*. CuO nanoparticles. ZnO nanoparticles. Toxicity. X-ray fluorescence. X-ray absorption.



## RESUMO

RASERA, J. R. S. **Avaliação da distribuição, especiação química e efeitos tóxicos de nanopartículas de CuO e ZnO em *Daphnia magna* e *Danio rerio***. 2021. 111 p. Tese (Doutorado em Ciências) – Centro de Energia Nuclear na Agricultura, Universidade de São Paulo, Piracicaba, 2021.

O uso de produtos com nanopartículas vem crescendo nos últimos anos. Atualmente, há a aplicação de nutrientes na forma nanoparticulada na agricultura. Com este crescimento, é importante expandir com segurança o seu uso e avaliar o risco ambiental provocada por elas, visto que pode ocorrer descargas próximo a fluxos d'água. Neste trabalho, foi avaliado a toxicidade, a distribuição, concentração e forma química de nanopartículas de CuO e ZnO em dois organismos modelos de ecotoxicologia - *Daphnia magna* e *Danio rerio*. Cobre e zinco foram escolhidos devido a sua importância agronômica. Neste estudo, foi determinado maior toxicidade para nanopartículas menores de CuO e CuSO<sub>4</sub> em ambos os organismos. Para ZnO, a toxicidade dependeu do tamanho da partícula e da presença de surfactante, sendo também maior para nanopartículas menores. A análise de especiação química mostrou que ocorreu biotransformação de CuO (25 nm) e CuSO<sub>4</sub> em Cu<sub>3</sub>(PO<sub>4</sub>)<sub>2</sub> em *D. magna*; entretanto não houve transformação em *D. rerio*. A distribuição de cobre e zinco foi semelhante em ambos os organismos, sendo que a maior concentração ocorreu no sistema intestinal e gastrointestinal para *D. magna* e *D. rerio*, respectivamente. Neste estudo, não houve depuração de ZnO em *D. magna* observadas por 24 h.

**Palavras-chave:** *Daphnia magna*. *Danio rerio*. Nanopartículas de CuO. Nanopartículas de ZnO. Toxicidade. Fluorescência de raios X. Absorção de raios X.



## SUMMARY

1 INTRODUCTION .....	17
1.1 Hypothesis .....	19
1.2 Objectives .....	20
1.3 Structure of the thesis .....	20
References.....	20
2 TOXICITY, BIOACCUMULATION AND BIOTRANSFORMATION OF Cu OXIDE NANOPARTICLES IN <i>Daphnia magna</i> .....	23
Abstract.....	23
2.1 Introduction.....	23
2.2 Materials and Methods.....	25
2.2.1 Nanoparticle and dispersion characterization .....	25
2.2.2 Toxicity Assessments .....	26
2.2.2.1 Experimental conditions .....	26
2.2.2.2 Preparation of dispersions and dilution for acute and chronic assays .....	27
2.2.2.3 Sensitivity, acute and chronic assays .....	27
2.2.3 Decomposition of H <sub>2</sub> O <sub>2</sub> by nCuO and CuSO <sub>4</sub> .....	29
2.2.4 X-ray fluorescence microanalysis (μ-XRF).....	29
2.2.5 Microprobe X-ray absorption near edge spectroscopy (μ-XANES) .....	30
2.3 Results and discussion .....	31
2.3.1 Characterization of nCuO .....	31
2.3.2 Acute and chronic assays .....	34
2.3.3. Spatial distribution of Cu in dead daphnids.....	41
2.3.4 μ-XANES chemical speciation of Cu within Cu hotspots.....	44
2.4 Partial Conclusions .....	46
References.....	47
3 UPTAKE, TOXICITY AND PERSISTENCE OF ZnO NANOPARTICLES IN <i>Daphnia magna</i> .....	53
Abstract.....	53
3.1 Introduction.....	53
3.2 Material and methods.....	54
3.2.1. Nanoparticles characterization and dispersion analysis.....	54
3.2.2. Experimental conditions .....	57
3.2.2.1. Stock culture of <i>Daphnia magna</i> .....	57

3.2.3. Exposure of daphnids to nZnO dispersions.....	58
3.2.3.1. Sensitivity assays.....	58
3.2.3.2. Acute assays .....	58
3.2.3.3. Depuration assays.....	59
3.2.4. X-ray fluorescence microanalysis ( $\mu$ -XRF) .....	59
3.2.4.1. Zn quantitative maps of daphnids exposed to acute assays.....	59
3.2.4.2. Zn quantitative maps of daphnids from depuration assays .....	60
3.3 Results and discussion.....	61
3.3.1. Nanoparticles characterization and dispersion analysis .....	61
3.3.2. Experimental conditions.....	61
3.3.3. Acute assays .....	61
3.3.4. X-ray fluorescence microanalysis ( $\mu$ -XRF) .....	64
3.3.4.1. Zn quantitative maps of daphnids exposed to acute assays.....	64
3.3.4.2. Zn quantitative maps of <i>Daphnia</i> at depuration assays.....	66
3.4 Partial Conclusions.....	74
References .....	74
<b>4 X-RAY IMAGING AND CHEMICAL SPECIATION ASSISTING TO UNDERSTAND THE TOXIC EFFECTS OF COPPER OXIDE NANOPARTICLES ON ZEBRAFISH (<i>Danio rerio</i>) .....</b>	<b>79</b>
Abstract .....	79
4.1 Introduction .....	79
4.2 Material and methods .....	81
4.2.1 Characterization.....	81
4.2.1.1 Nanoparticles and dispersion.....	81
4.2.2 Experimental conditions.....	81
4.2.2.1 Maintenance of zebrafish .....	81
4.2.3 Acute assays .....	81
4.2.4 Total copper concentration in the zebrafish .....	83
4.2.5 X-ray fluorescence microanalysis ( $\mu$ -XRF) .....	84
4.2.6 Microprobe X-ray absorption near edge spectroscopy ( $\mu$ -XANES) .....	85
4.3 Results and discussion.....	86
4.3.1 Characterization.....	86
4.3.1.1 Nanoparticles and dispersion.....	86
4.3.2 Acute assays .....	87
4.3.3 Total Cu inside zebrafish.....	91
4.3.3.1 Atomic absorption spectrophotometer .....	91



4.3.4 Spatial distribution of Cu inside <i>Danio rerio</i> X-ray fluorescence microanalysis ( $\mu$ -XRF) .....	94
4.3.5 Microprobe X-ray absorption near edge spectroscopy ( $\mu$ -XANES) applied zebrafish	96
4.4 Partial Conclusions .....	99
References .....	99
5 GENERAL CONCLUSIONS .....	105
ANNEX .....	107



## 1 INTRODUCTION

Nanomaterials: a trade of between benefits and environmental risks?

Currently, there are many definitions in the scientific community about what nanoparticles or nanomaterials are. IUPAC adopts that nanoparticles are those with dimensions of approximately 1 to 100 nm (IUPAC, 2018). According to the definition of the international Organization for Standardization (ISO/TR 18401:2017), nanotechnology is application of scientific knowledge to manipulate and control matter predominantly in the nanoscale to make use of size- and structure-dependent properties and phenomena distinct from those associated with individual atoms or molecules, or extrapolation from larger sizes of the same material.

The Nanotech project inventory reports that about 1800 products currently marketed contain nanomaterials. They are found in various shapes, sizes and chemical composition and are used in sunscreens, cosmetics, the textile industry, medicine, batteries and agriculture (MOORE, 2006; PASCHOALINO; MARCONE; JARDIM, 2010). However, this is not always explicit mentioned on product packages. CuO NPs are components of catalysts, antifouling paints, metallic coating polymers, solar cells, semiconductors, among others (ADAM et al., 2015). ZnO NPs are components of plastics, ceramics, glass, rubbers, paints, cosmetic batteries among others (MA; WILLIAMS; DIAMOND, 2013). Thus, a large number of nanomaterials have come to the market and in people's lives and, as a result, we are already exposed to them daily.

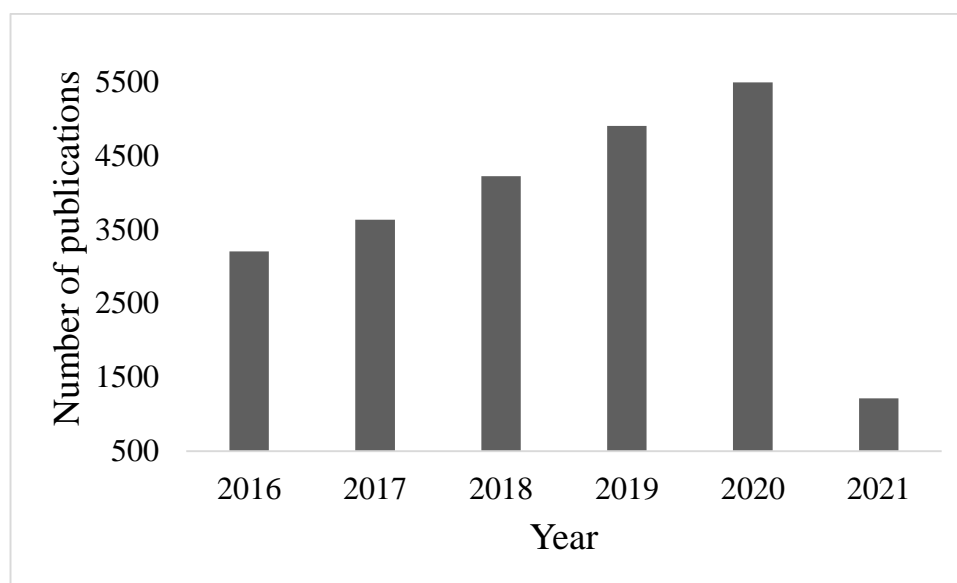
In this scenario, nanotechnology offers the prospect of major breakthroughs that could improve human quality of life, especially in food production. Agriculture is one of the main sectors of production that needs to innovate. Current agricultural practices rely heavily on the use of agrochemicals (pesticide fertilizers) that are inefficiently applied with most of these inputs finally lost or unavailable to crops (ROSER, 2019). Currently, nanomaterials are also present in agriculture, but their use is still modest (GREEN; BEESTMAN, 2007).

Cu nanoparticles can provide increased agricultural productivity as copper is an essential element in plant metabolism and participates in enzymatic processes. Zn nanoparticles have the potential to stimulate plant germination and growth as well as disease suppression (SINGH et al., 2018).

With the increase of nanoparticles in various products and sectors - such as agriculture – follows environmental risks (BASHIRNEZHAD et al., 2015). Nanomaterials can be released indirectly and dispersed into the environment/ecosystems. Little is known about the metabolism of nanomaterials, their effects on plants and their behavior on the soil, since nanoparticles may

remain in organic matter or be leached. Figure 1 shows the number of Web of Science (accessed date: April 02, 2021) publications using the words “nanoparticles” and “environment”. The graph shows that in the last 6 years, there has been a growing research in these areas, which emphasizes the importance in these studies.

Figure 1. Number of publications and citations on Web of Science with the search term “nanoparticles” and “environmental” grouped annually. Accessed date: April 2021



The risks associated with the widespread spread of nanoparticles in the environment are more noteworthy as they differ in scale in size, surface and volume from other materials. Plants and animals can carry these nanomaterials as they can be absorbed into cells when inhaled or ingested (ADAM et al., 2015). In the aquatic environment, they can be transferred to other organisms through the food chain or to future generations during reproduction (KLAINE et al., 2008). In this context, the effects caused by nanoparticles on organisms and the aquatic environment need to be investigated (BASHIRNEZHAD et al., 2015).

The aquatic ecosystem is one of the final destinations of many pollutants and particles that can interact and affect aquatic organisms. Thus, comparative studies between materials and organisms of different trophic levels are important for making a full evaluation. The species *Danio rerio* (zebrafish) is a model organism in research on acute toxicity, malformation of sublethal effects (KNÖBEL et al., 2012). Daphnids species are ideal for toxicity tests, as they are sensitive to various substances, cultivation is easy in many laboratory and is a source of food for fish (ZAGATO; BERTOLETTI, 2006). The results of this research may help the

legislators and the scientific community delimitation of maximum permissible levels in environmental compartments.

X-ray fluorescence spectroscopy (XRF) is a multi-element, non-destructive technique, which consists of exposing the sample to high-energy X-rays; so electrons from the innermost shell are excited and ejected out of the atom. When this occurs, another electron in the upper layer fills the vacancy and, in this transition, energy is released in the form of x-rays characteristic of a certain element. Thus, it is possible to know which elements make up the material, for example biological sample, through a simple preparation or without any preparation, such as seeds (DURAN et al., 2017; SAVASSA et al., 2018) and plant tissues (CRUZ et al., 2017; RODRIGUES et al., 2018). Using synchrotron based X-ray absorption spectroscopy (XAS) technique; a beam of x-rays scans the sample over a range of energies below and above the absorption edge of the element of interest, creating a spectrum. Thus, it is possible to know the structural and chemical environment of an absorbing atom.

First studies with XRF applied to *Daphnia magna* were made by Jackson et al. (2009) and De Samber et al. (2008; 2010), with CdSe / ZnS and Zn (quantum dots) where, CdSe / ZnS and Zn were concentrated in the intestinal region of daphnids. However, there are no works in the literature using XAS in daphnids and zebrafish. Thus, this thesis presents new data in the area of ecotoxicology, such as the chemical environment of copper in *D. magna* and *D. rerio*; in addition to data on toxicity and distribution of copper and zinc by XRF after exposure of copper and zinc nanoparticles.

## 1.1 Hypothesis

This study tested the following hypotheses:

- ✓ Nanoparticles (CuO and ZnO) are toxic to *Daphnia magna* and *Danio rerio* (zebrafish) organisms;
- ✓ Nanoparticles may cause morphological changes to *D. magna* and zebrafish organisms;
- ✓ Nanoparticles can accumulate in different parts of *D. magna* and zebrafish organisms;
- ✓ Nanoparticles can be biotransformed upon exposure to *D. magna* and zebrafish organisms;

## 1.2 Objectives

The aims of this thesis were to evaluate the effects of CuO and ZnO nanoparticles on two model organisms: *Daphnia magna* and *Danio rerio*. For this evaluation, the following experiments were realized:

- i. Characterization of nanoparticles by: dynamic light scattering (DLS), X-ray diffraction (XRD) and scanning electron microscopy (SEM) and transmission electron microscopy TEM);
- ii. Acute and chronic exposure of various concentrations of nanoparticles to the models organisms to determine morphological changes and mortality and effect dose affecting 50% of organisms;
- iii. Micro X-ray fluorescence spectroscopy ( $\mu$ XRF) and X-ray absorption near edge structure (XANES) analysis to estimate the distribution of the element of interest and the chemical environment in model organisms after exposure to nanoparticles;

## 1.3 Structure of the thesis

This thesis is organized in four chapters. The first one brings this general introduction while the followings present:

- Chapter 2: Toxicity, bioaccumulation and biotransformation of Cu oxide nanoparticles in *Daphnia magna*. The data herein was published in the *Environmental Science Nano*. 2019, 6, 2897-2906.  
<https://doi.org/10.1039/c9en00280d>.
- Chapter 3: Uptake, toxicity and persistence of ZnO nanoparticles in *Daphnia magna* [This chapter will be sent to publication].
- Chapter 4: X-ray spectrometry imaging and chemical speciation assisting to understand the toxic effects of copper oxide nanoparticles in zebrafish (*Danio rerio*). This chapter will be sent to publication].

## References

ADAM, N. et al. The chronic toxicity of CuO nanoparticles and copper salt to *Daphnia magna*. **Journal of Hazardous Materials**, v. 283, p. 416–422, 2015.

BASHIRNEZHAD, K. et al. A comprehensive review of last experimental studies on thermal conductivity of nanofluids. **Journal of Thermal Analysis and Calorimetry**, v. 122, n. 2, p.863-884, 2015.

CRUZ, T. N. M. da et al. Shedding light on the mechanisms of absorption and transport of ZnO nanoparticles by plants via in vivo X-ray spectroscopy. **Environmental Science: Nano**, v. 4, p. 2367-2376, 2017.

DE SAMBER, B. et al. A combination of synchrotron and laboratory X-ray techniques for studying tissue-specific trace level metal distributions in *Daphnia magna*. **Journal of Analytical Atomic Spectrometry**, v. 23, n. 6, p. 829-839, 2008.

DE SAMBER, B. et al. Dual detection X-ray fluorescence cryotomography and mapping on the model organism *Daphnia magna*. **Powder Diffraction**, v. 25, n. 2, p. 169–174, 2010.

DURAN, N. M. et al. X-ray spectroscopy uncovering the effects of Cu based nanoparticle concentration and structure on *Phaseolus vulgaris* germination and seedling development. **Journal of Agricultural and Food Chemistry**, v. 65, p. 7874-7884, 2017.

GREEN, J. M.; BEESTMAN, G. B. Recently patented and commercialized formulation and adjuvant technology. **Crop Protection**, v. 26, n. 3, p. 320-327, 2007.

INTERNATIONAL ORGANIZATION FOR STANDARDIZATION - ISO. **ISO/TR 18401:2017(en)**: Nanotechnologies - Plain language explanation of selected terms from the ISO/IEC 80004 series. Geneva, Switzerland, 2017. 13 p.

IUPAC. **Compendium of Chemical Terminology. The Gold Book**: Nanogel. 2. ed. Research Triangle Park, 2018. Available at: <https://doi.org/10.1351/goldbook>. Accessed: 12 Apr. 2018.

JACKSON, B. P. et al. Synchrotron X-ray 2D and 3D elemental imaging of CdSe/ZnS quantum dot nanoparticles in *Daphnia magna*. **Analytical and Bioanalytical Chemistry**, v. 394, n. 3, p. 911–917, 2009.

KLAINÉ, S. J. et al. Nanomaterials in the environment: Behavior, fate, bioavailability, and effects. **Environmental Toxicology and Chemistry**, v.27, p.1825-1851, 2008.

KNÖBEL, M. et al. Predicting adult fish acute lethality with the zebrafish embryo: Relevance of test duration, endpoints, compound properties, and exposure concentration analysis. **Environmental Science and Technology**, v. 46, n. 17, p. 9690-9700, 2012.

MA, H.; WILLIAMS, P. L.; DIAMOND, S. A. Ecotoxicity of manufactured ZnO nanoparticles - A review. **Environmental Pollution**, v.172, p.76-85, 2013.

MOORE, M. N. Do nanoparticles present ecotoxicological risks for the health of the aquatic environment? **Environment International**, v. 32, n. 8, p.967-976, 2006.

PASCHOALINO, M. P.; MARCONE, G. P. S.; JARDIM, W. F. Os Nanomateriais E a Questão Ambiental. **Química Nova**, v. 33, n. 2, p. 421–430, 2010.

RODRIGUES, E. S. et al. Laboratory microprobe X-ray fluorescence in plant science: emerging applications and case studies. **Frontiers in Plant Science**, v. 9, p. 1588, 2018.

ROSER, M. **Future population growth**. Oxford: University of Oxford, 2019. Available at: <https://ourworldindata.org/future-population-growth>. Accessed date: 2 Apr. 2021.

SAVASSA, S. M. et al. Effects of ZnO Nanoparticles on Phaseolus vulgaris Germination and Seedling Development Determined by X-ray Spectroscopy. **ACS Applied Nano Materials**, v. 11, p. 6414-6426, 2018.

SINGH, A. et al. Zinc oxide nanoparticles: a review of their biological synthesis, antimicrobial activity, uptake, translocation and biotransformation in plants. **Journal of Materials Science**, v.53, p.185-201, 2018.

ZAGATO, P. A.; BERTOLETTI, E. **Ecotoxicologia aquática: princípios e aplicações**. 1. ed. São Carlos: RiMa, 2006. 464 p.



## 2 TOXICITY, BIOACCUMULATION AND BIOTRANSFORMATION OF Cu OXIDE NANOPARTICLES IN *Daphnia magna*

### Abstract

This study investigated the toxicity, bioaccumulation and biotransformation of copper oxide nanoparticles (nCuO) and CuSO<sub>4</sub> in *Daphnia magna*. We performed acute and chronic assays, and analyzed the organisms by  $\mu$ -XRF and  $\mu$ -XANES. In acute assays 25 nm nCuO (LC<sub>50</sub> – lethal concentration that kills 50% of organisms -  $0.05 \pm 0.011$  mg Cu L<sup>-1</sup>) and CuSO<sub>4</sub> (LC<sub>50</sub>  $0.16 \pm 0.015$  mg CuL<sup>-1</sup>) were most toxic, while 40 nm and 80 nm nCuO had similar toxicity (LC<sub>50</sub>  $2.34 \pm 0.479$  and  $2.26 \pm 0.246$  mg Cu L<sup>-1</sup>, respectively). In chronic assays, CuSO<sub>4</sub> (EC<sub>50</sub> – effect concentration in 50% of organisms -  $1.7 \times 10^{-4} \pm 1.0 \times 10^{-4}$  mg Cu L<sup>-1</sup>) was most toxic followed by 25 nm nCuO (EC<sub>50</sub>  $1.8 \times 10^{-3} \pm 8.0 \times 10^{-4}$  mg Cu L<sup>-1</sup>), while 40 and 80 nm nCuO were least toxic (EC<sub>50</sub>  $2.10 \pm 0.669$  and  $1.95 \pm 0.568$  mg Cu L<sup>-1</sup>, respectively).  $\mu$ -XRF showed that Cu was accumulated in the intestine and appendages of the daphnids.  $\mu$ -XANES showed that 25 nm nCuO and CuSO<sub>4</sub> were biotransformed into Cu<sub>3</sub>(PO<sub>4</sub>)<sub>2</sub> (acute assays), whereas 40 and 80 nm nCuO remained as CuO (chronic assays). The higher toxicity exhibited by CuSO<sub>4</sub> and 25 nm nCuO can be explained from their higher chemical reactivity (probed by catalytic decomposition of H<sub>2</sub>O<sub>2</sub> and  $\mu$ -XANES) compared to 40 and 80 nm nCuO.

**Keywords:** *Daphnia magna*; toxicity; CuO; nanoparticles; X-ray; XRF, XANES

### 2.1 Introduction

Pesticides and fertilizers have been of major importance for meeting the demand for food, feed and biomass. However, their indiscriminate use can lead to soil, water and crop contamination.

Copper is an essential element for plant (BURKHEAD et al., 2009; WELCH; SHUMAN, 1995) its concentration in vegetal tissues ranges from 1-5 mg Cu kg<sup>-1</sup> dry mass (WHITE; BROWN, 2010). Due to the conversion of Cu<sup>2+</sup> to Cu<sup>+</sup> and vice versa, this element plays key roles in the photosynthetic electron transport chain, in respiration and as a cofactor of enzymes (MARSCHNER, 1995). Since Cu is exported from fields after each crop harvest, it must be resupplied as fertilizer. This keeps its adequate level in the soil without decreasing crop yield. The most common chemical forms in Cu-containing fertilizers are EDTA chelates, sulphates and oxides (LARNEY et al., 2006; SCHULTE; KELLING, 1931). Cu-based compounds, such as oxides, hydroxides, sulphates, carbonates and organic complexes, are also

employed as pesticides for controlling weeds mollusks, algae, bacteria and fungi (FISHEL, 2015; HOU et al., 2017; (AMERICAN SOCIETY OF TESTING AND MATERIALS - ASTM, E1193-97, 2012; INTERNATIONAL ORGANIZATION FOR STANDARDIZATION -ISO 6341, 2012; US ENVIRONMENTAL PROTECTION AGENCY - US EPA, 64405-1, 2014).

Nanotechnology-based products ready for use as fertilizer or pesticide can be found on the shelf of stores (MILLER; SENJEN, 2008). Moreover, the inventory of the 'Project on Emerging Nanotechnologies', which has been founded in the United States and since 2005 provides information on nanotechnologies, lists 10 products containing copper nanomaterials in water filter cartridges, food supplements and skin care products (WOODROW WILSON INTERNATIONAL CENTER FOR SCHOLARS, 2005). The world production of copper oxide nanoparticles (nCuO) is expected to be 1,600 tons by 2025 (HOU et al., 2017).

In agriculture, the application of nCuO was able to increase plant growth (OCHOA et al., 2017; RAWAT et al., 2018), improve seedling weight gain and reduce stress (KASANA et al., 2017). Copper oxide nanoparticles have also been applied in catalysts (LIU et al., 2012), photodetectors (WANG et al., 2011), biosensors (RAHMAN et al., 2010) and batteries (YANG et al., 2009). A common problem of all these types of usage is the fact that nCuO might eventually reach the environment such as soil and water streams.

The literature reports on the acute and chronic toxicity of nanoparticles to aquatic organisms like bacteria (YANG et al., 2012), algae (ATES et al., 2015), plants (ATHA et al., 2012), crustaceans (ADAM et al., 2015; ROSSETTO et al., 2014) and fish (ATES et al., 2015; DHARSANA et al., 2015). However, few studies report on the spatial distribution and chemical speciation of the nanoparticles or released metal ions inside the test organisms. This type of information could help to understand the causes of toxicity.

Currently, most studies on *Daphnia magna* indicate oxidative stress (HEINLAAN et al., 2008; JO et al., 2012; KIM et al., 2017; LU et al., 2017; ROSSETTO et al., 2014; SAIF et al., 2016; SEO et al., 2014; THIT et al., 2016) and dissolved copper (HEINLAAN et al., 2008; JO et al., 2012; KIM et al., 2017; ROSSETTO et al., 2014; SAIF et al., 2016; SEO et al., 2014) as the main causes of toxicity in this organism. Reactive oxygen species can be formed by chemical species, such as  $\text{Cu}^{2+}$ , which causes oxidative stress in the organism (ROSSETTO et al., 2014). This stress can cause damage to lipids, carbohydrates, proteins and DNA (HEINLAAN et al., 2008; ROSSETTO et al., 2014). Radical specie scan impair the cell membrane and lead to loss of cellular functions (HEINLAAN et al., 2008). Other studies have reported relationship of the toxicity of nanomaterials with particle size (THIT et al., 2016). The

daphnids can absorb particles (THIT et al., 2016) which can block the gastrointestinal tract resulting in malnutrition (LU et al., 2017).

X-ray fluorescence microanalysis ( $\mu$ -XRF) combined with microprobe near edge X-ray absorption spectroscopy ( $\mu$ -XANES) are non-destructive analytical tools that can reveal the elemental spatial distribution of a nanomaterial and its chemical environment in biological tissues.

The present study aimed at evaluating and comparing the toxicity of commercially available copper oxide particles (25, 40 and 80 nm, according to the supplier) to *D. magna*. Acute and chronic assays were performed to assess the LC<sub>50</sub> for effects on survival and EC<sub>50</sub> for effects on reproduction, respectively. In addition, we employed  $\mu$ -XRF and  $\mu$ -XANES to understand how the internal distribution of the Cu and its chemical speciation could help explaining nCuO toxicity to the daphnids.

## 2.2 Materials and Methods

### 2.2.1 Nanoparticle and dispersion characterization

Three commercial Cu oxide-based nanoparticles were employed in this study, having nominal sizes of 25, 40 and 80 nm (US Nanomaterials Research Inc). The size and shape of then CuO nanoparticles were characterized in dispersions at 10 mg Cu L<sup>-1</sup> by transmission electron microscopy (TEM) (JEM-1011, Carl Zeiss AG, Germany). The dispersions were sonicated with a Sonic Dismembrator (Model 705, Fisher Scientific, USA) at 95 W, amplitude of 50% and 50 J for 4 cycles of 5 min each and intervals of 3 min between cycles. The crystal structure of then CuO was determined by Cu-K $\alpha$  radiation X-ray diffraction (XRD) using a PM 1877 diffractometer (Philips, Netherlands).

To estimate the solubility of nCuO, we prepared 50 mL aqueous dispersions in deionized water and daphnid culture medium with the 25, 40 and 80 nm CuO particles at 100 mg Cu L<sup>-1</sup>. A solution of CuSO<sub>4</sub> at the same concentration was also prepared for comparison. The time and parameters of the sonication were the same for TEM, except that the dispersions were kept at room temperature for 24 h. Then, 1 mL of each dispersion was centrifuged using a microcentrifuge (Mikro120, Hettich, Germany) for 1 h at 13,000 rpm. We dripped 15  $\mu$ L of supernatant of nCuO dispersions and CuSO<sub>4</sub> solution salt were dripped in a 6.3 window cuvette assembled with five micrometer thick polypropylene film and dried the samples at 60°C in a laboratory oven. This procedure was repeated twice and samples were measured in triplicate using a rhodium X-ray tube operating at 50 kV. Spectra were acquired by a Si (Li) detector during 200 s. The quantification was made using external standard

calibration and Ga as the internal standard, and using the formula shown below, limits of quantification (LOQ) was calculated. For the soluble concentration of Cu in deionized water and culture medium, the LOQ was 0.18 and 0.11 mg L<sup>-1</sup>, respectively. Measurements were performed in triplicate in deionized water and culture medium.

$$LOQ = \frac{10 \sqrt{BG} \text{ (cps)}}{\text{time (s)} \times \text{electric current } (\mu A)}$$

For zeta potential and dynamic light scattering (DLS) analysis, dispersions of nCuO at 100 mg Cu L<sup>-1</sup> were prepared as describe above. The measurements were carried out in water and culture medium (without algae) using a Zetasizer Nano (Malvern Instruments, U.K).

Geochem (SHAFF et al., 2010) was employed to assess Cu chemical species in water and culture medium. The software it was possible to simulate the reactions between main solutions of the culture medium of *D. magna*, according Associação Brasileira de Normas Técnicas (ABNT NBR 12713, 2016), with CuSO<sub>4</sub>. The software works with the properties of the daphnids culture medium, which had a pH of 7-7.5.

In addition to CuSO<sub>4</sub>, the following salt concentrations were used as in put for the test solutions: KCl: 5.8x10<sup>-3</sup> g L<sup>-1</sup>; MgSO<sub>4</sub>.7H<sub>2</sub>O: 0.1233 g L<sup>-1</sup>; CaCl<sub>2</sub>.2H<sub>2</sub>O: 0.2940 g L<sup>-1</sup>; K<sub>2</sub>HPO<sub>4</sub>: 1.84x10<sup>-4</sup> g L<sup>-1</sup>; H<sub>3</sub>BO<sub>3</sub>: 2.85x10<sup>-3</sup> g L<sup>-1</sup>; Na<sub>2</sub>MoO<sub>4</sub>: 6.3x10<sup>-5</sup> g L<sup>-1</sup>; MnCl<sub>2</sub>.4H<sub>2</sub>O: 7.21x10<sup>-4</sup> g L<sup>-1</sup>; SrCl<sub>2</sub>.6H<sub>2</sub>O: 3.04x10<sup>-4</sup> g L<sup>-1</sup>; LiCl: 6.12x10<sup>-4</sup> g L<sup>-1</sup>; RbCl: 1.4x10<sup>-4</sup> g L<sup>-1</sup>; CuCl<sub>2</sub>.H<sub>2</sub>O: 3.35x10<sup>-5</sup> g L<sup>-1</sup>; ZnCl<sub>2</sub>: 2.6x10<sup>-5</sup> g L<sup>-1</sup>; Fe(SO<sub>4</sub>).7H<sub>2</sub>O: 9.95x10<sup>-4</sup> g L<sup>-1</sup>; KH<sub>2</sub>PO<sub>4</sub>: 1.43x10<sup>-5</sup> g L<sup>-1</sup>; Na<sub>2</sub>EDTA.2H<sub>2</sub>O: 2.5x10<sup>-3</sup>g L<sup>-1</sup>.

## 2.2.2 Toxicity Assessments

### 2.2.2.1 Experimental conditions

*Daphnia magna* neonates were grown in 2 L beakers stored in an incubator at 22 ± 1° C and 12 hours photoperiod. The culture medium was prepared with deionized water at pH 7-7.5, according to ABNT 12713 (2016). The daphnids were fed three times a week with suspensions of *Raphidocelis subcapitata* (density 10<sup>6</sup> cells mL<sup>-1</sup>) and trout feed solution (5 g L<sup>-1</sup>). The medium was changed three times per week.

### 2.2.2.2 Preparation of dispersions and dilution for acute and chronic assays

Three stock dispersions of 25, 40 and 80 nm nCuO and a stock solution of CuSO<sub>4</sub>·7H<sub>2</sub>O (P.A. Synth), both at 50 mg Cu L<sup>-1</sup>, were prepared in deionized water. Then, the dispersions were sonicated as described above.

### 2.2.2.3 Sensitivity, acute and chronic assays

Prior to the acute and chronic assays, sensitivity assays were performed with the reference substance NaCl, exposing neonates to concentrations of 1, 3, 5 and 7 g L<sup>-1</sup>. Sensitivity and acute assays were performed with five neonates ( $\leq$  24 hold) per replicate. The acute assays with nCuO were performed according to ABNT 12713 (2016). CuSO<sub>4</sub> was used as positive control and culture medium as negative control. The Table 1 shows the concentrations of nCuO and CuSO<sub>4</sub> in the culture medium ranged from 0.015 to 16 mg Cu L<sup>-1</sup>, using five test concentrations. The daphnids were exposed in polyethylene flasks containing 30 mL of test solution and kept in an incubator at 22  $\pm$  1°C and 12 h photoperiod for 48 h. During the exposures, no precipitation of nCuO was observed on the bottom of the flasks. After this period, the dead or immobile individuals were counted. The Probit method was used to calculate the concentration that killed or immobilized 50% of the organisms (LC<sub>50</sub>) (SAKUMA, 1998).

Table 1. Concentrations and pH of CuSO<sub>4</sub> and nCuO solutions used for determining dose-response curves for the acute toxicity to *Daphnia magna*

TREATMENT	[ ] MG CU L <sup>-1</sup> / PH											
	[ ]	pH	[ ]	pH	[ ]	pH	[ ]	pH	[ ]	pH	[ ]	pH
CUSO <sub>4</sub>	0	7.4	0.04	7.4	0.08	7.4	0.16	7.4	0.24	7.3	0.32	7.3
NCUO 25 NM	0	7.3	0.03	7.3	0.066	7.3	0.1	7.3	0.13	7.3	0.16	7.3
NCUO 40 NM	0	7.2	1	7.1	2.5	7.2	3.5	7.2	4.5	7.3	5	7.3
NCUO 80 NM	0	7.2	1.5	7.1	1.6	7.1	3.2	7	10	7	16	7

The chronic assays were performed according to guidelines for Testing of Chemicals (OECD - 211, 1998). The Table 2 shows test concentrations ranged from 1.6 x 10<sup>-4</sup> to 1.9 mg Cu L<sup>-1</sup>, using four concentrations in culture medium, which was chosen based on preliminary tests. Neonates, less than 24 h old, were exposed individually in polyethylene flasks containing 100 mL culture medium spiked with nCuO dispersions or CuSO<sub>4</sub> solution. For each treatment and negative control (culture medium), 10 replicates were prepared and maintained at 22  $\pm$  1 °C with photoperiod of 12 hours. Treatment solutions, culture medium and feed (*R. subcapitata*, at 10<sup>3</sup> cells mL<sup>-1</sup>) were replaced three times per week, and tests lasted

for 21 days. Every day the numbers of new-borns were assessed. At the end of the assays, the averages of posture and reproduction were calculated as described below:

Average of broods = total number of broods/number of fertile daphnids;

Average of reproduction = average of (sum of n° neonates generated from a fertile daphnid/n° of broods from a fertile daphnid)

Table 2. Concentrations and pH of CuSO<sub>4</sub> and nCuO solutions used for determining dose-response curves for the acute toxicity to *Daphnia magna*

Treatment (mg Cu L <sup>-1</sup> )	pH	% mortality	Average of broods	Day of 1 <sup>st</sup> brood	Average of reproduction	Total number of neonates
Control	7.4	0	4.2	8 <sup>th</sup>	25.0	1019
nCuO 25 (0.01248) nm	7.3	50	4.4	10 <sup>th</sup>	5.8	125
nCuO 25 (0.00624) nm		40	4	10 <sup>th</sup>	7.29	175
nCuO 25 nm (0.00312)		30	3.71	8 <sup>th</sup>	9.61	272
nCuO 25 nm (0.00156)	7.2	10	3.77	8 <sup>th</sup>	11.9	408
nCuO 40 nm (1.90)	7.2	40	3.33	9 <sup>th</sup>	23.7	719
nCuO 40 nm (1.17)		30	3.77	8 <sup>th</sup>	21.2	831
nCuO 40 nm (0.585)		20	5.4	8 <sup>th</sup>	15.2	837
nCuO 40 nm (0.292)	7.2	10	4.3	8 <sup>th</sup>	19.9	877
nCuO 80 nm (1.86)	7.2	30	4.44	8 <sup>th</sup>	15.7	678
nCuO 80 nm (1.13)		30	4.44	8 <sup>th</sup>	20.1	790
nCuO 80 nm (0.565)		30	4.7	8 <sup>th</sup>	20.1	918
nCuO 80 nm (0.282)	7.3	10	4.4	8 <sup>th</sup>	20.8	955
CuSO <sub>4</sub> (0.00128)	7.4	80	4.5	10 <sup>th</sup>	9.42	77
CuSO <sub>4</sub> (0.00064)		40	4.33	9 <sup>th</sup>	6.02	157
CuSO <sub>4</sub> (0.00032)		30	3.66	8 <sup>th</sup>	9.19	206
CuSO <sub>4</sub> (0.00016)	7.4	10	5.11	8 <sup>th</sup>	10.6	474

### 2.2.3 Decomposition of H<sub>2</sub>O<sub>2</sub> by nCuO and CuSO<sub>4</sub>

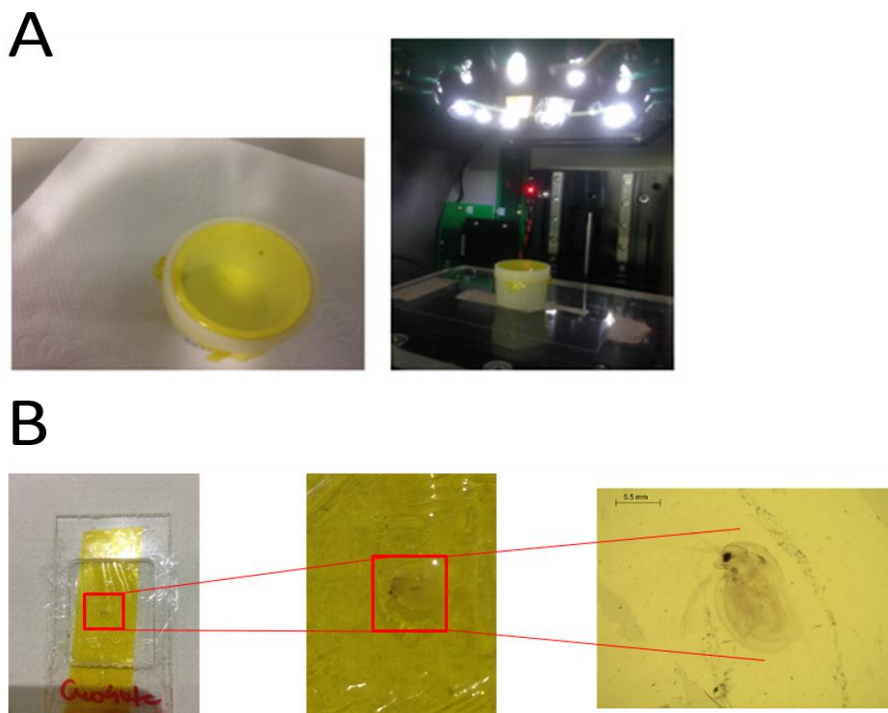
To assess the surface reactivity of then CuO, the decomposition rate of H<sub>2</sub>O<sub>2</sub> was evaluated in terms of the volume of O<sub>2</sub> generated. For this, 19.5 mL of a 1,000 mg Cu L<sup>-1</sup> dispersion of nCuO or a solution of CuSO<sub>4</sub> was prepared in deionized water and in culture medium. Similar solutions were prepared in culture medium at concentrations corresponding to the LC<sub>50s</sub>. For 1,000 mg Cu L<sup>-1</sup>, the samples were placed in a 25 mL sealed flask, connected to a syringe and to a 25 mL pipette placed in the water column. Then, 0.5 mL of H<sub>2</sub>O<sub>2</sub> 30% v/v was added and the volume of O<sub>2</sub> produced was measured every five minutes for 300 minutes or until it exceeded the graduation limits of the 25 mL pipette. The tests were repeated twice. The same procedure was applied three times for concentrations corresponding with the LC<sub>50</sub> using a 5 mL pipette for 48 h.

### 2.2.4 X-ray fluorescence microanalysis (μ-XRF)

μ-XRF was employed to map the 2D spatial distribution of Cu taken up by the daphnids that died up on exposure to nCuO and CuSO<sub>4</sub>. This allowed uncovering the Cu location at the moment of death. The daphnids were removed from the test media, washed three times with phosphate buffer (PBS) (Na<sub>2</sub>HPO<sub>4</sub>, NaH<sub>2</sub>PO<sub>4</sub>.H<sub>2</sub>O, pH 7-7.5) and fixated in 4% paraformaldehyde solution (PFA) over night, washed again three times with PBS and kept under PBS at 4°C till analysis.

The daphnids were taken from the PBS with a pipette and transferred to the top of a Kapton<sup>TM</sup> (polyamide) thin film mounted on an XRF cuvette, how show the Figure 1 (A). The Cu spatial distribution was determined using a benchtop μ-XRF system (EDAX, Orbis PC USA). X-rays were generated by a Rh anode. The 30 μm X-ray beam (for the Mo-Kα) was focused on the samples by poly-capillary optics, and the detection was carried out by a 30 mm<sup>2</sup> silicon drift detector operating at 140 eV resolution for Mn-Kα. The maps were recorded using a matrix of 64 x 50 points summing up to 3,200 XRF spectra for each image. The maps for daphnids from the acute assays were acquired using 40 kV, 300 μA and 1.5 s dwell time per point while the maps for daphnids from the chronic assays were registered under 50 kV, 800 μA and 6 s dwell time per point. The latter measurements were performed using a 25 μm Ti primary filter. All maps were recorded under a dead time lower than 3%.

Figure 1. (A) *Daphnia magna* on top of a Kapton™ (polyamide) film prepared for  $\mu$ -XRF analysis, (B) Scheme of a sample of *D. magna* covered by a 4  $\mu$ m Ultralene™ (polyethylene) film for XANES



The Cu instrumental sensitivity was determined using a CuS thin film Micromatter™ standard containing  $42.3 \mu\text{g Cu cm}^{-2}$  (serial #6323). X-ray transmission assays (not shown here) revealed that the neonates are infinitely thin samples for Cu  $K\alpha$  radiation. Then, Cu quantification was performed by dividing the number of XRF Cu- $K\alpha$  Counts (cps) by the elemental sensitivity ( $\text{cps } \mu\text{g}^{-1} \text{cm}^{-2}$ ). The thickness of adult *D. magna* (intermediate sample) did not allow performing quantitative analyses and therefore only qualitative Cu maps will be presented.

### 2.2.5 Microprobe X-ray absorption near edge spectroscopy ( $\mu$ -XANES)

Cu-K edge  $\mu$ -XANES spectra were recorded at the XRF beamline of the 1.37 GeV Brazilian Synchrotron Light Laboratory (LNLS, Campinas). In this facility X-rays were provided by a bending magnet device, monochromatized by a double crystal Si(111), and the  $20 \times 25 \mu\text{m}^2$  X-ray beam was focused on the sample by a KB mirror system. The detection was carried out in XRF mode using an element Si drift detector (KETEK GmbH, Germany). At least six  $\mu$ -XANES spectra were recorded per sample, each of them recorded in c. 40 min in the same position. The energy step in the edge region was 0.5 eV. The spectra were subsequently merged to improve the signal to noise ratio.



Chemical distribution maps previously recorded in our laboratory helped to define the appropriate regions of the daphnids to be measured by  $\mu$ -XANES. The spots with higher Cu content were analyzed. The chemically fixed samples (same procedure as described for  $\mu$ -XRF) were selected for these analyses. To prevent dehydration, the samples were covered with a 4  $\mu$ m Ultralene<sup>TM</sup> (polyethylene) film, Figure 1 (B).

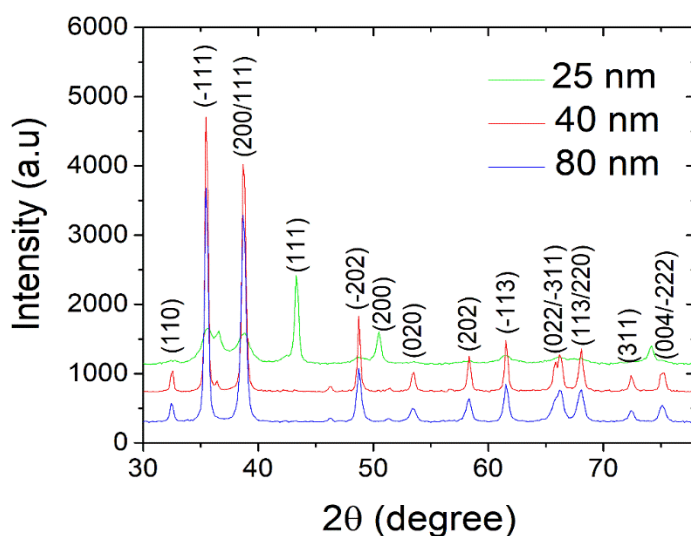
In addition to these samples, Cu reference compounds previously synthesized in our laboratory were measured. The complexation procedure was similar to that for Zn reported by Sarret et al. (2009). The mixtures of aqueous  $\text{Cu}(\text{NO}_3)_2$  and salts at pH 5 were stirred for 24 h and freeze dried. The  $\mu$ -XANES spectra were energy calibrated using a reference Cu foil. The data was normalized using the Athena software of the IFEFFIT package (RAVEL; NEWVILLE, 2005).

## 2.3 Results and discussion

### 2.3.1 Characterization of nCuO

X-ray diffraction patterns (Figure 2) shows that the 40 and 80 nm CuO particles were monoclinic CuO, the 25 nm CuO particles contained a fraction of face centric cubic (fcc) metallic phase in addition to monoclinic CuO. In a previous study we showed that the 25 nm CuO particles had a core-shell structure (DURAN et al., 2017).

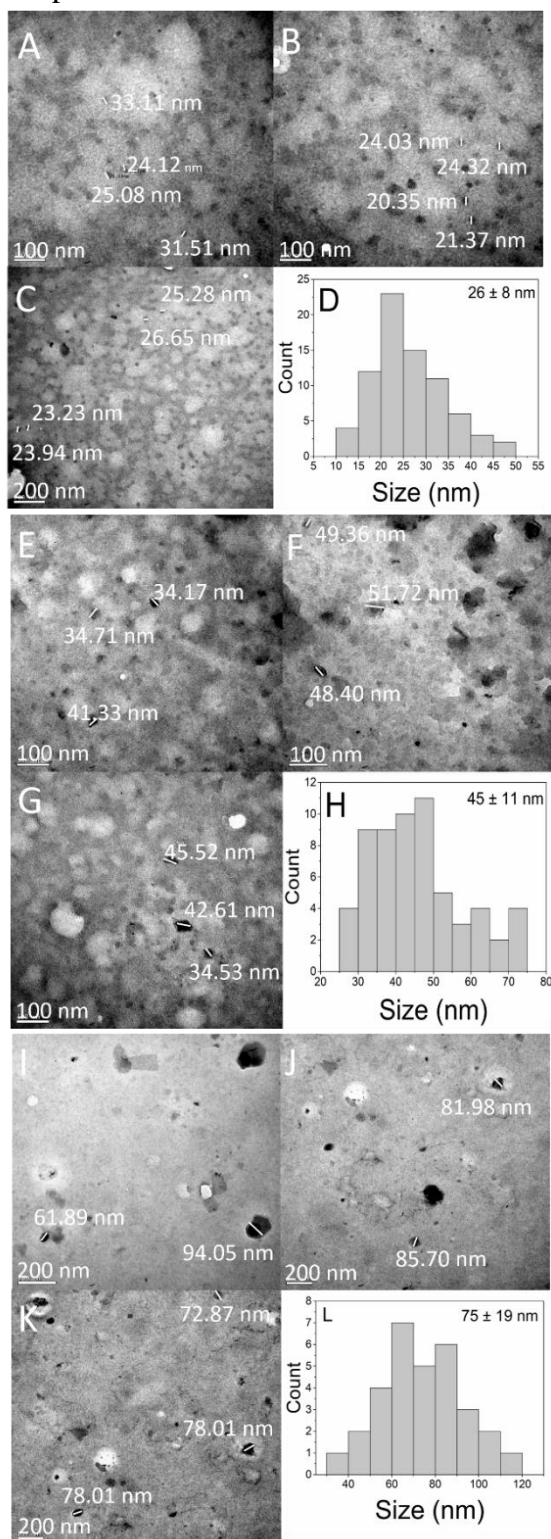
Figure 2. XRD patterns for 25, 40 and 80 nm nCuO



The average particle size determined by TEM (Figure 3) were close to the values reported by the supplier. nCuO 25 nm ( $26 \pm 8$  nm) were of spherical shape, 40 nm ( $45 \pm 11$  nm) of elliptical shape and 80 nm ( $75 \pm 19$  nm) of quadratic shape. Nevertheless, for the sake of

clarity, we decided to keep the nominal size mentioned by the supplier when reporting the results obtained.

Figure 3. Characterization of dispersions of nCuO at 10 mg Cu L<sup>-1</sup> (50% deionized water and 50 % isopropanol) of (A, B, C) 25 nm, (E, F, G) 40 nm and (I, J, K) 80 nm by transmission electronic microscopy (TEM). (D, H, L) histograms showing the size distribution of nanoparticle counts for nCuO 25 nm, 40 nm and 80 nm, respectively



For reasons of feasibility, DLS and zeta potential measurements (Table 3) were performed using concentrations above those used in the bioassays. The dispersed particles aggregated. In agreement with a previous study, the hydrodynamic diameters in culture medium were larger than those recently reported for dispersions in deionized water (LIU et al., 2009). This is partially explained by the decrease in zeta potential, which ultimately leads to lower electric repulsion between the particles. Other studies also reported aggregate size and zeta potentials in the same orders of magnitude (-17.6mV,-9.6mV and 935.5 nm 1,095 nm, respectively) (JO et al., 2012; WU et al., 2017).

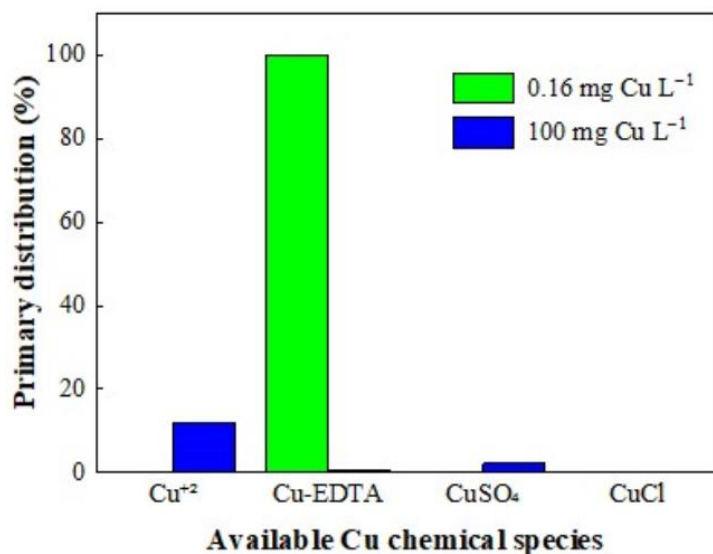
Table 3. Physical-chemical characterization of the treatments of nCuO and CuSO<sub>4</sub>

Treatment	Hydrodynamic Diameter (nm)		Zeta Potential (mV)		Dissolved Cu (mg L <sup>-1</sup> )	
	dw	cm	dw	cm	dw	cm
<b>25 nm</b>	263 ± 3	819 ± 353	16 ± 0.1	-10 ± 0.2	1.0 ± 0.3	1.0 ± 0.7
<b>40 nm</b>	153 ± 45	171 ± 91	-20 ± 0.6	-8 ± 0.7	0.6 ± 0.2	0.1 ± 0.06
<b>80 nm</b>	214 ± 3	292 ± 3	-17 ± 0.2	-11.8 ± 0.2	0.2 ± 0.01	0.3 ± 0.3
<b>CuSO<sub>4</sub></b>	-	-	-	-	117 ± 10	40 ± 7

\*dw = deionized water; cm = culture medium.

Table 3 shows that in water and culture media, Cu solubility was inversely proportional to nanoparticle size. This trend is in agreement with the literature (LIU et al., 2009). The solubility of CuSO<sub>4</sub> was higher in deionized water than in culture medium, which suggests that part of the Cu<sup>2+</sup> ions had precipitated. Calculations performed by Geochem (SHAFF et al., 2010) showed that 85% of the Cu was precipitated with OH<sup>-</sup> in the 100 mg Cu L<sup>-1</sup> solution (Figure 4). Thus, when interpreting the dose-response curves one should keep in mind that a significant fraction of the putative active free or ionic Cu may actually be precipitated.

Figure 4. Cu chemical interactions in the daphnid culture medium and after adding different concentrations of CuSO<sub>4</sub>



### 2. 3.2 Acute and chronic assays

The acute assays revealed the concentrations necessary to kill 50 % of the daphnid population within 48 hours exposure. The chronic assays focused on the effects of low concentrations during along-term exposure. Therefore, these tests are complementary.

Figure 5 shows the sensitivity of *D. magna* neonates to the reference substance NaCl. The LC<sub>50</sub> of 4,370 mg L<sup>-1</sup> was close to the values of 4,868 mg L<sup>-1</sup> and 4,765 mg L<sup>-1</sup> reported in the literature (MOUNT et al., 1997; STRUEWING et al., 2015). This confirms that the organisms used were in good condition.

Figure 5. Dose-response curve for the acute toxicity of the reference chemical NaCl to *Daphnia magna*

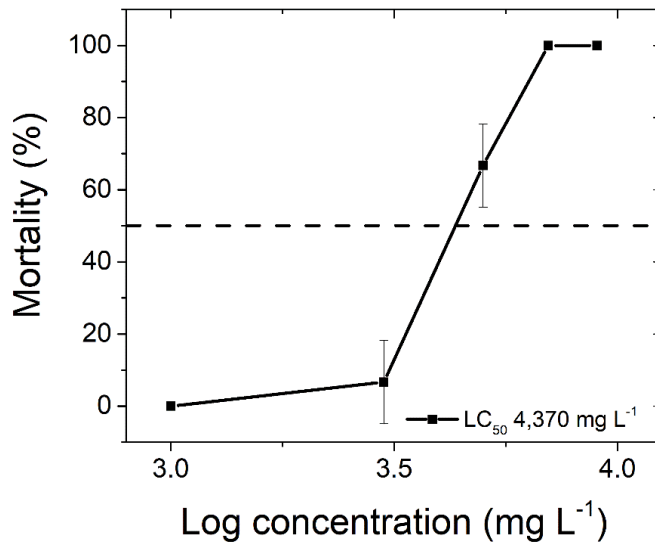


Figure 6 shows the mortality (dose-response curve) of the daphnids exposed to 25, 40 and 80 nm nCuO and the CuSO<sub>4</sub> positive control. The 25 nm CuO and CuSO<sub>4</sub> were the most toxic with LC<sub>50</sub>s of  $0.05 \pm 0.011$  mg Cu L<sup>-1</sup> and  $0.16 \pm 0.015$  mg Cu L<sup>-1</sup>, respectively. The LC<sub>50</sub> values for 40 and 80 nm nCuO were similar at  $2.34 \pm 0.0479$  and  $2.26 \pm 0.246$  mg Cu L<sup>-1</sup>, respectively. According to the statistical analysis presented in Figure 7, the order of acute toxicity was: 25 nmCuO = CuSO<sub>4</sub> > 40 nm nCuO = 80 nm.

Figure 6. Dose-response curves for the acute toxicity of nCuO and CuSO<sub>4</sub> to *Daphnia magna* neonates

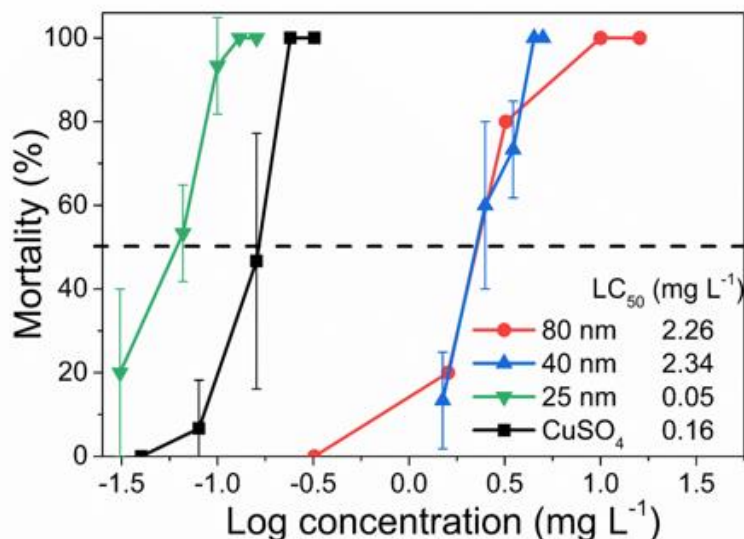
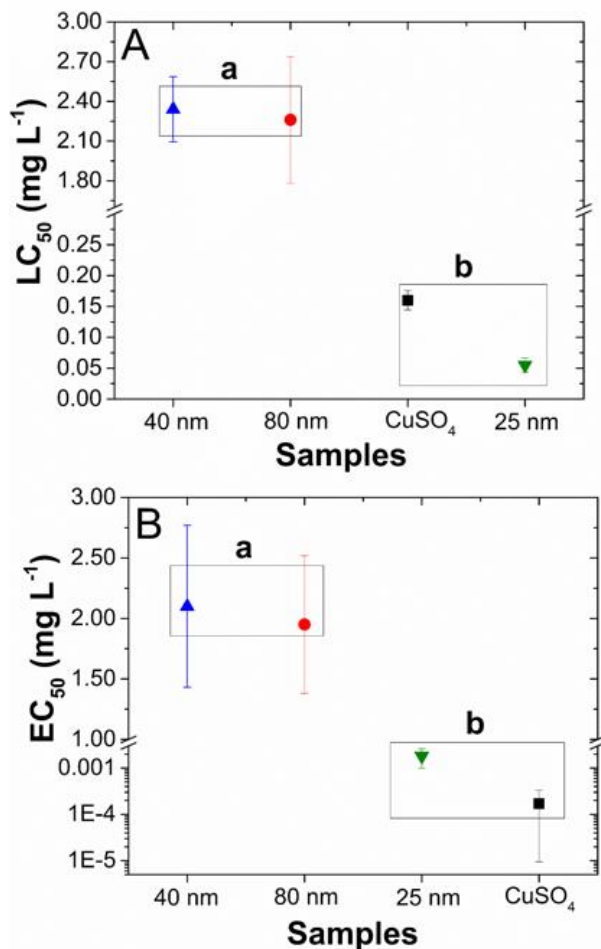


Figure 7. Effects of nCuO and CuSO<sub>4</sub> on survival and sublethal endpoint in assays with *Daphnia magna*. Comparison of (A) LC<sub>50</sub> values from acute assays and (B) EC<sub>50</sub> values from chronic assays. Values followed with the same indices do not differ significantly according to the Tukey test ( $p < 0.05$ )



The calculation performed by the Geochem code showed that in the 0.16 mg Cu L<sup>-1</sup> CuSO<sub>4</sub> solution most of the copper was precipitated as CuEDTA. Thus, if the toxic effect was caused by free Cu<sup>2+</sup> ions, the actual Cu ionic concentration corresponded to nearly one tenth of that supplied as CuSO<sub>4</sub>. This means that the Cu ionic toxic threshold is actually lower than supposed.

Table 4 compiles the LC<sub>50</sub> values found by other research groups evaluating the acute toxicity of nCuO to *D. magna*. According to Table 4, nCuO smaller than 100 nm yielded LC<sub>50</sub> values from 0.08 to 4.0 mg Cu L<sup>-1</sup> while LC<sub>50</sub>s for CuSO<sub>4</sub> ranged from 0.04 to 0.17 mg Cu L<sup>-1</sup>. The CuSO<sub>4</sub> LC<sub>50</sub> reported in the present study is in close agreement with Heinlaan et al. (2008); and Rossetto et al. (2014) however, it strongly differs from (THIT et al., 2016).

Table 4. LC<sub>50</sub> values found in the present study and in the literature for *Daphnia magna* exposed for 48 hours to the CuO nanoparticles, CuSO<sub>4</sub> and other Cu salts. For CuO nanoparticles the LC<sub>50</sub> varied from 0.05 to 4.0 mg Cu L<sup>-1</sup>, whereas for positive controls (soluble Cu forms) it ranged from 0.02 to 0.80 mg Cu L<sup>-1</sup>

Reference	nCuO (nm)	LC <sub>50</sub> nCuO (mg Cu L <sup>-1</sup> )	LC <sub>50</sub> (mg Cu L <sup>-1</sup> )
Heinlaan et al. (2008)	30	3.2	CuSO <sub>4</sub> – 0.17
Rossetto et al. (2014)	200-300	22	CuSO <sub>4</sub> – 0.10
Jo et al. (2012)	< 50	2.79	CuCl <sub>2</sub> – LC <sub>50</sub> not report
Kim et al. (2017)	30 -50	1.09	Cu(NO <sub>3</sub> ) <sub>2</sub> – 0.02
Seo et al. (2014)	30-50	0.98	CuSO <sub>4</sub> – 0.04
Thit et al. (2016)	6	0.08	-
Saif et al. (2016)	50	0.102	Cu(NO <sub>3</sub> ) <sub>2</sub> – 0.02
Lu et al. (2017)	< 100	0.63	-
In this study	25	0.05	CuSO <sub>4</sub> – 0.16
In this study	40	2.34	same as above
In this study	80	2.6	same as above

Although the values reported in Table 4 give an idea of the toxicity of Cu salts and nCuO, it is difficult to compare the LC<sub>50</sub> data generated by these studies. In spite of recommendations in the test guidelines (ASTM, E1193-97, 2012; ISO 6341, 2012; US EPA 232, 2002) some of the above mentioned studies (HEINLAAN et al., 2011; KIM et al., 2017; LU et al., 2017; SAIF et al., 2016) did not determine the sensitivity of the daphnids to a reference substance, e.g. NaCl. Therefore, to facilitate data comparison future studies should also report this parameter.

In principle, the observed toxicity to neonates may relate to an imbalance of dissolved ions, channel obstruction or reactions taking place on the surface of the particles. Previous studies evaluating the effects of several nanoparticles on microbes suggest that the contribution of dissolved ions may be negligible (SONG et al., 2015). However, for *D. magna*, the LC<sub>50</sub> reported in the present study for CuSO<sub>4</sub> combined to the solubility of nanoparticles, suggests that dissolved ions may contribute to the toxicity. Heinlaan et al. (2008) detailed the importance of dissolved ions for the toxic effects of nanoparticles. The toxicity of nano CuO and bulk CuO was almost identical to that of free Cu<sup>2+</sup> from CuSO<sub>4</sub> (bioavailable Cu). In addition, they showed that the nanoparticles do not have to enter the cells to cause harm, as the contact between the nanoparticle and gut cells may cause changes in the microenvironment such as generation of extracellular ROS.

Figure 8. Effect of differently sized nCuO particles and CuSO<sub>4</sub> (A) on the survival (bars), average reproduction (line) and (B) average number of broods (bars) and average number of neonates (line) in the chronic assay with *Daphnia magna*. The raw data is presented in table 2. The effects on reproductive output of *D. magna* were more pronounced for 25 nm nCuO and CuSO<sub>4</sub>

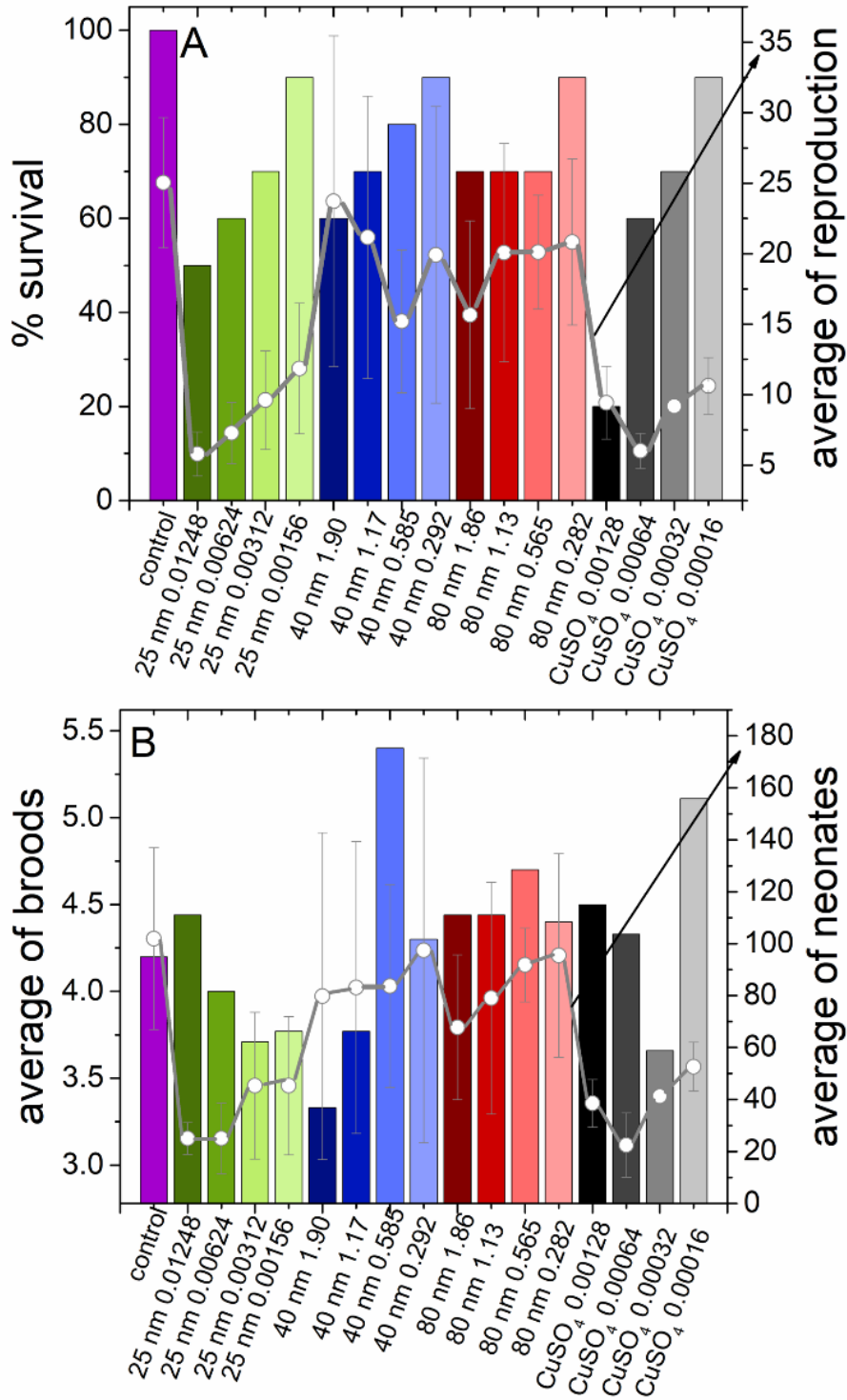
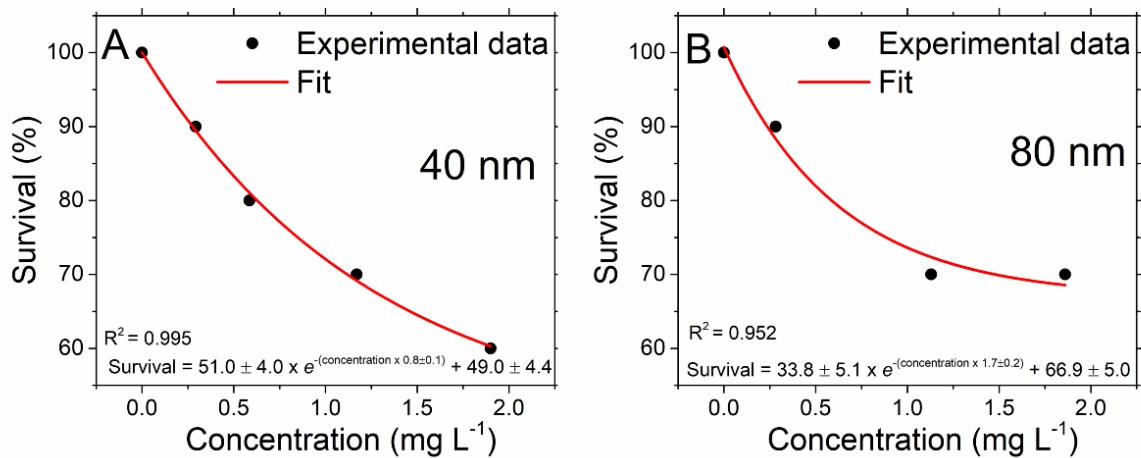




Figure 9. Effect of (A) 40 nm and (B) 80 nm nCuO on the survival of *Daphnia magna* in chronic tests



The average reproduction shown in Figure 8(A) followed the survival trend for the 25 nm nCuO and CuSO<sub>4</sub>, while for 40 nm and 80 nm nCuO no tendency was observed. The statistical analysis (Figure 10(A)) confirmed that the lowest average reproduction was obtained for CuSO<sub>4</sub> and 25 nm nCuO, especially at 0.00064 mg Cu L<sup>-1</sup> and 0.01248 mg Cu L<sup>-1</sup>, respectively. The average reproduction (Figure 10(A)) did not significantly differ for the 40 and 80 nm CuO.

Figure 10. (A) Average reproduction and (B) average number of neonates produced by *Daphnia magna* in 21-day chronic toxicity assays. Values followed with the same indices do not differ significantly according to the Tukey test ( $p < 0.05$ )

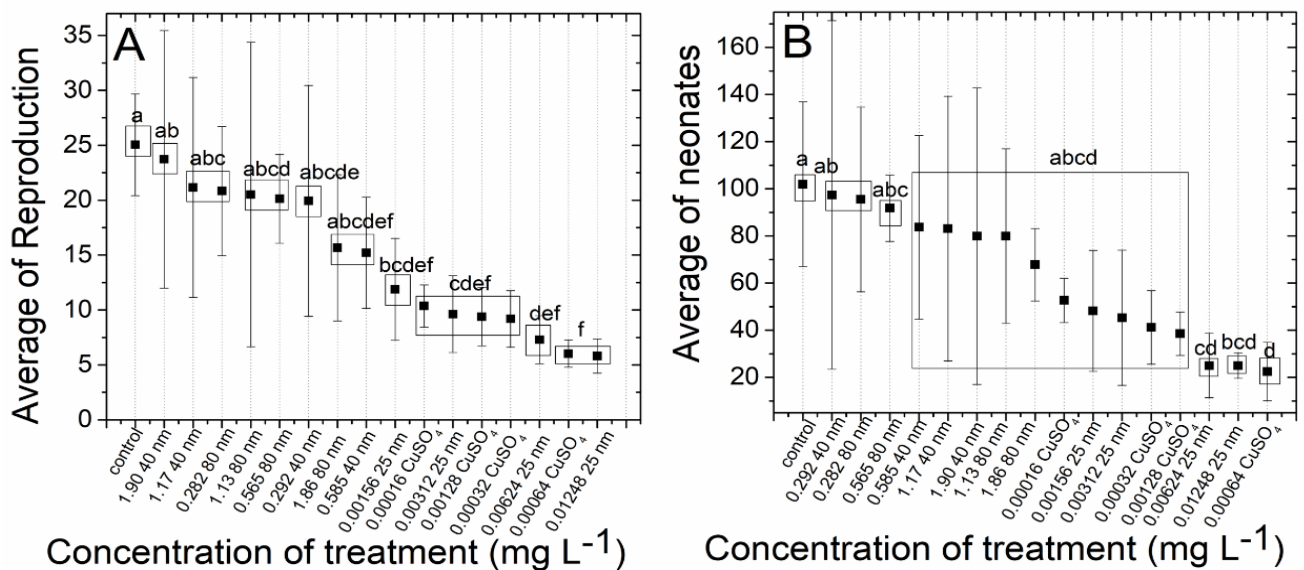


Figure 8 (B) shows that the average number of broods per daphnid increased following exposure to the nanoparticles while the average number of neonates decreased. Hence, although more broods were produced, the average number of neonates (offspring) was lower.

Table 2 shows that the time to the 1<sup>st</sup> brood was practically the same for treatments and control. Similar results were reported by Lu et al. (2017) who found no significant effect on offspring numbers and time to 1<sup>st</sup> brood at 0.4  $\mu\text{g Cu L}^{-1}$  (nCuO < 100 nm). Analogous to the average reproduction, the lowest average numbers of neonates were found for CuSO<sub>4</sub> and 25 nm nCuO (Figure 10 (B)).

The EC<sub>50</sub> values for the reduction of neonate numbers caused by 40, 80, 25 nm nCuO and CuSO<sub>4</sub> were 2.10, 1.95, 0.0018, and 0.00017 mg Cu L<sup>-1</sup>, respectively. According to the Tukey test, the toxicity order was the same as found for the LC<sub>50</sub>s (Figure 7(B)). Overall, the statistical analysis showed that the 40 and 80 nm nCuO presented similar effects on the daphnids. And the 25 nm nCuO has a similar toxicity as the CuSO<sub>4</sub>.

Reduction of the time of first brood and the number of neonates were also reported for *D. magna* exposed for 21 days to nano CuO, ZnO, Au, and TiO<sub>2</sub> (LIU et al., 2014). In agreement to the present study, a positive relationship between harmful effects and dissolved ion concentrations were reported. Likewise, in 21-days assays, Adam et al. (2015) reported a reduction of average brood number per female, from  $3.9 \pm 0.3$  in the control to  $1 \pm 1.4$  and  $3 \pm 0.8$  for CuCl<sub>2</sub> and CuO, respectively.

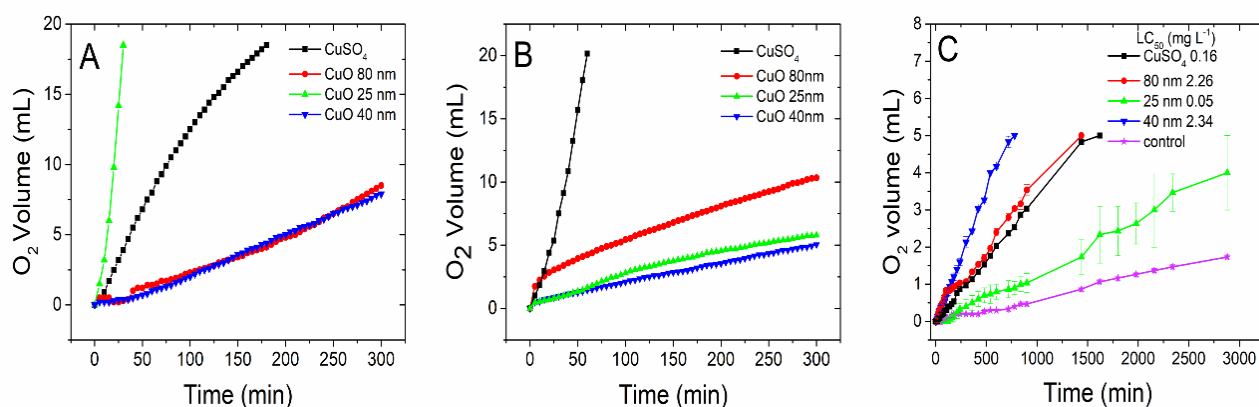
The effects of nanoparticles on reproductive parameters may be hypothesized in the light of the available literature. Using a combination PIXE/RBS/STIM, Pinheiro et al. (2013) showed the presence of Ti in the egg shell and eggs of *D. magna* exposed for four days to TiO<sub>2</sub> at 2.8 mg Ti L<sup>-1</sup>. Although the limits of detection and lateral resolution imposed by XRF in the present study did not allow detecting Cu in these tissues, one can suppose it might affect the reproduction of the daphnids.

Wang et al. (2015) investigated the effects of micro/nano-Cu<sub>2</sub>O crystals (450 – 900 nm at 10  $\mu\text{g L}^{-1}$ ) on *D. magna*. The time to the first brood and offspring growth were evaluated during 30 days of exposure. In agreement to the present study, the time to first brood was affected by the treatments (2 days delayed for daphnids exposed to Cu<sub>2</sub>O vertex-truncated octahedron shapes). All six micro/nano-Cu<sub>2</sub>O crystals reduced the length of individuals compared to the control. In the most extreme case, the treatment reduced the length by 48.7%.

To better understand the biological effects of then CuO particles on the daphnids, their chemical reactivity was evaluated in terms of H<sub>2</sub>O<sub>2</sub> decomposition. The O<sub>2</sub> evolution curves showed that 25 nm nCuO was the most reactive particle in both deionized water and culture

medium for  $1,000 \text{ mg Cu L}^{-1}$  (Figure 11 (A) (B)). At concentrations corresponding to the  $LC_{50s}$ , the amount of  $O_2$  produced by the 25 nm nCuO was lower than for the other nCuO particles and  $CuSO_4$  (Figure 11 (C)), which may be justified by its low concentration. The reactivity of  $CuSO_4$  was lower in culture medium than in water, which might be related to its chemical availability since a fraction of the Cu ions was precipitated as Cu phosphate. The amount of  $O_2$  produced by 40 and 80 nm nCuO was similar, regard less of the liquid media. In the literature there is no consensus as to whether toxicity is caused by the dissolved copper or by nanoparticles (HOU et al., 2017; LU et al., 2017; THIT et al., 2016). Since the trend in  $H_2O_2$  decomposition was in line with the results of the toxicological assays, it seems that the redox reactivity of Cu ions and nanoparticles may play a role in the mechanism of toxicity.

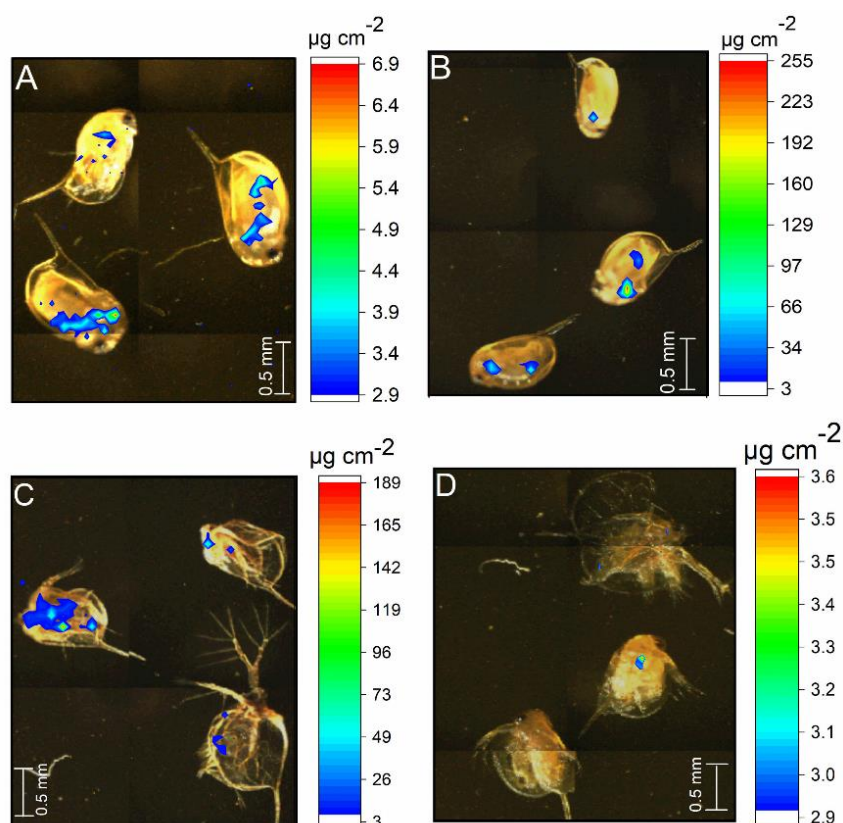
Figure 11. Oxygen volume generated during the decomposition of  $H_2O_2$  in the presence of nCuO and  $CuSO_4$  at  $1,000 \text{ mg Cu L}^{-1}$  in (A) deionized water, (B) daphnid culture medium and (C) at concentrations in daphnid culture medium corresponding with the  $LC_{50s}$  for the effects of these compounds on the survival of *Daphnia magna*



### 2. 3.3. Spatial distribution of Cu in dead daphnids

Figure 12 presents quantitative maps revealing the spatial distribution of Cu in the *D. magna* exposed to nCuO and  $CuSO_4$  during the acute assays. The local concentration is expressed as  $\mu\text{g}$  of Cu per  $\text{cm}^{-2}$ . The concentration of Cu in the spots varied from 2.9 up to  $255 \mu\text{g cm}^{-2}$ .

Figure 12. Quantitative spatial distribution of copper in the body of *Daphnia magna* neonates exposed for 48 h to nCuO and CuSO<sub>4</sub> at concentrations killing all organisms (LC<sub>100</sub>) in the acute assays. (A) neonates exposed to 25 nm nCuO at 0.15 mg Cu L<sup>-1</sup>, (B) neonates exposed to 40 nm nCuO at 4.5 mg Cu L<sup>-1</sup>, (C) neonates exposed to 80 nm nCuO at 16 mg Cu L<sup>-1</sup>, (D) neonates to CuSO<sub>4</sub> at 0.32 mg Cu L<sup>-1</sup>. Cu accumulation hotspots were found in the intestine and soft tissues



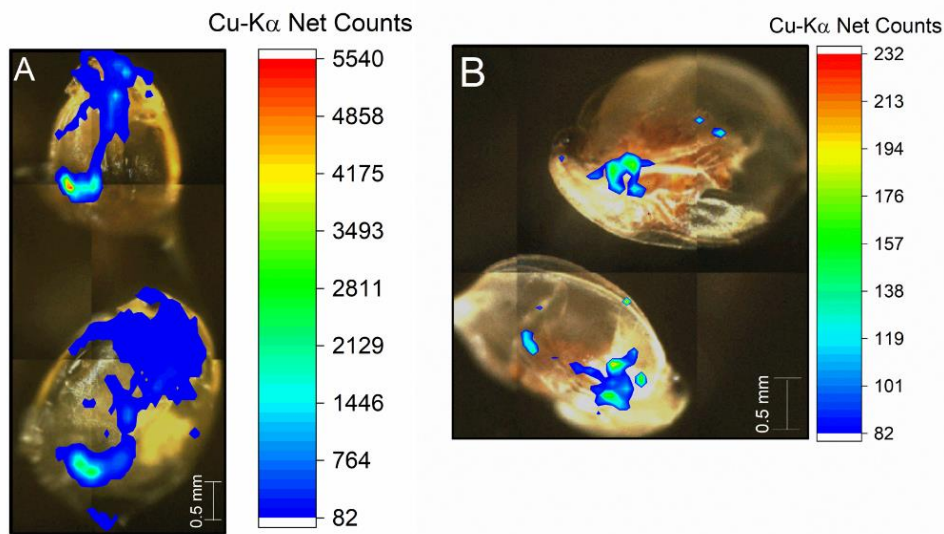
Instead of appearing homogeneously distributed along the carapace, Cu was found as spots in the gut region. This suggests that Cu was stored in the soft parts of the daphnids, such as the intestine and appendages. These findings are in agreement with scanning electron microscopy results reported by Wang et al. (2015).

The daphnids exposed to CuSO<sub>4</sub> showed a ruptured carapace, which helps explaining the low internal concentrations since the Cu concentrated inside may have leached out due to these ruptures. It is worth highlighting that the fixation procedure did not alter the elemental spatial distribution, considering a lateral resolution of tens of micrometres.

Figure 13 shows the spatial distribution of Cu in the body of adult daphnids exposed for 21 days to (A) 80 nm nCuO at 1.86 mg Cu L<sup>-1</sup> and (B) 40 nm Cu at 1.90 mg Cu L<sup>-1</sup>. Similar to the acute assays, the Cu was mainly accumulated in the intestine and soft parts. We did not find

any other reports comparing the spatial distribution of the same nanoparticles within neonates and adults. Due to the thickness of adult *D. magna*, it was not possible to transform the XRF counts in to concentrations. Nevertheless, the number of Cu-K $\alpha$  counts is directly proportional to the Cu content. Thus, the brighter points in Figure 13 indicate Cu hotspots. It was not possible to detect XRF signals for Cu in the daphnids exposed to 25 nm Cu and CuSO<sub>4</sub>.

Figure 13. Spatial distribution maps of copper in the body of *Daphnia magna* exposed for 21 days to (A) 80 nm nCuO at 1.86 mg Cu L<sup>-1</sup> and (B) 40 nm nCuO at 1.90 mg Cu L<sup>-1</sup>. Cu accumulation hotspots were found in the intestine and soft tissues



In agreement to our findings, CdSe/ZnS quantum dots (JACKSON et al., 2009), C60 (17-23 nm) (HEINLAAN et al., 2011) and CuO nanoparticles (30 and 30-50 nm) (HEINLAAN et al., 2011; HOU et al., 2017) were shown to be concentrated in the gut of daphnids (HEINLAAN et al., 2011; HOU et al., 2017; LOVERN; OWEN; KLAPER, 2008). Adult *D. magna* exposed to 0.12 mg L<sup>-1</sup> dissolved Zn (from quantum dots) for one week accumulated Zn mainly in the gut region and eggs, where concentrations reached 30  $\mu\text{g cm}^{-2}$  (DE SAMBER et al., 2008; 2010).

In agreement to the present study, SEM images showed that micro/nano-Cu<sub>2</sub>O tended to agglomerate inside the gut. This suggests that damage can be caused by low concentrations of dissolved metal ions in the gut and that the concentration of soluble copper is higher at the octahedron shape of micro/nano-Cu<sub>2</sub>O (WANG et al., 2015).

The literature describes several mechanisms by which particles and ions can harm or compromise the health of *D. magna*, including intracellular effects, mobility and obstruction effects.

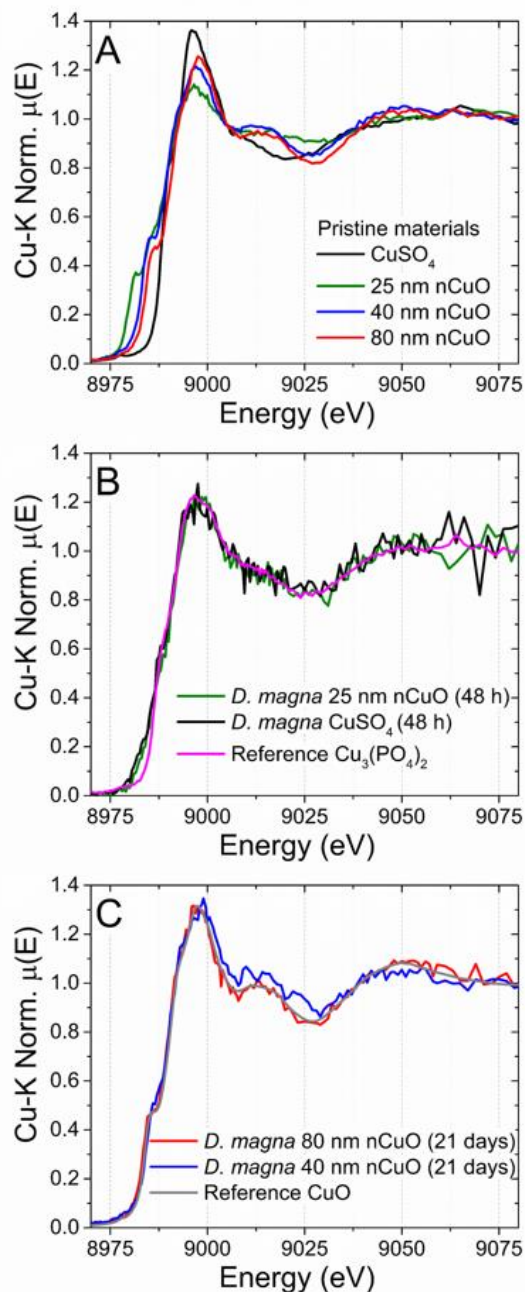
Daphnids are filter feeders. A 2-3 mm wide *D. magna* can filter up to 400 mL of liquid medium per day (MCMAHON, 1965). Upon filtration, particles can get trapped inside the organisms and ions can be taken up in to cells by endocytosis (ADAM et al., 2015; MCMAHON, 1965). Ions can also be absorbed by ion channels or by ionic pumps located on cells of the intestine (BIANCHINI; WOOD, 2008; SIMKISS; TAYLOR, 1989). In *Gammarus pulex* the excess of ions and particles was shown to compromise the osmoregulation process generating a metabolic expense in the organism (LU et al., 2017). Specifically, Cu ions can reduce sodium absorption (HEINLAAN et al., 2011).

Nanoparticles can adhere to the carapace and therefore hinder the mobility of the daphnid, leading to a change in its swimming behavior (LU et al., 2017). The movement of appendages in daphnids is constant and occurs even in the absence of food. This movement, besides aiding in the filtration of particles, acts in the circulation of the aqueous medium in the carapace and facilitates respiration. Movements can also transfer particles located in the appendages towards the intestine (LOVERN; OWEN; KLAPER, 2008). Another study reported that diamond nanoparticles can accumulate within the gastrointestinal tract and block the absorption of nutrients by the intestinal cells in *D. magna* (MENDONÇA et al., 2011). Deficiency in nutrient absorption can lead to slow growth and reduced fecundity.

#### **2.3.4 $\mu$ -XANES chemical speciation of Cu within Cu hotspots**

The chemical speciation of the Cu taken up by the daphnids was investigated by measuring XANES on the Cu K edge. Figure 14 (A) shows the XANES spectra for then CuO and CuSO<sub>4</sub> pristine materials used in the exposure assays. Figure 14 (B) shows that the  $\mu$ -XANES spectra of daphnids exposed to 25 nm nCuO and CuSO<sub>4</sub> for 48 h are similar to that of Cu<sub>3</sub>(PO<sub>4</sub>)<sub>2</sub>. This indicates that 25 nm nCuO and CuSO<sub>4</sub> were converted into Cu<sub>3</sub>(PO<sub>4</sub>)<sub>2</sub>. The Cu<sub>3</sub>(PO<sub>4</sub>)<sub>2</sub> inside *D. magna* possibly was formed after reaction with the phosphate buffer used to preserve the carapace of the daphnids, so copper analysed was inside the daphnids. More research is needed to address the possible changes occurring during sample preparation. Figure 14(C) shows that the Cu chemical neighbourhood inside daphnids exposed for 21 days to 40 nm and 80 nm nCuO remained as CuO.

Figure 14. Spectra generated by XANES analysis of (A) pristine  $\text{CuSO}_4$  and 25 nm CuO materials, (B) of *Daphnia magna* exposed for 48 h to  $\text{CuSO}_4$  and nCuO 25 nm at  $16 \text{ mg Cu L}^{-1}$ , and (C) of *D. magna* exposed for 21 days to 80 and 40 nm at  $1.86$  and  $1.90 \text{ mg Cu L}^{-1}$ , respectively.  $\text{CuSO}_4$  and 25 nm CuO were transformed into a compound chemically similar to  $\text{Cu}_3(\text{PO}_4)_2$ , while 40 nm and 80 nm CuO remained mainly as CuO



The  $\mu$ -XANES findings agreed with the results of the  $\text{H}_2\text{O}_2$  decomposition tests. Since the 40 and 80 nm nCuO were not transformed, it confirms their lower reactivity, and therefore availability, compared to 25 nm nCuO and  $\text{CuSO}_4$ .

Using XANES, Sávolý et al. (2013) demonstrated that  $\text{CuSO}_4$  was biotransformed in the nematode *Xiphinema vuittenezi* exposed to  $1 \text{ mmol L}^{-1}$   $\text{CuSO}_4$ . They found Cu binding species similar to glycine, glutamate acid and histidine.

Ivask et al. (2017) employed XANES to investigate the chemical environment of Cu in a T-lymphocyte cell line exposed to a nontoxic concentration ( $2 \mu\text{g Cu mL}^{-1}$ ) of 15 nm CuO and CuSO<sub>4</sub>. Different from our results, they reported Cu-cysteine (55–58%) as the major species for both treatments. In addition, minor fractions of Cu-histidine (11–20%), Cu-citrate (4–11%), and CuO (15–22%) were detected. The same Cu species, but in different proportions, were found for the treatments in culture medium without cells. Copper II oxide was found even in the cells and culture medium exposed to CuSO<sub>4</sub>.

## 2.4 Partial Conclusions

The combination of  $\mu$ -XANES and  $\mu$ -XRF showed that Cu is accumulated in the intestine of daphnids as Cu<sub>3</sub>(PO<sub>4</sub>)<sub>2</sub> and Cu oxide, the chemical form depending on the type of nanoparticle. Since 25 nm nCuO and CuSO<sub>4</sub> were more reactive, low concentrations were used in the acute ( $0.031\text{--}0.32 \text{ mg Cu L}^{-1}$ ) and chronic ( $1.248 \times 10^{-3}\text{--}1.6 \times 10^{-4} \text{ mg Cu L}^{-1}$ ) assays and therefore less Cu was found within the *D. magna*. The highest reactivity of 25 nm nCuO and CuSO<sub>4</sub> might have favored their conversion into Cu<sub>3</sub>(PO<sub>4</sub>)<sub>2</sub>.

On the other hand, 40 and 80 nm nCuO presented higher LC<sub>50</sub> and EC<sub>50</sub> values, in turn more Cu was absorbed by the organisms making their detection by  $\mu$ -XRF easier (Figure 12). Since  $\mu$ -XANES showed that then CuO did not undergo biotransformation, the exhibited toxic effects might mainly be related to physical hindrance phenomena. Obstruction of the intestine seems to be at least partially responsible for the biological effects.

An imbalance of dissolved Cu could also have induced toxic effects, with a similar mechanism of action as that of the ionic Cu dosed as CuSO<sub>4</sub>. The Cu ions could be admitted within the cells and the toxicity mechanism would be intracellular. Copper ions may pass through the membrane (cells) and enter into the cytoplasm. This passage can generate reactive oxidative species (ROS) which leads to oxidative stress; both are toxicological mechanisms for cell damage induced by nanoparticles.

The highest toxicity exhibited by the 25 nm nCuO might be related to their core-shell structure that consisted of a Cu metal core covered by oxidized Cu<sub>2</sub>O and CuO layers. The highest toxicity might be related also to their higher solubility that increased Cu availability in the medium. Besides hindering the proper absorption of nutrients, it is likely that the 25nm nCuO might have promoted oxidation or reduction of biomolecules that negatively affected the daphnids.



Altogether, the results show that in addition to particle size, composition and concentration, the structure might influence the toxicological behavior and the environmental impact of CuO nanoparticles.

## References

ADAM, N. et al. The chronic toxicity of CuO nanoparticles and copper salt to *Daphnia magna*. **Journal of Hazardous Materials**, v. 283, p. 416–422, 2015.

ASSOCIAÇÃO BRASILEIRA DE NORMAS TÉCNICAS - ABNT. **NBR12713 de 05/2016**: Ecotoxicologia aquática - Toxicidade aguda - Método de ensaio com *Daphnia* spp (Crustacea, Cladocera). São Paulo, 2016. 33 p.

AMERICAM SOCIETY OF TESTING AND MATERIALS - ASTM. **ASTM E1193-97**: Standard Guide for Conducting *Daphnia magna* Life-Cycle Toxicity Tests. West Conshohocken, PA, 2012.

ATES, M. et al. Accumulation and toxicity of CuO and ZnO nanoparticles through waterborne and dietary exposure of goldfish (*Carassius auratus*). **Environmental Toxicology**, v. 30, n. 1, p. 119–128, 2015.

ATHA, D. H. et al. Copper Oxide Nanoparticle Mediated DNA Damage in Terrestrial Plant Models. **Environmental Science and Technology**, v. 46, n. 3, p. 1819–1827, 2012.

BIANCHINI, A.; WOOD, C. M. Does sulfide or water hardness protect against chronic silver toxicity in *Daphnia magna*? A critical assessment of the acute-to-chronic toxicity ratio for silver. **Ecotoxicology and Environmental Safety**, v. 71, n. 1, p. 32–40, 2008.

BURKHEAD, J. L. et al. Copper homeostasis, **New Phytologist**, v.182, 799–816, 2009.

DE SAMBER, B. et al. A combination of synchrotron and laboratory X-ray techniques for studying tissue-specific trace level metal distributions in *Daphnia magna*. **Journal of Analytical Atomic Spectrometry**, v. 23, n. 6, p. 829-839, 2008.

DE SAMBER, B. et al. Dual detection X-ray fluorescence cryotomography and mapping on the model organism *Daphnia magna*. **Powder Diffraction**, v. 25, n. 2, p. 169–174, 2010.

DHARSANA, U. S. et al. Sulfidation modulates the toxicity of biogenic copper nanoparticles. **RSC Adv.**, v. 5, n. 38, p. 30248–30259, 2015.

DURAN, N. M. et al. X-ray Spectroscopy Uncovering the Effects of Cu Based Nanoparticle Concentration and Structure on *Phaseolus vulgaris* Germination and Seedling Development. **Journal of Agricultural and Food Chemistry**, v. 65, n. 36, p. 7874–7884, 2017.

FISHEL, F. M. Pesticide Toxicity Profile : Neonicotinoid Pesticides. **IFAS Extention**, PI-67, p. 10–12, 2015.

HEINLAAN, M. et al. Toxicity of nanosized and bulk ZnO, CuO and TiO<sub>2</sub> to bacteria *Vibrio fischeri* and crustaceans *Daphnia magna* and *Thamnocephalus platyurus*. **Chemosphere**, v. 71, p. 1308–1316, 2008.

HEINLAAN, M. et al. Changes in the *Daphnia magna* midgut upon ingestion of copper oxide nanoparticles: A transmission electron microscopy study. **Water Research**, v. 45, 179–190, 2011.

HOU, J. et al. Ecotoxicological effects and mechanism of CuO nanoparticles to individual organisms. **Environmental Pollution**, v. 221, p. 209–217, 2017.

INTERNATIONAL ORGANIZATION FOR STANDARDIZATION - ISO. **ISO 6341**: Water quality – determination of the inhibition of the mobility of *Daphnia magna* (Cladocera, Crustacea) – Acute toxicity test. Geneva, Switzerland, 2012. 22 p.

IVASK, A. et al. Complete transformation of ZnO and CuO nanoparticles in culture medium and lymphocyte cells during toxicity testing. **Nanotoxicology**, v. 11, p. 150-156, 2017.

JACKSON, B. P. et al. Synchrotron X-ray 2D and 3D elemental imaging of CdSe/ZnS quantum dot nanoparticles in *Daphnia magna*. **Analytical and Bioanalytical Chemistry**, v. 394, n. 3, p. 911–917, 2009.

JO, H. J. et al. Acute toxicity of Ag and CuO nanoparticle suspensions against *Daphnia magna*: The importance of their dissolved fraction varying with preparation methods. **Journal of Hazardous Materials**, v. 227–228, p. 301–308, 2012.

KASANA, R. C. et al. Biosynthesis and effects of copper nanoparticles on plants. **Environmental Chemistry Letters**, v. 15, p. 233–240, 2017.

KIM, S. et al. Time-Dependent Toxicity Responses in *Daphnia magna* Exposed to CuO and ZnO Nanoparticles. **Bulletin of Environmental Contamination and Toxicology**, v. 98, n. 4, p. 502–507, 2017.

LARNEY, F. J. et al. The role of composting in recycling manure nutrients. **Canadian Journal of Soil Science**, v. 86, n. 4, p. 597–611, 2006.

LIU, J. et al. Tailoring CuO nanostructures for enhanced photocatalytic property. **Journal of Colloid and Interface Science**, v. 384, n. 1, p. 1–9, 2012.

LIU, J. et al. Effects of ZnO, CuO, Au, and TiO<sub>2</sub> nanoparticles on *Daphnia magna* and early life stages of zebrafish *danio rerio*. **Environment Protection Engineering**, v. 40, p. 139-140, 2014.

LIU, P. C. et al. Dissolution of Cu nanoparticles and antibacterial behaviors of TaN-Cu nanocomposite thin films. **Thin Solid Films**, v. 517, n. 17, p. 4956–4960, 2009.

LOVERN, S. B.; OWEN, H. A.; KLAPER, R. Electron microscopy of gold nanoparticle intake in the gut of *Daphnia magna*. **Nanotoxicology**, v. 2, n. 1, p. 43–48, 2008.

LU, G. et al. Toxicity of Cu and Cr Nanoparticles to *Daphnia magna*. **Water, Air, and Soil Pollution**, v. 228, art. 18, 2017.

MARSCHNER, H. **Mineral nutrition of higher plants**. San Diego: Academic Press, 1995. 889 p.

MCMAHON, J. W. Some physical factors influencing the feeding behavior of *Daphnia Magna* Straus. **Canadian Journal of Zoology**, v. 43, n. 4, p. 603–611, 1965.

MENDONÇA, E. et al. Effects of diamond nanoparticle exposure on the internal structure and reproduction of *Daphnia magna*. **Journal of Hazardous Materials**, v. 186, n. 1, p. 265–271, 2011.

MILLER, G.; SENJEN, R. **Out of the laboratory and on to our plates: Nanotechnology in food & agriculture**. 2. ed. Collingwood, VIC, 2008. 68 p.

MOUNT, D. R. et al. Statistical models to predict the toxicity of major ions to *Ceriodaphnia dubia*, *Daphnia magna* and *Pimephales promelas* (fathead minnows). **Environmental Toxicology and Chemistry**, v. 16, n. 10, p. 2009–2019, 1997.

OCHOA, L. et al. Modulation of CuO nanoparticles toxicity to green pea (*Pisum sativum* Fabaceae) by the phytohormone indole-3-acetic acid. **Science of the Total Environment**, v. 598, p. 513–524, 2017.

ORGANISATION FOR ECONOMIC CO-OPERATION AND DEVELOPMENT - OECD. **Guidelines for Testing of Chemicals - OECD 211: *Daphnia magna* Reproduction Test**. Paris, 1998. 21 p.

PINHEIRO, T. et al. Nuclear microscopy as a tool in TiO<sub>2</sub> nanoparticles bioaccumulation studies in aquatic species. **Nuclear Instruments and Methods in Physics Research. Section B: Beam Interactions with Materials and Atoms**, v. 306, p. 117-120, 2013.

RAHMAN, M. M. et al. A comprehensive review of glucose biosensors based on nanostructured metal-oxides. **Sensors**, v. 10, n. 5, p. 4855–4886, 2010.

RAVEL, B.; NEWVILLE, M. ATHENA, ARTEMIS, HEPHAESTUS: Data analysis for X-ray absorption spectroscopy using IFEFFIT. **Journal of Synchrotron Radiation**, v.12, p. 537–541, 2005.

RAWAT, S. et al. Impacts of copper oxide nanoparticles on bell pepper (*Capsicum annum* L.) plants: a full life cycle study. **Environmental Science: Nano**, v. 5, p. 83-95, 2018.

ROSSETTO, A. L. de O. F. et al. Comparative evaluation of acute and chronic toxicities of CuO nanoparticles and bulk using *Daphnia magna* and *Vibrio fischeri*. **Science of the Total Environment**, v. 490, p. 807–814, 2014.

SAIF, S. et al. Plant Mediated Green Synthesis of CuO Nanoparticles: Comparison of Toxicity of Engineered and Plant Mediated CuO Nanoparticles towards *Daphnia magna*. **Nanomaterials**, v. 6, n. 11, p. 205, 2016.

SAKUMA, M. Probit analysis of preference data. **Applied Entomology and Zoology**, v. 33, n. 3, p. 339–347, 1998.

SARRET, G. et al. Zinc distribution and speciation in *Arabidopsis halleri* × *Arabidopsis lyrata* progenies presenting various zinc accumulation capacities. **New Phytologist**, v. 184, n. 3, p. 581–595, 2009.

SÁVOLY, Z. et al. Investigation of distribution and oxidation state of copper in soil-inhabiting nematodes by means of synchrotron radiation. **X-Ray Spectrometry**, v. 42, n. 4, p. 321–329, 2013.

SCHULTE, E. E.; KELLING, K. A. **Soil and Applied Copper**. SR 07/99. Madison: Wisconsin Cooperative Extension, 1999. 2 p. (Publication A2527: Understanding Plant Nutrients).

SEO, J. et al. Effects of physiochemical properties of test media on nanoparticle toxicity to *daphnia magna* straus. **Bulletin of Environmental Contamination and Toxicology**, v. 93, n. 3, p. 257–262, 2014.

SHAFF, J. E. et al. GEOCHEM-EZ: A chemical speciation program with greater power and flexibility. **Plant and Soil**, v. 330, n. 1, p. 207–214, 2010.

SIMKISS, K.; TAYLOR, M. G. Convergence of cellular systems of metal detoxification. **Marine Environmental Research**, v. 28, n. 1-4, p. 211–214, 1989.

SONG, L. et al. Assessing toxicity of copper nanoparticles across five cladoceran species. **Environmental Toxicology and Chemistry**, v. 34, n. 8, p. 1863–1869, 2015.

STRUEWING, K. A. et al. Part 2: Sensitivity comparisons of the mayfly *Centroptilum triangulifer* to *Ceriodaphnia dubia* and *Daphnia magna* using standard reference toxicants; NaCl, KCl and CuSO<sub>4</sub>. **Chemosphere**, v. 139, p. 597–603, 2015.

THE PROJECT ON EMERGING NANOTECHNOLOGIES. Available at: <https://nanotechproject.tech>. Acced date: 2 May. 2019.

THIT, A. et al. Acute toxicity of copper oxide nanoparticles to *Daphnia magna* under different test conditions. **Toxicological & Environmental Chemistry**, v. 2248, p. 1–15, 2016.

US ENVIRONMENTAL PROTECTION AGENCY - USEPA. **Methods for Measuring the Acute Toxicity of Effluents and Receiving Waters to Freshwater and Marine Organisms**. 5. ed. Washington, DC, 2002. 275 p. (EPA-821-R-02-012).

US ENVIRONMENTAL PROTECTION AGENCY - USEPA. Office Pesticides Program - About Pesticides | Pesticides. Washington, DC, 2014. (EPA, 64405-1).

WANG, H. et al. Chronic effects of six micro/nano-Cu<sub>2</sub>O crystals with different structures and shapes on *Daphnia magna*. **Environmental Pollution**, v. 203, p. 60-68, 2015.

WANG, S. B. et al. A CuO nanowire infrared photodetector. **Sensors and Actuators, A: Physical**, v. 171, n. 2, p. 207–211, 2011.

WELCH, R. M.; SHUMAN, L. Critical Reviews in Plant Sciences Micronutrient Nutrition of Plants Micronutrient Nutrition of Plants. **Critical Reviews in Plant Sciences**, v. 14, n. 1, p. 49–8249, 1995.

WHITE, P. J.; BROWN, P. H. Plant nutrition for sustainable development and global health. **Annals of Botany**, v. 105, n. 7, p. 1073–1080, 2010.

WOODROW WILSON INTERNATIONAL CENTER FOR SCHOLARS. **The Project on Emerging Nanotechnologies**. Washington, DC, 2005. Available at: Accessed in 02<sup>th</sup> Apr. 2021. <https://www.wilsoncenter.org/publication-series/project-emerging-nanotechnologies>

WU, F. et al. Uptake and toxicity of CuO nanoparticles to *Daphnia magna* varies between indirect dietary and direct waterborne exposures. **Aquatic Toxicology**, v. 190, p. 78–86, 2017.

YANG, H. et al. Comparative study of cytotoxicity, oxidative stress and genotoxicity induced by four typical nanomaterials: The role of particle size, shape and composition. **Journal of Applied Toxicology**, v. 29, n. 1, p. 69–78, 2009.

YANG, Y. et al. Defense mechanisms of *Pseudomonas aeruginosa* PAO1 against quantum dots and their released heavy metals. **ACS Nano**, v. 6, n. 7, p. 6091–6098, 2012.



### 3 UPTAKE, TOXICITY AND PERSISTENCE OF ZnO NANOPARTICLES IN *Daphnia magna*

#### Abstract

Size is a key factor controlling the rate of dissolution of nanoparticles, such property can be explored for producing controlled release fertilizers. Hence, one can expect the increasing discharge of nanoparticles closer to water streams in the near future. In this study, we employed the model fresh water organism *Daphnia magna* to investigate the uptake, acute toxicity and depuration of ZnO nanoparticles. The lethal concentration that kills 50% of population (LC<sub>50</sub>) depended on particle size and the presence of surfactant; for positive control ZnSO<sub>4</sub> (2.15 mg L<sup>-1</sup>), 20 nm ZnO (1.68 mg L<sup>-1</sup>), and 40 nm ZnO (1.71 mg L<sup>-1</sup>) were statistically the same, while the addition of surfactant increased the LC<sub>50</sub> of 40 nm and 60 nm to 2.93 and 3.24 mg L<sup>-1</sup>, respectively. The 300 nm ZnO was the least toxic nanoparticle presenting LC<sub>50</sub> of 6.35 mg L<sup>-1</sup>. X-ray fluorescence chemical imaging revealed that Zn accumulated along the digestive system regardless the particle size. Finally, contrary to what have been reported by several papers, the present study did not detect any depuration of ZnO nanoparticles during 24 hours. Thus, the ability of organisms to expel ingested nanomaterials might be dependent on specific physical-chemical features of such nanomaterials.

**Keywords:** *Daphnia magna*; toxicity; ZnO; nanoparticles;  $\mu$ -XRF; depuration

#### 3.1 Introduction

Concentrate suspensions of zinc oxide microparticles are commonly used as fertilizers, in this context, zinc oxide nanoparticles (nZnO) emerges as a possible input for crops (MA; WILLIAMS; DIAMOND, 2013). It was recently shown that the size of nZnO controls the rate of Zn<sup>2+</sup> dissolution, and hence the velocity of Zn<sup>2+</sup> uptake by plants (DA CRUZ et al., 2017; SAVASSA et al., 2018). Such property can back up the development of smarter fertilizers in which the rate of nutrient release matches the plant uptake curve, hence reducing the losses through leaching or runoff. Thus, the end use of nZnO in agricultural areas, therefore close to water streams, may increase in the near future.

In Europe, nZnO has been found in natural surface water (10 ng nZnO L<sup>-1</sup>) and in treated waste water (430 ng nZnO L<sup>-1</sup>) (GOTTSCHALK et al., 2009). This is a matter of concern since reports indicate that nZnO can affect aquatic organisms disturbing them at the level of the

hepatic, renal, intentional, pulmonary, cardiovascular, immune, and nervous systems (TANGAA et al., 2016; YANG et al., 2017).

Water fleas are small Cladocera found in stagnant waters in various parts of the world (BLAISE; FÉRARD, 2005). They are filtering organisms having thoracic legs with bristles that act as sieves, retaining algae, bacteria and particles found in water. Particles and food are transferred to the mouth, ground by the jaws and directed to the digestive tract (ZAGATO; BERTOLETTI, 2006). Species of the genus *Daphnia* are an important source of food for fish and ideal for use in toxicity tests, since they are sensitive to pollutants and easily grown in the laboratory. One of the most employed species in toxicological studies is *Daphnia magna*.

The toxicity of zinc on *D. magna* has been previously described in the literature. Effects, zinc can accumulate intracellularly and internalize in the gastrointestinal tract, which is the main entry of nanoparticles in *D. magna*. This accumulation can cause the over absorption of zinc by the intestine; alteration of the permeability of the mitochondria membrane and consequently disturb the electron transport chain that causes the production of reactive oxygen species (ADAM et al., 2014). The consequences of this process are histological and structural changes, such as swelling in mitochondria, multilaminar bodies and autophagy vacuums (ADAM et al., 2015; BACCHETTA et al., 2016; 2017).

In this study, we evaluated the acute toxicity of several nZnO, with and without surfactants, on *Daphnia magna*. We also employed a non-destructive method based on microprobe X-ray fluorescence spectrometry to determine the spatial distribution of zinc inside of the organisms exposed to nZnO through acute assay; finally, employing the imaging method, we evaluated whether the accumulated zinc was depurated as a function of time.

## **3.2 Material and methods**

### **3.2.1. Nanoparticles characterization and dispersion analysis**

Five commercial nZnO were employed in this study - three nZnO containing surfactant with sizes of 40, 60 (US Nanophase Technologies Corporation) and 300 nm (Agrichem), two nZnO without surfactant with sizes of 20 and 40 nm (M K Impex Corp.).

The crystal structure (Figure 1) was determined by Cu-K $\alpha$  radiation X-ray diffraction (XRD) using a PM 1877 diffractometer (Philips, Netherlands). The shape and size of the nZnO (Figure 2) were determined by scanning electron microscopy (SEM) (Inspect F50 microscope, FEI Company, USA).



Figure 1. XRD patterns for (A) 40 and 20 nm and (B) 60 and 40 nm with surfactant of nZnO

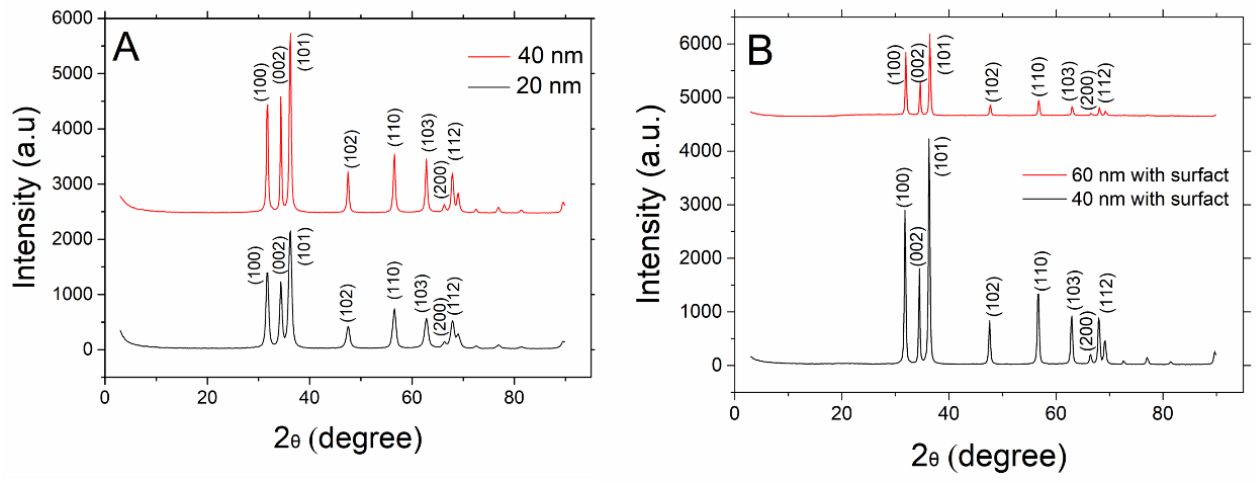
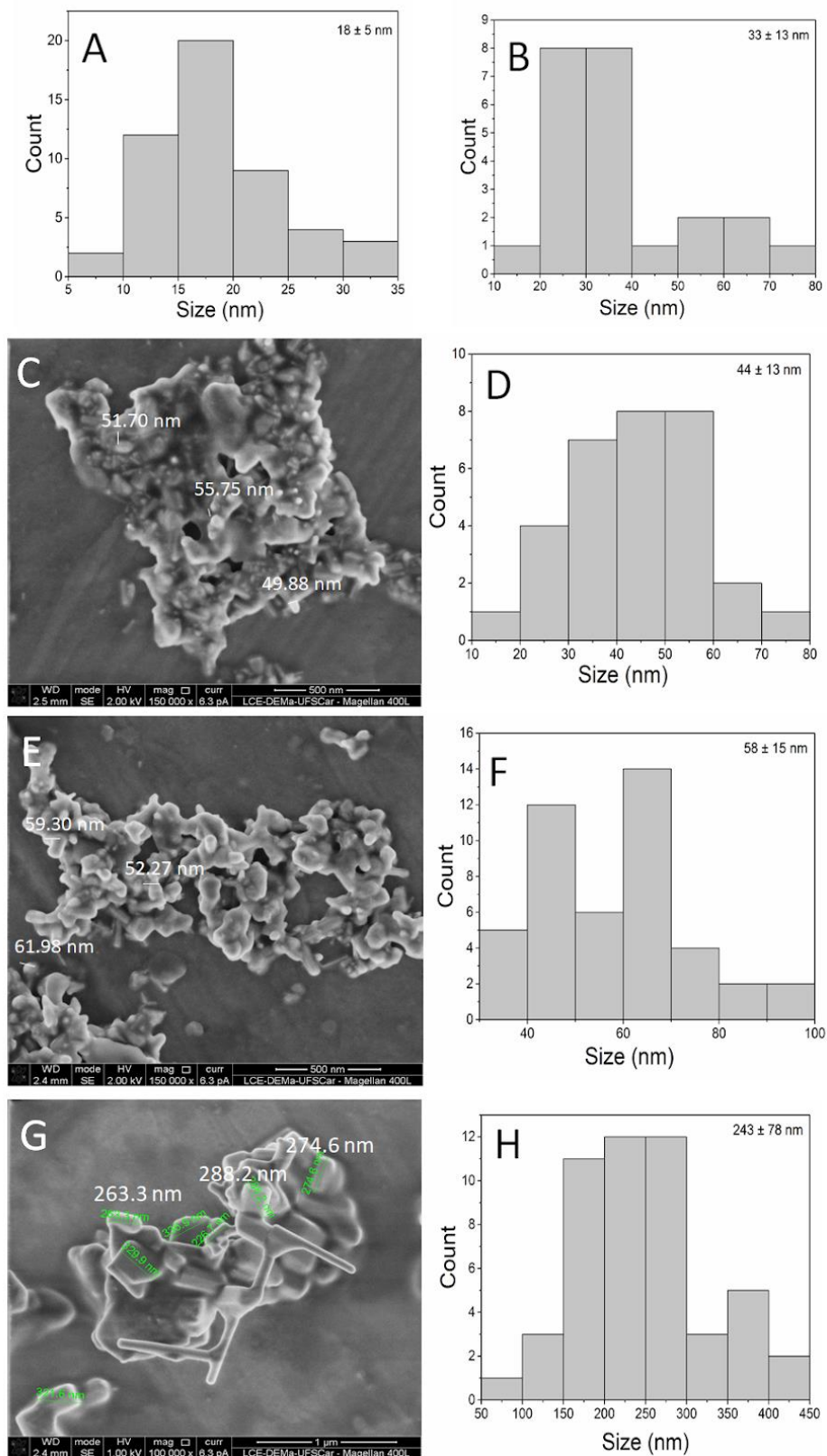


Figure 2. Characterization of nZnO (A, B, D, F, H) histograms of nCuO 20 nm, 40 nm, 40 nm with surfact, 60 nm with surfact and 300 nm with surfact, respectively. (C) 40 nm with surfact (E) 60 nm with surfact (G) 300 nm with surfact by scanning electron microscopy, (SEM)



For zeta potential and dynamic light scattering (DLS) analysis, each nZnO was dispersed in deionized water and culture medium of *D. magna* at 100 mg Zn L<sup>-1</sup>. The nanoparticles were dispersed using a Sonic dismembrator (Model 705, Fischer Scientific, USA) at 95 W, amplitude of 50 J for 2 cycles of 3 min each and interval of 30 s between each cycle. Zeta potential and DLS (Table 1) were determined using a Zetasizer Nano (Malvern Instruments, U.K.) in triplicate.

Table 1. Hydrodynamic Diameter and Zeta potential of differently nZnO particles dispersed in deionized water and culture medium of *Daphnia magna* at 100 mg ZnO L<sup>-1</sup>

nZnO	Hydrodynamic diameter - nm (DLS)		Zeta Potential (mV)	
	d.w.	c.m.	d.w.	c.m.
20 nm	3052 ± 744	2505 ± 118	-6 ± 0.9	-5 ± 0.3
40 nm	2883 ± 1040	2220 ± 79	-15 ± 0.6	-7 ± 0.2
300 nm + surfact	230 ± 2	995 ± 51	-25 ± 0.3	-18 ± 07
60 nm + surfact	216 ± 3	221 ± 2	-21 ± 0.6	-9.01
40 nm + surfact	165 ± 2	178 ± 2	-19 ± 0.3	-8 ± 0.4

d.w. = deionized water;

c.m. = culture medium of *D. magna*;

### 3.2.2. Experimental conditions

#### 3.2.2.1. Stock culture of *Daphnia magna*

*Daphnia magna* (neonates) were grown in culture medium (Table 2) in 2 L beaker, incubated at 22 ± 1°C, 12 h photoperiod and pH 7.0-7.5, according to Associação Brasileira de Normas Técnicas (ABNT NBR 1213, 2016). Culture medium and feed were replaced three times a week with the separation of neonates when the daphnids became adult. The feed consisted of a suspension of *Raphidocelis subcapitata* (density 10<sup>6</sup> cells mL<sup>-1</sup>) and trout feed solution (5 g L<sup>-1</sup>).

Table 2. Composition of culture medium of *D. magna*

Stock solution	Reagents	g L <sup>-1</sup>
Solution 1	CaCl <sub>2</sub> . 2H <sub>2</sub> O	73.52
Solution 2	MagSO <sub>4</sub> . 7H <sub>2</sub> O	123.3
Solution 3	KCl	5.8
Solution 4	NaHCO <sub>3</sub>	64.8
Solution 5	MnCl <sub>2</sub> . 4H <sub>2</sub> O	7.21
	LiCl	6.12
	RbCl	1.42
	SrCl <sub>2</sub> . 6H <sub>2</sub> O	3.04
	CuCl <sub>2</sub> . 2H <sub>2</sub> O	0.335
	ZnCl <sub>2</sub>	0.260
	CoCl <sub>2</sub> . 6H <sub>2</sub> O	0.2
Solution 6	H <sub>3</sub> BO <sub>3</sub>	5.719
	NaBr	0.032
	Na <sub>2</sub> MoO <sub>4</sub> . 2H <sub>2</sub> O	0.126
	KI	0.0065
	Na <sub>2</sub> SeO <sub>3</sub>	0.00438
	NH <sub>4</sub> VO <sub>3</sub>	0.00115
	NaNO <sub>3</sub>	0.548
Solution 7	Na <sub>2</sub> SiO <sub>3</sub>	0.021465
Solution 8	FeSO <sub>4</sub> . 7H <sub>2</sub> O	0.1991
	Na <sub>2</sub> EDTA. 2H <sub>2</sub> O	0.500
Solution 9	KH <sub>2</sub> PO <sub>4</sub> . 4H <sub>2</sub> O	0.286
	K <sub>2</sub> HPO <sub>4</sub>	0.368
Solution 10	thiamine hydrochloride	0.750
	cyanocobalamin	0.01
	biotin	0.075

### 3.2.3. Exposure of daphnids to nZnO dispersions

#### 3.2.3.1. Sensitivity assays

Neonates were evaluated for their sensitivity in assays with NaCl as the reference substance in culture medium (ABNT 12713, 2016). Five neonates ( $\leq 24$  h) per replicate were exposed for 48 h to concentrations from one to 9 g NaCl L<sup>-1</sup> in polyethylene flasks containing 30 mL of tested solution. The assays were carried out in an incubator chamber at  $22 \pm 1^\circ\text{C}$ , 12 h photoperiod (ABNT 12713, 2016).

#### 3.2.3.2. Acute assays

Stock dispersions of 50 mg Zn L<sup>-1</sup> of each nZnO and ZnSO<sub>4</sub>. 7H<sub>2</sub>O (Merck) were prepared for the acute assays. ZnSO<sub>4</sub> was used as the positive control and culture medium as negative control. The nZnO dispersions were sonicated as described above.

Five neonates ( $\leq 24$  h) per replicate were exposed to nZnO and ZnSO<sub>4</sub> at concentrations from 0.5 to 15 mg Zn L<sup>-1</sup> (Table 3) for 48 h, under the same conditions as the sensitivity assays (ABNT 12713, 2016).

Table 3. Concentration used in the sensibility and acute assays

Treatment	mg Zn L <sup>-1</sup>						
	0	1000	3000	5000	7000	9000	
NaCl	0	1000	3000	5000	7000	9000	
nZnO 40 nm	0	0.5	1	1.5	2	2.5	
nZnO 20 nm	0	0.5	1	1.5	2	2.5	3
nZnO 40 nm + surfact	0	1	3	5	10	12	
nZnO 60 nm + surfact	0	1	3	5	10	12	
nZnO 300 nm + surfact	0	2.5	5	7.5	10	15	
ZnSO <sub>4</sub>	0	2	2.74	4.11	5.78	7.15	8.5

During the assays, no precipitation of nZnO was observed. After 48 h, immobile or dead individuals were counted and the Pribrobit program was used to estimate the concentration that killed or immobilized 50% of the organisms (lethal concentration - LC<sub>50</sub>) (SAKUMA, 1998).

### 3.2.3.3. Depuration assays

Neonates were exposed to 1 mg Zn L<sup>-1</sup> of 40 nm nZnO in three replicates. The exposure conditions were the same as described above. After 48 h, the neonates were transferred to culture medium containing neither nZnO nor food. Then, they were analyzed by microprobe X-ray fluorescence after 2 h, 6 h, 12 h and 24 h of depuration. Table 4 details the number of transfers of daphnids to the clean culture medium during the depuration assays.

Table 4. Number of transfers to clean daphnids culture medium in the depuration assays with *D. magna*

Time of depuration	Transfers of the culture medium (n°)
0 h (5 min)	1
2 h	2
6 h	7
12 h	13
24 h	14

### 3.2.4. X-ray fluorescence microanalysis (μ-XRF)

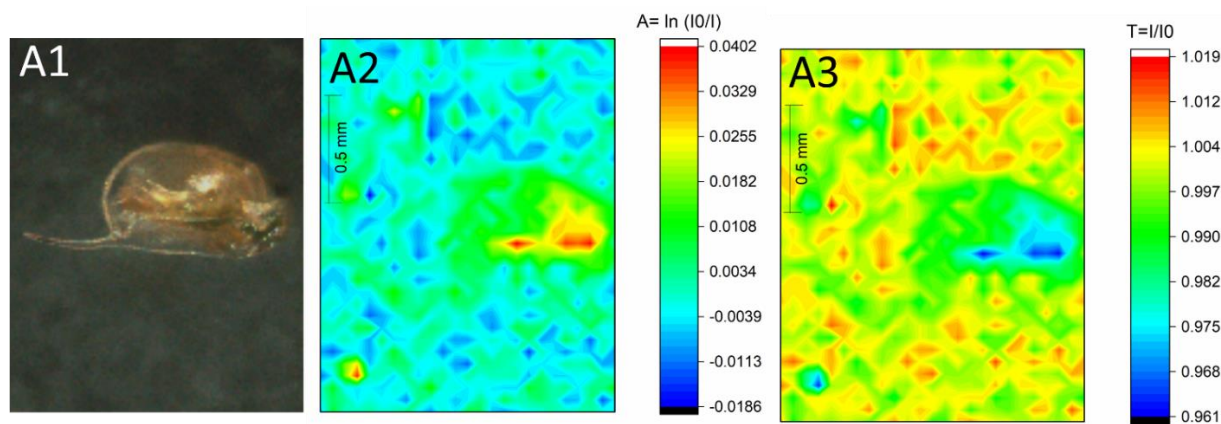
#### 3.2.4.1. Zn quantitative maps of daphnids exposed to acute assays

μ-XRF was used to reveal the spatial distribution of zinc absorbed by the daphnids exposed to LC<sub>100</sub> during acute assays. After the exposure, daphnids were collected, washed three times with phosphate buffer (PBS) (Na<sub>2</sub>HPO<sub>4</sub>, NaH<sub>2</sub>PO<sub>4</sub>.H<sub>2</sub>O, pH 7-7.5), fixed in paraformaldehyde solution 4% (PFA) overnight, washed again three times with PBS and kept under PBS in refrigerator at 4°C until analysis by μ-XRF. In total, 18 individuals were mapped.

Using a pipette the daphnids were transferred from the PBS and put to the top of a Kapton™ (polyamide) thin film on an XRF cuvette. The measurements were performed using a benchtop  $\mu$ -XRF system (EDAX, Orbis PC, USA) which X-rays were generated by an Rh anode. The 30  $\mu\text{m}$  X-ray beam (for Mo-K $\alpha$ ) was focused on the samples by a polycapillary optics, and the detection was carried out by a 30 mm<sup>2</sup> silicon drift detector operating at 140 eV resolution for Mn-K $\alpha$ . The maps were constructed employing a matrix of 64 x 50 points summing up to 3,200 XRF spectra for each image, 40 kV, 100  $\mu\text{A}$  and 1.0 s dwell time per point. The dead time of each map was lower than 3%.

The Zn instrumental sensitivity was calculated using a ZnTe thin film Micromatter™ standard containing 16.16  $\mu\text{g Zn cm}^{-2}$ . The test for infinitely thin film conditions was carried out measuring the attenuation of the Zn- K $\alpha$  by the daphnids. Since the neonates were infinitely thin for Zn K $\alpha$  energy, Zn was quantified by dividing the number of XRF Zn K $\alpha$  counts by the elemental sensitivity (Figure 3).

Figure 3. Maps of transmittance and absorbance of Zn K $\alpha$  radiation by *Daphnia magna*. (A1) *D. magna* adult, (A2) absorbance of adult, (A3) transmittance of adult



#### 3.2.4.2. Zn quantitative maps of daphnids from depuration assays

The maps revealing the distribution of Zn inside the daphnids during the depuration assays were obtained similarly to described above. The matrix employed was 32 x 25 points summing up to 800 XRF spectra for each image. X-ray were generated at 40 kV and 900  $\mu\text{A}$ , the dwell time was 3 s per point. The spectra were recorded using a 25  $\mu\text{m}$  Ni primary filter. The dead time of each maps was less than 3%. In the total, 60 individuals were mapped.

In order to obtain quantitative information from the chemical images, the average median zinc concentration and the total zinc content for each image were determined. Only

pixels whose values were above the limit of quantification of zinc were considered. Since each measurement was carried out using three biological replicates (four daphnids per replicate), the median zinc concentration for each time measurement were arithmetically averaged and divided by the average median concentration found at the beginning of the depuration (time = 0 h).

Additionally, the counts of pixels above the limit of quantification in each imaged were summed, giving the total number of counts of zinc in the image yielding a quantity named zinc content.

### **3.3 Results and discussion**

#### **3.3.1. Nanoparticles characterization and dispersion analysis**

Figure 1 shows XRD patterns, which confirm ZnO wurtzite crystalline phase. The SEM images (Figure 2) show that the nanoparticles actual size is close to that indicated by the manufacturer. SEM images of 20 nm and 40 nm nZnO are shown in Da Cruz et al. (2017).

Except for the 300 nm ZnO, DLS shows that the nZnO aggregated under water and culture medium (Table 1). Such aggregates were higher for nanoparticles dispersed without the aid of surfactants, for example 40 nm nZnO surfactant in culture medium presented hydrodynamic diameter of  $178 \pm 2$  nm while the one without surfactant was  $2220 \pm 79$  nm. In culture medium, all nanoparticles were negatively charged.

#### **3.3.2. Experimental conditions**

#### **3.3.3. Acute assays**

Figure 4 presents the dose response curves of acute assays to the nZnO. The  $LC_{50}$  to the NaCl is  $4,370 \text{ mg L}^{-1}$ . The sensitivity assays indicated that organisms are healthy and suitable for the further mortality tests shown herein. The mortality assays were performed using three replicates (summing up 15 organisms per treatment). Figure 5 shows statistical differences assessed by Tukey test among the  $LC_{50}$ s. The  $LC_{50}$ s of nZnO and ZnSO<sub>4</sub> ranged from  $1.68 \pm 0.22$  to  $6.35 \pm 0.80 \text{ mg Zn L}^{-1}$ . The order of toxicity of nZnO and ZnSO<sub>4</sub> is  $20 \text{ nm} = 40 \text{ nm} = \text{ZnSO}_4 > 40 \text{ nm} + \text{surfact} = 60 \text{ nm} + \text{surfact} > 300 \text{ nm} + \text{surfact}$ . Table 5 details the statistical parameters of model plateau linear assumed by Probit software and  $LC_{50}$  e  $LC_{10}$  of nZnO and ZnSO<sub>4</sub>.

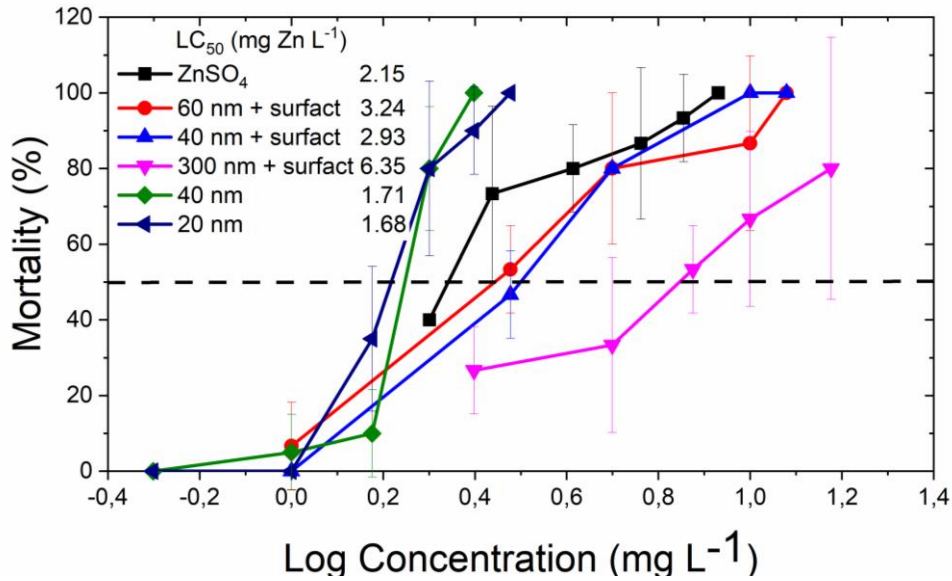
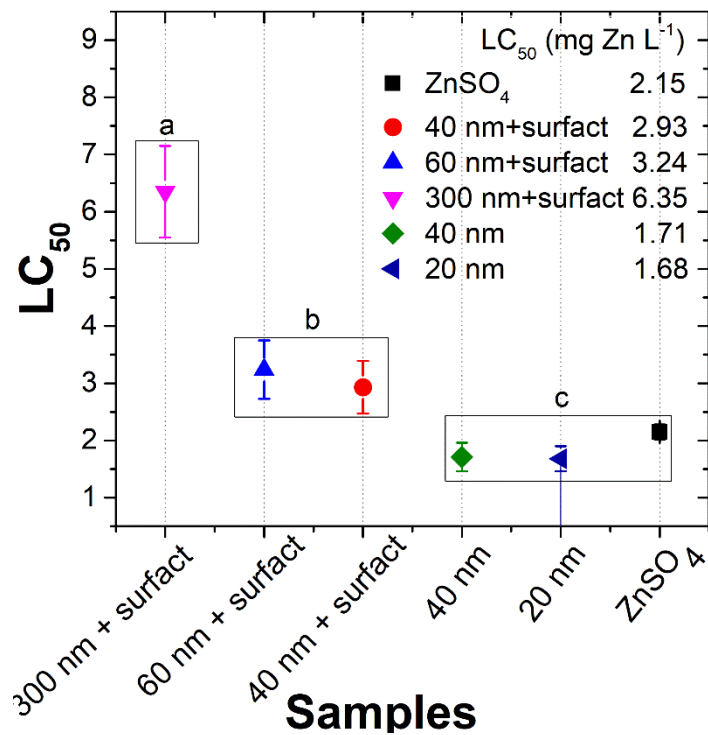
Figure 4. Dose-response curves for the acute toxicity of nZnO and ZnSO<sub>4</sub> to *Daphnia magna*Figure 5. Effects of nZnO and ZnSO<sub>4</sub> on survival of *Daphnia magna* and lethal concentration that kills 50% of organisms (LC<sub>50</sub>). Values followed with the same indices do not differ significantly according to the Tukey test ( $p < 0.05$ ). 40 and 20 nm nZnO without surfactant were as toxic as ZnSO<sub>4(aq)</sub>



Table 5. Plateau linear model ( $y = a + bx$ ) of nZnO and ZnSO<sub>4</sub>

Treatment	a	b	LC <sub>50</sub>	LC <sub>10</sub>
nZnO 20 nm	-2.14 ± 0.45	9.45 ± 1.63	1.68 ± 0.22	1.12 ± 0.01
nZnO 40 nm	-2.62 ± 0.96	11.17 ± 3.65	1.71 ± 0.23	1.31 ± 0.12
nZnO 40 nm + surfact	-1.37 ± 0.38	2.94 ± 0.57	2.93 ± 0.46	1.07 ± 0.032
nZnO 60 nm + surfact	-2.70 ± 0.85	5.26 ± 1.42	3.24 ± 0.51	1.85 ± 0.26
nZnO 300 nm	-1.57 ± 0.51	1.96 ± 0.59	6.35 ± 0.80	1.41 ± 0.15
ZnSO <sub>4</sub>	-1.05 ± 0.46	3.15 ± 0.80	2.15 ± 0.33	0.84 ± 0.07

Lower LC<sub>50</sub>s were reported for *D. magna*, Xiao et al. (2015), Lopes et al. (2014), and Ma et al. (2014) studied the exposure of ZnO nanoparticles of 43; 30, 80-100 nm; 30-50 nm, and <100 nm, respectively, and they found LC<sub>50</sub> of 0.99 mg Zn L<sup>-1</sup>; 1.02 mg Zn L<sup>-1</sup>, 1.10 mg Zn L<sup>-1</sup>; 0.54 mg Zn L<sup>-1</sup> and 1.53 mg Zn L<sup>-1</sup>, respectively. In agreement with the present study, these reports showed that toxicity increased as the particle size decreased. Since the nanoparticles were not more toxic than the positive control, this relationship might be related to the dissolution rate (BACCHETTA et al., 2016).

However, other studies suggest that acute nanoparticle toxicity is not only dependent on particle size alone, suggesting that this issue is far from being fully understood and requires further investigation. For example, skjolding, Winther-Nielsen and Baun, (2014); Adam et al. (2014), and Heinlaan et al. (2008) found LC<sub>50</sub>s of 1.90 mg Zn L<sup>-1</sup>; 1.12 mg Zn L<sup>-1</sup> and 2.25 mg Zn L<sup>-1</sup> and 3.2 mg Zn L<sup>-1</sup>, respectively, for nZnO of ≤ 5 μm; 40 and 30 nm and 50-70 nm, respectively.

Anyway, ZnSO<sub>4</sub> positive control shows that dissolved zinc contributes to toxicity. It was associated with morphological changes at the cellular level of daphnids (BACCHETTA et al., 2016). LC<sub>50</sub> values for dissolved zinc, in the same order of magnitude of those found in the present study, were presented by Bacchetta et al. (2016), Heinlaan et al. (2008) with ZnSO<sub>4</sub> and Adam et al. (2014) with ZnCl<sub>2</sub> which find LC<sub>50</sub> 1.35 mg Zn L<sup>-1</sup>; 6.1 mg Zn L<sup>-1</sup> and 2.30 mg Zn L<sup>-1</sup>, respectively.

In comparison with other compounds used in industry, the LC<sub>50</sub> of the present study showed toxicity less than or equal to compounds of different chemical classes (4-nonylphenol 0.21± 0.02; pentachlorophenol 0.68 ± 0.13; carbaryl 1.9 ± 0.3) and some pesticides (dichloroaniline 0.2 ± 0.17; pentachlorophenol 0.39 ± 0.37; endosulfan 0.62 ± 0.54; lindane 1.64 ± 1.15) tested by Milam et al. (2005) and Ferrando, Andreu-Moiner and Fernández-Casalderry (1992), respectively. However, the Sánchez-Bayo; Goka (2006) study with imidacloprid - agrochemicals used in agriculture - showed an LC<sub>50</sub> of 65-133 mg / L, which indicates less toxicity to daphnids.

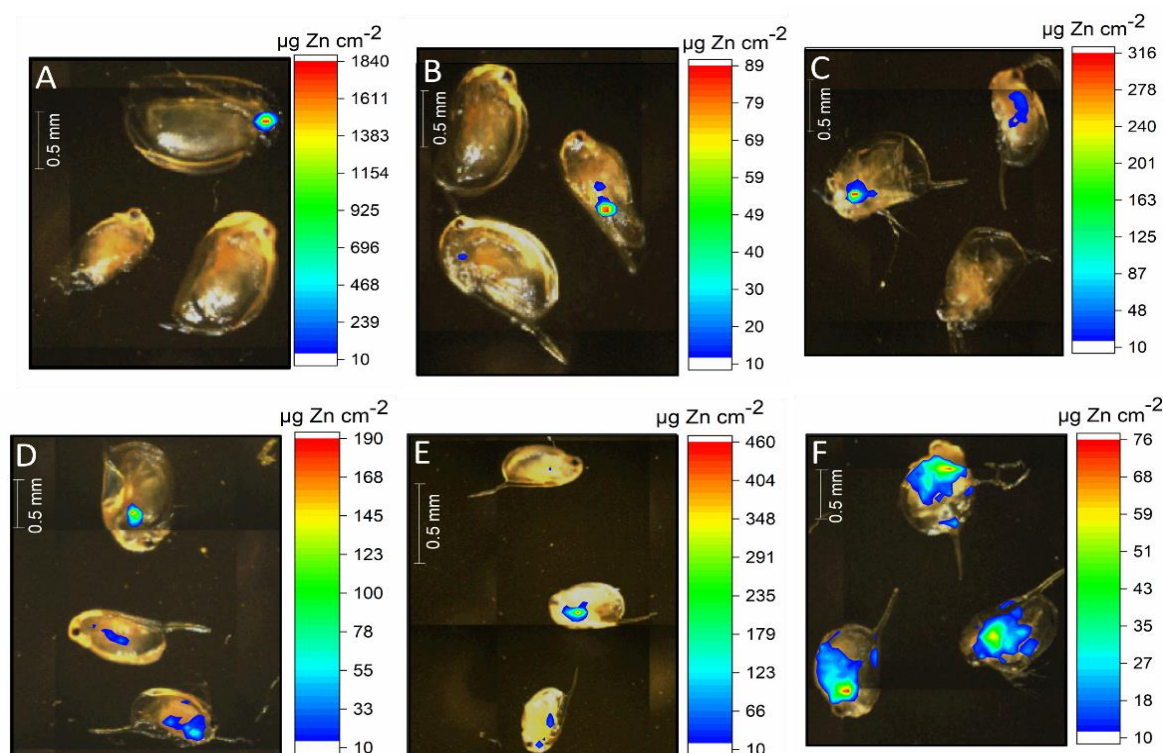
Regarding nanoparticles containing surfactants, Oleszczuk, Josko and Skwarek (2015) estimated the effect of surfactants (CTAB, TX100 and SDBS) on the toxicity of ZnO, TiO<sub>2</sub> and Ni nanoparticles in *D. magna* in acute assays. Like the present study, the researchers also observed less toxicity of nanoparticles with surfactants. The study concluded that this reduction is probably related to the formation of aggregates that inhibited their availability to organisms. Our study showed aggregation in all of the nanoparticles tested; however, the most aggregated were those with the absence of surfactant, which indicates that there may be other mechanisms related to toxicity.

### **3.3.4. X-ray fluorescence microanalysis ( $\mu$ -XRF)**

#### **3.3.4.1. Zn quantitative maps of daphnids exposed to acute assays**

The quantitative maps (Figure 6) show that Zn from ZnSO<sub>4</sub> was broadly distributed inside the body of organisms, while Zn from nanoparticulate sources were concentrated in certain regions. For 20 nm, 40 nm and 40 nm + surfact treatments, Zn was more concentrated near the mouth. Conversely, the 60 nm, 300 nm ZnO and ZnSO<sub>4</sub> treatments presented more Zn in the region near the anus. The Zn concentration found in neonates after exposure was proportional to exposure concentration (LC<sub>100</sub>), except for the 20 nm ZnO treatment in which the maximum concentration within the neonates reached 1840  $\mu\text{g cm}^{-2}$ .

Figure 6. Quantitative spatial distribution of Zn inside of *Daphnia magna* neonates exposed for 48 h to nZnO and ZnSO<sub>4</sub> at lethal concentrations that kills 100% of organisms (LC<sub>100</sub>). (A) neonate exposed to 20 nm nZnO at 2.54 mg L<sup>-1</sup>, (B) neonate exposed to 40 nm nZnO at 2.46 mg L<sup>-1</sup> (C) neonate exposed to 40 nm + surfact nZnO at 12 mg L<sup>-1</sup>, (D) neonate to 60 nm + surfact nZnO 10 mg L<sup>-1</sup>, (E) neonate exposed to 300 nm + surfact at 15 mg L<sup>-1</sup>, (F) neonate exposed to ZnSO<sub>4</sub> at 8.52 mg L<sup>-1</sup>



Previous studies investigated the distribution of zinc in *D. magna* exposed to higher concentration than those reported in the present study. The organisms were analyzed by  $\mu$ -XRF with/or association with other techniques. De Samber et al. (2008) studied the distribution of zinc in adult *D. magna* exposed to 120 mg Zn L<sup>-1</sup> (from ZnCl<sub>2</sub>) for 7 days and chemically fixed with acetone. Differently from our work, zinc was distributed among the appendages (12  $\mu\text{g cm}^{-2}$ ), eggs (15  $\mu\text{g cm}^{-2}$ ) and intestine (30  $\mu\text{g cm}^{-2}$ ).

Exposed of *D. magna* to quantum dots corroborate the spatial distribution pattern of shown in Figure 6. Using synchrotron radiation Jackson et al. (2009) imaged *D. magna* exposed for 36 h to quantum dots (CdSe/ZnS – 6 nm) and found that zinc was concentrated in the intestine. De Samber et al. (2013) also analyzed neonates exposed to 1 mg L<sup>-1</sup> (from ZnCl<sub>2</sub>) for 48 h cryogenically frozen and analyzed by nano-XRF. Zinc was found in the gut; however, the concentration was lower than our study (2.5  $\mu\text{g cm}^{-2}$ ).

In partial agreement with the present study, Muna et al. (2017) showed that particulate forms trend to accumulate in higher amounts than dissolved ones. *D. magna* exposed to CuO nanoparticles (22-25 nm) and CuSO<sub>4</sub> at 0.05 mg Cu L<sup>-1</sup> for 48 h absorbed 884 and 157 µg Cu g dry weight<sup>-1</sup>, respectively. This results are also in agreement with Adam et al. (2014) and can be attributed to filtration absorption and the resulting CuO nanoparticle accumulation in the intestine.

One reason for the accumulation/distribution of zinc in the gut is that daphnids are filtering crustaceans. There is also active selection by the feeding apparatus as well as diffusion or passive absorption alongside larger particles. For an adult *D. magna*, the largest ingestible particles are around 70 µm. Thus, it is possible aggregated particles to concentrate in the gut (GOPHEN; GELLER, 1984).

#### **3.3.4.2. Zn quantitative maps of *Daphnia* at depuration assays**

Since 40 nm ZnO presented the highest toxicity (statistically equal to 20 nm and ZnSO<sub>4</sub>), it was chosen for depuration assays, which were carried out at 1 mg Zn L<sup>-1</sup> exposure concentration, which corresponds to a value below the LC<sub>10</sub>.

Figure 7. A shows that Zn was detected during the 24 hours of depuration assay and no clear change in the pattern of spatial distribution was noticed over time. Additional maps obtained during the depuration assays are presented in Figure 8. Figure 7. (A) Concentration spatial distribution of Zn inside of *Daphnia magna* neonates exposed to  $1 \text{ mg Zn L}^{-1}$  40 nm and after depuration in culture medium over time; (B) average of median Zn concentration of replicates as a function of time; (C) Zn concentration of replicates over time

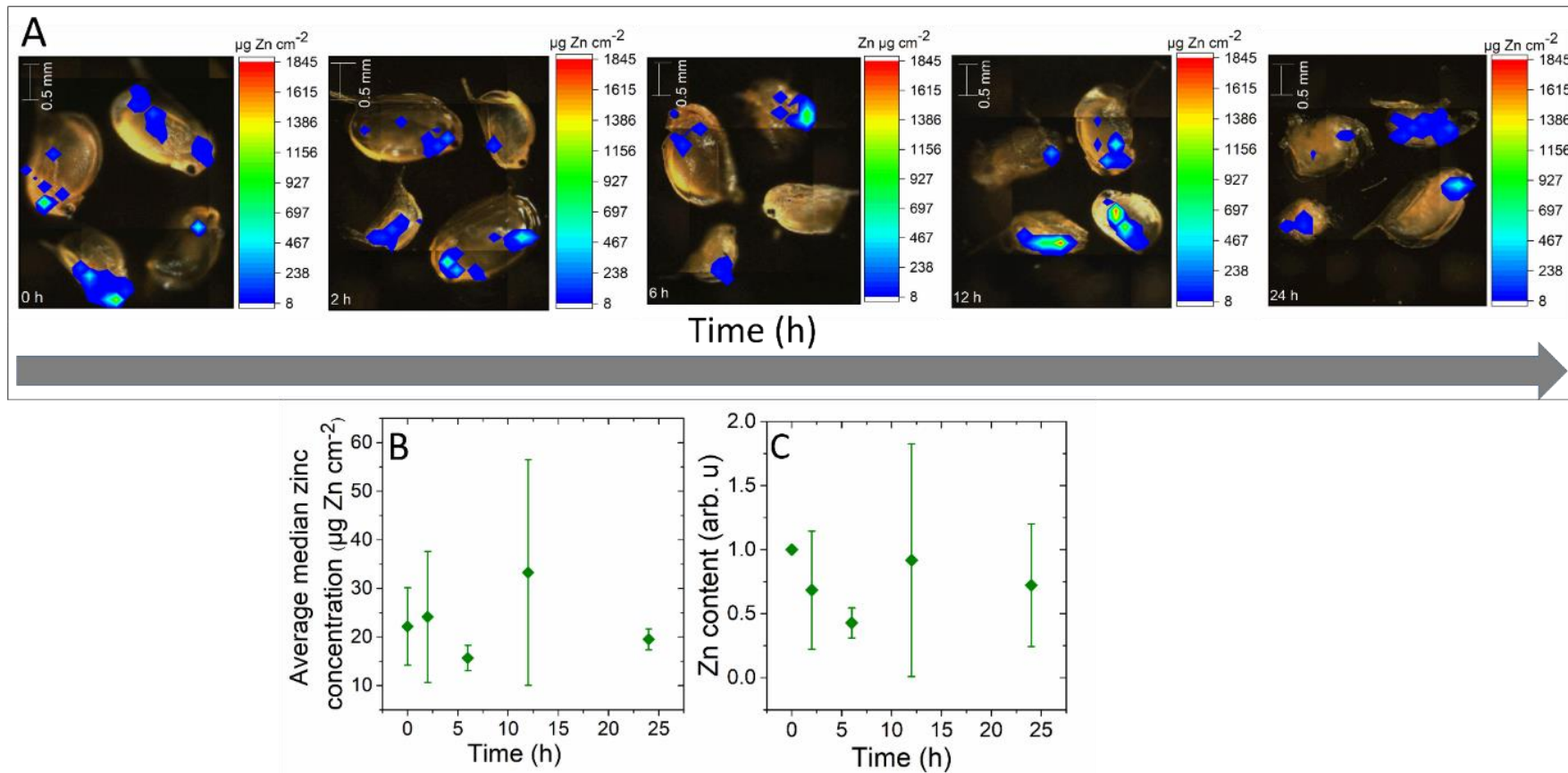




Figure 8. (A, B) Concentration spatial distribution of zinc inside of *Daphnia magna* neonates exposed to 1 mg Zn L<sup>-1</sup> 40 nm, and after depuration in culture medium over time

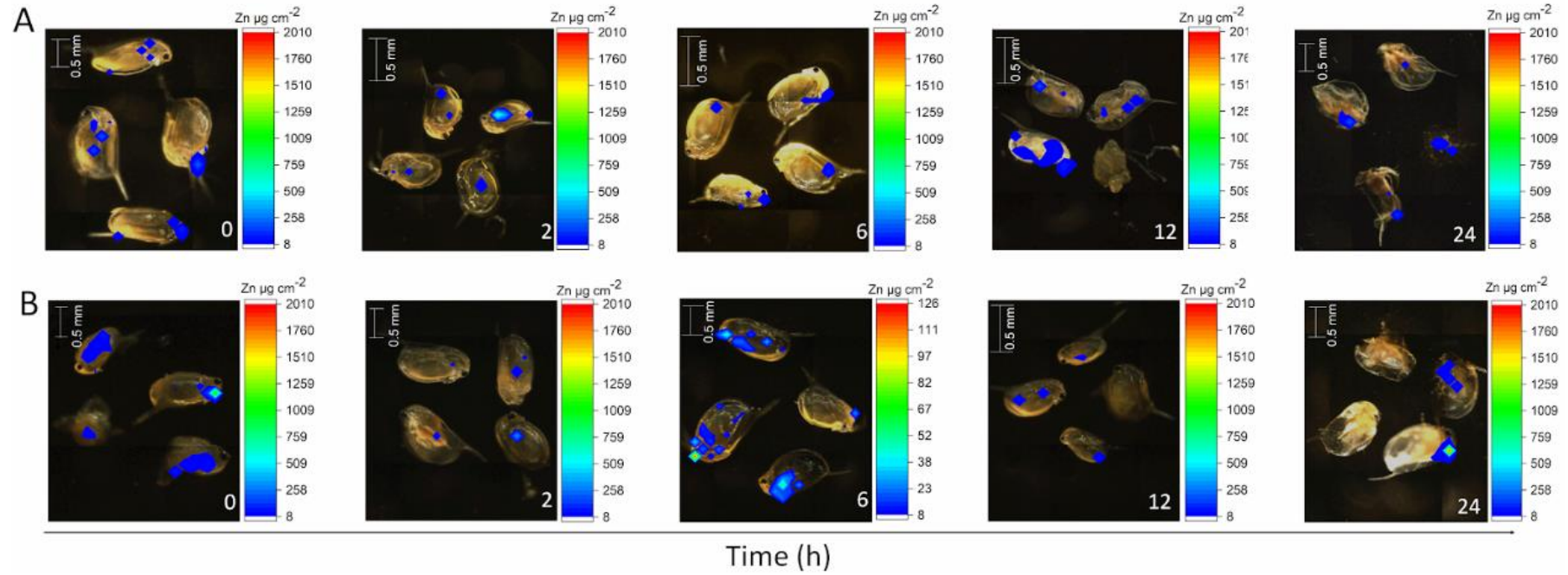






Figure 7B and 7C attempted at quantifying if Zn content varied as a function of time for the three replicates (12 organisms per each time point). Figure 8B shows that before the depuration started, the average median Zn local concentration was  $22.17 \pm 7.97 \mu\text{g cm}^{-2}$ . However, these values did not clearly decrease during the depuration assay, after 24 hours under culture medium free of nZnO and feed, the organisms presented  $19.52 \pm 2.14 \mu\text{g cm}^{-2}$  average median Zn local concentration.

Figure 7C represents the normalized ( $n = 3$  images, 12 organisms) total number of Zn counts. This quantity express the average integration of all zinc counts for a certain depuration time, divided by the total number of counts found at the beginning of the depuration, i.e. time = 0 h. Hence, it represents the total amount of zinc incorporated by the group of organisms at a certain time. If zinc was leaving the organism, i.e. undergoing depuration it was expected that the signal would decrease as a function of time. However, in Figure 7C it is clear that the content in the organisms did not reduce during the 24 hours of depuration.

Table 6 shows that uptake and depuration of nanoparticles by *D. magna* do not depend only on one factor such as composition or size. Like in the present study, the uptake of nanoparticles was in the range of parts per million in weigh. However, differently from our results, others studies reported partial depuration. Only Booth et al. (2016) using fluorescent nanoparticles (PMMA-FPNP, 86 - 125 nm) did not detect nanoparticles inside *D. magna* after 24 h.

The attempt of plotting the percentage of remaining particles within the organism as a function of particle size, using the data in Table 6, does shown return a correlation between the size and depuration.

At first glance, the results found by Skjolding et al. (2014) might suggest that smaller nanoparticles are more difficult to depurate. They found that for 10 nm Au, 53.66% and 74.66% (MUDA and CIT coating, respectively. See Table 6 for abbreviations) remained within the organism after 24 of depuration. On the other hand, for 30 nm 24 % & 17% (MUDA and CIT coating, respectively) remained inside the organism. Likewise, Rosenkranz et al. (2009) exposed *D. magna* to fluorescent carboxylated polystyrene nanoparticles (20 and 1000 nm at  $2 \mu\text{g L}^{-1}$ ), they noticed that the organisms retained more smaller particles (60%) than larger ones (8.27%) after 4 h of depuration.

Conversely, Fan et al. (2016) found that after 24 hours 30 nm TiO<sub>2</sub> depurated in larger quantities than 200 nm TiO<sub>2</sub>, they found that 25% and 50% of TiO<sub>2</sub>, respectively, remained in the organism. Skjolding et al. (2014) showed that there is no clear effect of stabilizing agent related depuration rate.

Muna et al. (2017) suggested that dissolved forms of copper are more recalcitrant than particulate ones. They showed that *D. magna* retained 44.6% of 22-25nm CuO (884 and 396 µg Cu g dry weight<sup>-1</sup>, for absorbed and retained, respectively) and 91.7% of CuSO<sub>4</sub> (157 and 144 µg Cu g dry weight<sup>-1</sup>, for absorbed and retained, respectively).

The studies shown in Table 6 argue that the main route of elimination of particles that pass through the body of *D. magna* is through excretion during fecal production. There are no depuration assays protocols; therefore, in depuration studies there is time variation after the exposure period as well as the presence/absence of food. In our study, we opted for the absence of food, because we intended to evaluate the depuration response regardless of the food variable. Gophen and Gold (1981) suggested that *Daphnia* spp. preserves food in the intestinal section during the period in which they are not fed, which may justify incomplete depuration in the evaluated period in our study. On the other hand, among the studies shown in Table 1, only Muna et al. (2017) and Sakka et al. (2016) fed the organisms during the depuration assay, but they all reported at least partial depuration.

Table 6. Literature survey on depuration of nanoparticles by *Daphnia magna*

Reference	NP	Size (nm)	Depuration (h)	Concentration after exposure	Concentration after depuration	Remaining nanoparticles (%)	Employed analytical technique
Skjolding et al. (2014a)	Au-MUDA & Au-CIT	10	24	30 and 15 ng $\mu\text{g dry wt.}^{-1}$ for Au-MUDA & Au-CIT, respectively	16.1 and 11.2 ng $\mu\text{g dry wt.}^{-1}$ for Au-MUDA & Au-CIT, respectively	53.66% and 74.66% for Au-MUDA & Au-CIT, respectively	ICP-OES
Skjolding et al. (2014a)	Au-MUDA & Au-CIT	30	24	5 ng $\mu\text{g dry wt.}^{-1}$ & 10 ng $\mu\text{g dry wt.}^{-1}$ for Au-MUDA & Au-CIT, respectively	1.2 ng $\mu\text{g dry wt.}^{-1}$ & 1.7 ng $\mu\text{g dry wt.}^{-1}$ for Au-MUDA & Au-CIT, respectively	24% & 17% for Au-MUDA & Au-CIT, respectively	ICP-OES
Skjolding et al. (2014b)	ZnO	30	24	7690 mg Zn kg dry wt. <sup>-1</sup>	<1250 mg Zn kg dry wt. <sup>-1</sup>	< 16.25%	ICP-OES
Booth et al. (2016)	PMMA-FPNP	86-125	24	intense fluorescence	no fluorescence	-	fluorescence spectrometry
Chen et al. (2014)	fullerene	139	24	1000 & 2100 mg kg <sup>-1</sup> respectively	800 & 1890 mg kg <sup>-1</sup> , respectively	80% & 90%, respectively	UV-visible spectrophotometry
Fan et al. (2016)	TiO <sub>2</sub>	30 & 200	1	15 & 35 mg g dry wt. <sup>-1</sup> , respectively	3.75 & 17.5 mg g dry wt. <sup>-1</sup> , respectively	25% & 50%, respectively	ICP-OES
Muna et al. (2017)	CuO	22-25	24	884 $\mu\text{g Cu g dry wt.}^{-1}$	396 $\mu\text{g Cu g dry wt.}^{-1}$	44.79%	TXRF
Rosenkranz et al. (2009)	PS-fluorescein	1000 & 20	4	1.45 ng & 0.055 ng per organism, respectively	0.12 ng & 0.033 ng per organism, respectively	8.27% & 60%, respectively	fluorimeter spectrometry
Sakka et al. (2016)	Ag-CIT	20-30	24h	0.69 ng per animal	0.27 ng per animal	40%	ICP-MS
Magro et al. (2018)	Fe <sub>3</sub> O <sub>4</sub>	< 100	3h	50 $\mu\text{g g}^{-1}$ daphnia	< 10 $\mu\text{g g}^{-1}$ daphnia	20%	ICP-AES

MUDA= mercaptoundecanoic acid, CIT= citrate, Carb= Carboxylated, PMMA-FPNP= PMMA polymer with fluorescent label copolymer, PS= polystyrene

Another reason for the absence of depuration regards the physical behavior of the particles in the aqueous medium; they can adhere to the surface of the exoskeleton and accumulate in the gastrointestinal tract, this leads to low absorption of nutrients and consequently malnutrition (BAUN et al., 2008; MENDONÇA et al., 2011; ROSSETTO et al., 2014). Thus, complete depuration suggests the absence of significant interactions between nanoparticles and intestinal epithelium, such as the retention and progressive degradation of metal ions from nanomaterials. In our study, there was no depuration and zinc intensity were found in the gut, which indicates interactions between nanoparticles and intestine.

### 3.4 Partial Conclusions

The toxicity was dependent on nanoparticle size and presence/absence of surfactants. Dissolved Zn contributes to greater toxicity. However, particulate forms trend to accumulate in higher amounts than dissolved ones. In addition, Zn from ZnSO<sub>4</sub> was broadly distributed inside the body of organism, while Zn from nanoparticles sources were concentrated in certain regions. Smaller Zn nanoparticles without surfactant have the same toxicity as the soluble source, ZnSO<sub>4</sub>.

μ-XRF analyzes show that neonates are considered infinitely thin samples, which facilitated the quantification of zinc. The chemical images showed that nanoparticulate forms of zinc accumulated mainly along the digestive tract.

Differently from several reports in literature, the depuration of zinc was not observed. This might be a consequence of presented strong adsorption of nZnO on the inner surface of the digestive tract, or the particles might also have agglomerated and block the digestive tube.

### References

ADAM, N. et al. The uptake of ZnO and CuO nanoparticles in the water-flea *Daphnia magna* under acute exposure scenarios. **Environmental Pollution**, v. 194, p. 130-137, 2014.

ADAM, N. et al. The uptake and elimination of ZnO and CuO nanoparticles in *Daphnia magna* under chronic exposure scenarios. **Water Research**, v. 68, p. 249-261, 2015.

ASSOCIAÇÃO BRASILEIRA DE NORMAS TÉCNICAS - ABNT. **NBR12713 de 05/2016**: Ecotoxicologia aquática - Toxicidade aguda - Método de ensaio com *Daphnia* spp (Crustacea, Cladocera). São Paulo, 2016. 33 p.

BACCHETTA, R. et al. Role of soluble zinc in ZnO nanoparticle cytotoxicity in *Daphnia magna*: A morphological approach. **Environmental Research**, v. 148, p. 376-385, 2016.

BACCHETTA, R. et al. Chronic toxicity effects of ZnSO<sub>4</sub> and ZnO nanoparticles in *Daphnia magna*. **Environmental Research**, v. 152, p. 128-140, 2017.

BAUN, A. et al. Ecotoxicity of engineered nanoparticles to aquatic invertebrates: A brief review and recommendations for future toxicity testing. **Ecotoxicology**, v. 17, p. 387-395, 2008.

BLAISE, C.; FÉRARD, J. F. **Small-scale freshwater toxicity investigations**. Volume 1: Toxicity test methods. 1. ed. Heidelberg: Springer, 2005. 572 p.

BOOTH, A. M. et al. Uptake and toxicity of methylmethacrylate-based nanoplastic particles in aquatic organisms. **Environmental Toxicology and Chemistry**, v. 35, p. 1641-1649, 2016.

CHEN, Q. et al. The effects of humic acid on the uptake and depuration of fullerene aqueous suspensions in two aquatic organisms. **Environmental Toxicology and Chemistry**, v. 33, p. 1090-1097, 2014.

DA CRUZ, T. N. M. et al. Shedding light on the mechanisms of absorption and transport of ZnO nanoparticles by plants: via in vivo X-ray spectroscopy. **Environmental Science: Nano**, v. 4, p. 2367-2376, 2017.

DE SAMBER, B. et al. A combination of synchrotron and laboratory X-ray techniques for studying tissue-specific trace level metal distributions in *Daphnia magna*. **Journal of Analytical Atomic Spectrometry**, v. 23, n. 6, p. 829-839, 2008.

DE SAMBER, B. et al. Hard X-ray nanoprobe investigations of the subtissue metal distributions within *Daphnia magna*. **Analytical and Bioanalytical Chemistry**, v. 405, p. 6061-6068, 2013.

FAN, W. et al. High bioconcentration of titanium dioxide nanoparticles in *Daphnia magna* determined by kinetic approach. **Science of the Total Environment**, v. 569-570, p. 1224-1231, 2016.

FERRANDO, M. D.; ANDREU-MOLINER, E.; FERNÁNDEZ-CASALDERREY, A. Relative Sensitivity of *Daphnia magna* and *Brachionus calyciflorus* to Five Pesticides. **Journal of Environmental Science and Health, Part B**, v. 27, n. 5, p. 511-522, 1992.

GOPHEN, M.; GELLER, W. Filter mesh size and food particle uptake by *Daphnia*. **Oecologia**, v. 64, p. 408-412, 1984.

GOPHEN, M.; GOLD, B. The use of inorganic substances to stimulate gut evacuation in *Daphnia magna*. **Hydrobiologia**, v. 80, p. 43-45, 1981.

GOTTSCHALK, F. et al. Modeled environmental concentrations of engineered nanomaterials (TiO<sub>2</sub>, ZnO, Ag, CNT, fullerenes) for different regions. **Environmental Science and Technology**, v. 43, p. 9216-9222, 2009.

HEINLAAN, M. et al. Toxicity of nanosized and bulk ZnO, CuO and TiO<sub>2</sub> to bacteria *Vibrio fischeri* and crustaceans *Daphnia magna* and *Thamnocephalus platyurus*. **Chemosphere**, v. 71, p. 1308-1316, 2008.

JACKSON, B. P. et al. Synchrotron X-ray 2D and 3D elemental imaging of CdSe/ZnS quantum dot nanoparticles in *Daphnia magna*. **Analytical and Bioanalytical Chemistry**, v. 394, n. 3, p. 911–917, 2009.

LOPES, S. et al. Zinc oxide nanoparticles toxicity to *Daphnia magna*: Size-dependent effects and dissolution. **Environmental Toxicology and Chemistry**, v. 13, p. 190-198, 2014.

MA, H. et al. Impact of solar UV radiation on toxicity of ZnO nanoparticles through photocatalytic reactive oxygen species (ROS) generation and photo-induced dissolution. **Environmental Pollution**, v. 193, p. 165-172, 2014.

MA, H.; WILLIAMS, P. L.; DIAMOND, S. A. Ecotoxicity of manufactured ZnO nanoparticles - A review. **Environmental Pollution**, v. 172, p. 76-85, 2013.

MAGRO, M. et al. The surface reactivity of iron oxide nanoparticles as a potential hazard for aquatic environments: A study on *Daphnia magna* adults and embryos. **Scientific Reports**, v. 8, p. 13017, 2018.

MENDONÇA, E. et al. Effects of diamond nanoparticle exposure on the internal structure and reproduction of *Daphnia magna*. **Journal of Hazardous Materials**, v. 186, n. 1, p. 265–271, 2011.

MILAM, C. D. et al. Acute toxicity of six freshwater mussel species (Glochidia) to six chemicals: Implications for daphnids and *Utterbackia imbecillis* as surrogates for protection of freshwater mussels (Unionidae). **Archives of Environmental Contamination and Toxicology**, v. 48, n. 2, p.166-173, 2005.

MUNA, M. et al. Evaluation of the effect of test medium on total Cu body burden of nano CuO-exposed *Daphnia magna*: A TXRF spectroscopy study. **Environmental Pollution**, v. 231, p. 1488-1496, 2017.

OLESZCZUK, P.; JOŚKO, I.; SKWAREK, E. Surfactants decrease the toxicity of ZnO, TiO<sub>2</sub> and Ni nanoparticles to *Daphnia magna*. **Ecotoxicology**, v. 24, n. 9, p. 1923-1932, 2015.

ROSENKRANZ, P. et al. A comparison of nanoparticle and fine particle uptake by *Daphnia magna*. **Environmental Toxicology and Chemistry**, v. 28, p. 2142-2149, 2009.

ROSSETTO, A. L. de O. F. et al. Comparative evaluation of acute and chronic toxicities of CuO nanoparticles and bulk using *Daphnia magna* and *Vibrio fischeri*. **Science of the Total Environment**, v. 490, p. 807-814, 2014.

SAKKA, Y. et al. Behavior and chronic toxicity of two differently stabilized silver nanoparticles to *Daphnia magna*. **Aquatic Toxicology**, v. 177, p. 526-535, 2016.

SAKUMA, M. Probit analysis of preference data. **Applied Entomology and Zoology**, v. 33, n. 3, p. 339–347, 1998.

SAVASSA, S. M. et al. Effects of ZnO Nanoparticles on *Phaseolus vulgaris* Germination and Seedling Development Determined by X-ray Spectroscopy. **ACS Applied Nano Materials**, v. 11, p. 6414-6426, 2018.

SÁNCHEZ-BAYO, F.; GOKA, K. Influence of light in acute toxicity bioassays of imidacloprid and zinc pyrethrin to zooplankton crustaceans. **Aquatic Toxicology**, v. 78, n. 3, p. 262-271, 2006.

SKJOLDING, L. M. et al. Uptake and depuration of gold nanoparticles in *Daphnia magna*. **Ecotoxicology**, v. 23, p. 1172-1183, 2014.

SKJOLDING, L. M.; WINTHER-NIELSEN, M.; BAUN, A. Trophic transfer of differently functionalized zinc oxide nanoparticles from crustaceans (*Daphnia magna*) to zebrafish (*Danio rerio*). **Aquatic Toxicology**, v. 157, p. 101-108, 2014.

TANGAA, S. R. et al. Trophic transfer of metal-based nanoparticles in aquatic environments: A review and recommendations for future research focus. **Environmental Science: Nano**, v. 6, p. 966-981, 2016.

XIAO, Y. et al. Toxicity and accumulation of Cu and ZnO nanoparticles in *daphnia magna*. **Environmental Science and Technology**, v. 49, p. 4657-4664, 2015.

YANG, Y. et al. Toxicity assessment of nanoparticles in various systems and organs. **Nanotechnology Reviews**, v. 6, p. 279-288, 2017.

ZAGATO, P. A.; BERTOLETTI, E. **Ecotoxicologia aquática: princípios e aplicações**. 1. ed. São Carlos: RiMa, 2006. 464 p.





## 4 X-RAY IMAGING AND CHEMICAL SPECIATION ASSISTING TO UNDERSTAND THE TOXIC EFFECTS OF COPPER OXIDE NANOPARTICLES ON ZEBRAFISH (*Danio rerio*)

### Abstract

Currently, copper nanoparticles are used in various sectors of industry, agriculture and medicine. To understand the effects induced by these nanoparticles, it is necessary to assess the environmental risk and safely expand its use. In this study, the toxicity of copper oxide (nCuO) nanoparticles in *Danio rerio* adults was evaluated, their distribution/concentration and chemical form after exposure. Such evaluation was done through the characterization of nCuO, acute exposure tests and analysis of distribution and concentration by X-ray fluorescence spectroscopy ( $\mu$ -XRF) and atomic absorption spectroscopy (GF-AAS). Synchrotron X-ray absorption spectroscopy (XAS) was performed to find out the chemical form of copper in hotspots. The results show that the toxicity values of fish exposed to nCuO were 2.4 mg L<sup>-1</sup> (25 nm), 12.36 mg L<sup>-1</sup> (40 nm), 149.03 mg L<sup>-1</sup> (80 nm) and 0.62 mg L<sup>-1</sup> (CuSO<sub>4</sub>, used as a positive control). The total copper found in the fish was in the order of mg kg and it was not directly proportional to the exposure concentration; most of the copper was concentrated in the gastric system. However, despite being concentrated, the analyzes showed that there was no chemical transformation of the accumulated copper.

**Keywords:** Zebrafish; CuO; nanoparticles; accumulation; X-ray; XRF; XANES

### 4.1 Introduction

Copper is an essential micronutrient for plants, humans, and animals. In biochemical reactions, copper can change between Cu<sup>2+</sup> and Cu<sup>+</sup> in enzymes and electron transporters catalyzing oxide reduction reactions involving oxygen (LIPPARD; BERG, 1994). Nanoparticulate forms of copper are used in a variety of good such as paints, cosmetics, bioactive coatings, nanofluids, electronics, textile sector, and food packaging (BUFFET et al., 2013; HEMMAT ESFE; BAHIRAEI; MIR, 2020; MILLER; SENJEN, 2008; MOTELICA et al., 2020). Recently, its applications in modern nanomedicine have also been intensively investigated (ALPHANDÉRY, 2020; CHATTOPADHYAY, 2020; DONG et al., 2020). Hence, if these products are not properly discarded, nanoparticles may end up in the environment.

Toxic effects of nCuO have been reported at several trophic levels, for example, in fish (BOYLE; CLARK; HANDY, 2020; GRIFFITT et al., 2007; NNAMDI et al., 2019), invertebrates (BUFFET et al., 2011; VOLLAND et al., 2018), protozoa (MORTIMER; KASEMETS; KAHRU, 2010; RUSAKOVA et al., 2015), bacteria (BAEK; AN, 2011;

SAGADEVAN et al., 2019; THAKUR et al., 2020) and yeasts (KASEMETS et al., 2009; SHARMIN et al., 2017).

Nanoparticles do not necessarily have to enter cells to harm the organisms. Changes in the microenvironment around the organism-particle contact area can increase metal solubilization or generate reactive oxygen species that can damage cell membranes (HEINLAAN et al., 2008). The bioavailability and toxicity of copper in aquatic organisms also depends on the chemical species of copper, which in turn is determined by factors such as pH, particle size, surface chemistry, sedimentation, dissolution, metal ion fraction, aggregation, and speciation among others (BOYLE; CLARK; HANDY, 2020; THIT et al., 2017). Thus, understanding the adverse effects induced by nCuO is of great importance for assessing environmental risk and safely expanding its use (ANDREANI et al., 2021; DING et al., 2020; HOU et al., 2017).

The zebrafish, *Danio rerio* (Pisces, Cyprinidae), is a freshwater tropical fish, native to northern India, and a model organism for vertebrate development and ecotoxicological studies. It can brood up to 200 embryos every seven days, which are transparent, small and rapidly developing (TAVARES; SANTOS LOPES, 2013). As a vertebrate model, zebrafish presents several advantages, such as a fully sequenced genome, embryological development outside the mother's body, and easy-to-observe behavior. Additionally, the homology between zebrafish and human genes is around 70%. Due to its genetic and biochemical mechanisms, the use of zebrafish reduces the number of larger animals in experiments as well as the amount of compounds needed for testing (GHENO et al., 2016). These characteristics become this organism to be considered as the “gold standard” for toxicological studies (JIA et al., 2019).

Hence, this study aimed at evaluating the toxicity caused by of nCuO on *D. rerio* adults. We evaluated the effects of nanoparticle composition, size and concentration on the survival of organisms. Additionally, we employed microprobe X-ray fluorescence spectroscopy ( $\mu$ -XRF) to locate the tissues in which copper accumulated within the organisms and synchrotron microprobe X-ray absorption spectroscopy (XAS) to carry out chemical speciation of copper in the hotspots.

## 4.2 Material and methods

### 4.2.1 Characterization

#### 4.2.1.1 Nanoparticles and dispersion

Three copper-based nanoparticles were studied: 25 nm particle made of a metallic core and passivated shell, 40 and 80 nm copper II oxide particles (US Nanomaterials Research Inc.). The nanoparticles were characterized by transmission electron microscopy (TEM), powder X-ray diffraction (XRD), zeta potential and dynamic light scattering (DLS).

Additional DLS and zeta potential measurements were performed for nCuO dispersed in *D. rerio* culture medium at 100 mg Cu L<sup>-1</sup> (Table 1). The measurements were performed using a Zetasizer Nano (Malvern Instruments, U.K.).

Table 1. Zeta potential and hydrodynamic diameter of differently size nCuO particles dispersed in culture medium of *Danio rerio* at 100 mg Cu L<sup>-1</sup>

nCuO (nm)	Hydrodynamic Diameter (nm)	Zeta Potential (mV)
25 nm	1491 ± 285	-17 ± 0.3
40 nm	436 ± 45	0.05 ± 0.21
80 nm	254 ± 9	-20 ± 0.4

### 4.2.2 Experimental conditions

#### 4.2.2.1 Maintenance of zebrafish

About 6-month-old *D. rerio* were bought from an aquarium commercial shop. The zebrafish were kept in a 30 L aquarium with approximately 25 fish per aquarium. Aquariums were conditioned at 23°C ± 2°C in the zebrafish culture medium (OECD 203, 1992), pH 7-7.5 and constant pump based aeration. The zebrafish were fed with flocculated feed – Tetra Min® - once a day.

### 4.2.3 Acute assays

Before the acute assays, the zebrafish (females and males) were kept in the aquarium for at least 12 days as quarantine time.

Stock dispersions of each nCuO and solution of CuSO<sub>4</sub>·7H<sub>2</sub>O (P.A. Synth) were prepared (50 to 500 mg Cu L<sup>-1</sup>) in the zebrafish culture medium (OECD 203, 1992). The nanoparticles were dispersed using Sonic Dismembrator (Fisher Scientific, USA, Model 705) at 95 W, 50% of amplitude and 50 J for 4 cycles of 5 min each and intervals of 3 min between cycles.

The zebrafish were not fed on the day before the assays. One fish per treatment concentration (seven replicates) was exposed individually in a beaker with 225 mL of nCuO dispersion or CuSO<sub>4</sub> solution, the beaker was aerated at 23°C ± 2°C, (Figure 1). CuSO<sub>4(aq)</sub> was employed as positive control and pristine culture medium as negative control. Tables 2 and 3 describe the composition of culture medium of zebrafish (OECD 203, 1992 with modification) and the concentration of nCuO dispersion and the CuSO<sub>4</sub> solution used in the acute assays, respectively.

Figure 1. (A) Scheme of replicates of exposure assays with zebrafish exposed to nCuO dispersions and CuSO<sub>4</sub> solutions for 96 h. (B) Fish were individually exposed

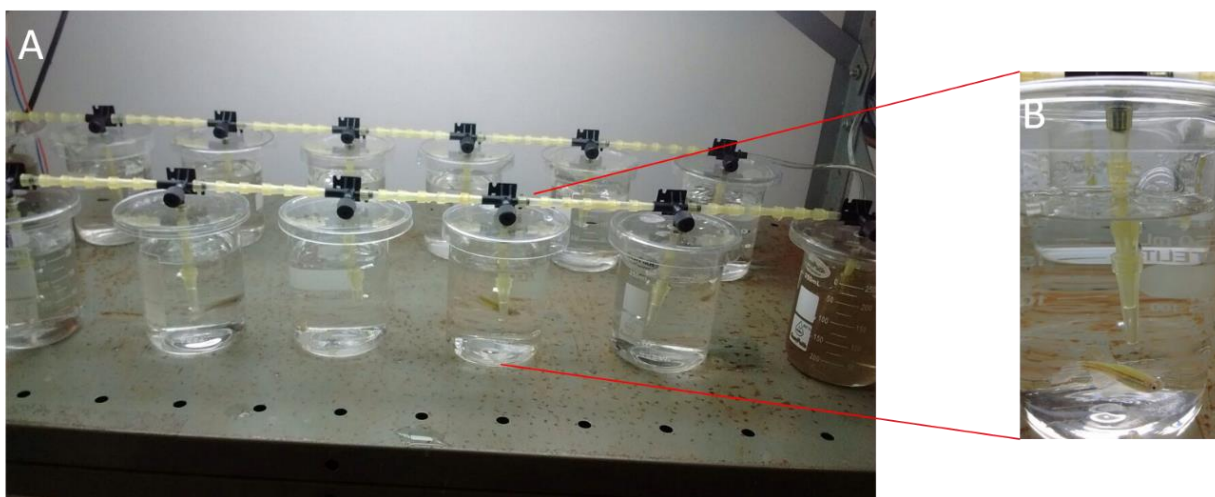


Table 2. Composition of the culture medium of *Danio rerio* (zebrafish). The pH was adjusted to 7.0-7.5

Solution	g L <sup>-1</sup>
Ca.Cl <sub>2</sub> . 2H <sub>2</sub> O	2.94
MgSO <sub>4</sub> . 7H <sub>2</sub> O	0.73
NaHCO <sub>3</sub>	2.59
KCl	0.23

Table 3. Concentrations of nCuO dispersions and CuSO<sub>4</sub> solution used in the acute assays with zebrafish. LC<sub>50</sub>, LC<sub>100</sub> determined in the exposure assays and pH

Treatment	Concentration ( mg L <sup>-1</sup> )							LC <sub>50</sub>	pH	LC <sub>100</sub>	pH
	0	0.5	1	1.5	2	2.5	3.5				
nCuO 25 nm	0	0.5	1	1.5	2	2.5	3.5	2.4	7.3	4.375	7.3
nCuO 40 nm	0	2.5	5	10	12	15	20	12.36	7.65	20	7.49
nCuO 80 nm	0	50	75	100	150	200	300	149.03	7.32	280	7.31
CuSO <sub>4</sub>	0	0.1	0.3	0.5	0.7	1	1.5	0.62	7.35	1.4	7.43

During the assays, the fishes were not fed. The nCuO dispersions, CuSO<sub>4</sub> solution and negative control medium were replaced every 24 h. After 96 h, the dead fish were counted. The Probit program was used to determine the concentration that killed 50% of the zebrafish (LC<sub>50</sub>) (SAKUMA, 1998). Data regarding the survival of zebrafish over time were subjected to survival analysis by applying the Weibull distribution through the survival package (THERNEAU; LUMLEY, 2018). All assays were done with permission of the institutional Ethics Committee on the Use of Animals (CEUA - n° 008-2016).

#### 4.2.4 Total copper concentration in the zebrafish

For determination of total Cu concentration in the zebrafish, six fish were exposed to concentrations equal to the LC<sub>50</sub> and LC<sub>100</sub> (Table 3). The exposure conditions were the same as for the acute assays. After exposure, the zebrafish were sacrificed in cold water, washed with phosphate buffer (PBS), frozen at -20°C and lyophilized.

The fishes were digested individually, in microwave flasks. Digestion was carried out using an Ultrawave (Table 4). The organisms dry body mass varied from 22 up to 170 mg, they were digested using 6 mL of HNO<sub>3</sub> (purified Merck at 20%) and 2 mL of H<sub>2</sub>O<sub>2</sub> (Exodo). In addition, 250 mg of a certified reference sample (DORM-4) was digested. After digestion, the content of the vials was made up to 15 mL with Milli-Q water. Copper detection was performed by graphite furnace atomic absorption spectroscopy (GF- AAS) (Perkin Elmer, Norwalk, USA).

Table 4. Temperature and energy programming of the microwave used for digestion of the *Danio rerio* (zebrafish) analysed for internal Cu concentrations

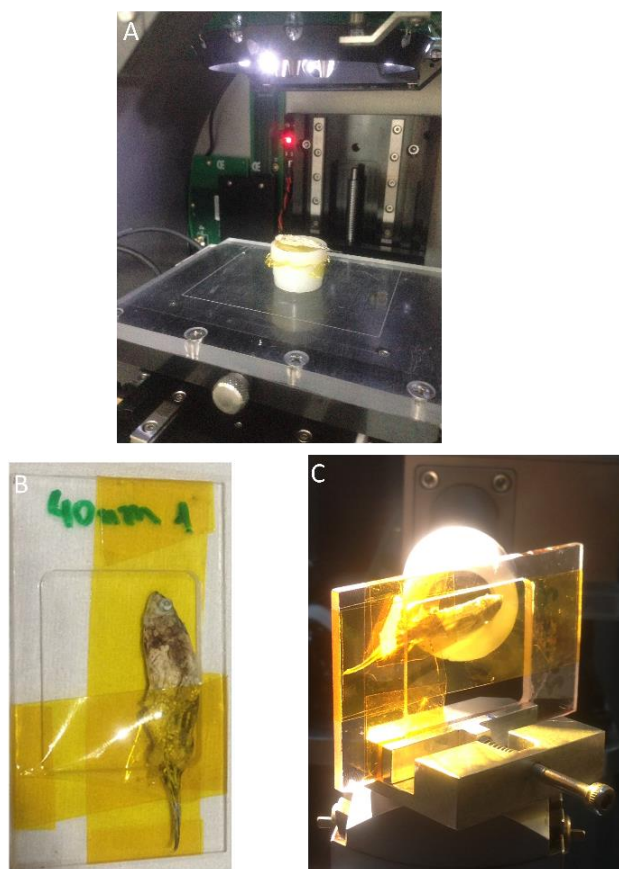
<b>Time (min)</b>	<b>P (W)</b>	<b>T1°C</b>	<b>T2°C</b>
5	1500	100	50
2	1500	160	50
5	1500	230	60
15	1500	230	60

#### 4.2.5 X-ray fluorescence microanalysis ( $\mu$ -XRF)

$\mu$ -XRF was used to map the 2D distribution of the Cu absorbed by the zebrafish that were exposed to nCuO. This provided information on the area (location) where Cu was concentrated inside the zebrafish. For this analysis, the zebrafish were exposed to concentrations equal to the LC<sub>100</sub> (two replicates) in the acute assays (Table 3). The choice of LC<sub>100</sub> for  $\mu$ -XRF is due to the higher copper concentration which makes the detection possible. After exposure, the zebrafish were sacrificed with cold water, washed with PBS, and partly dissected for analysis of the organs of the abdominal region.

Zebrafish were placed on a polyamide thin film (Kapton<sup>TM</sup>) mounted on a XRF cuvette. The Cu spatial distribution inside the zebrafish organs was determined by a benchtop  $\mu$ -XRF system (EDAX, ORBIS PC, USA). X-rays were generated by a Rh anode operating at 50 kV and 800  $\mu$ A, a 25  $\mu$ m Ti primary filter was employed to improve the signal-to-noise ratio. The 1 mm X-ray beam was delimited by a pin hole, and the detection carried out by a 30 mm<sup>2</sup> silicon drift detector operating at 6 s of dwell time, dead time below 3% and 140 eV resolution for Mn-K $\alpha$ . The maps were produced using a matrix of 32 x 25 points summing up to 800 XRF spectra for each image (Figure 2A).

Figure 2. Pictures of (A) *Danio rerio* (zebrafish) on top of a Kapton™ (polyamide) film prepared for  $\mu$ -XRF analysis, (B) zebrafish on the sample port, and (C) zebrafish on XANES analysis



#### 4.2.6 Microprobe X-ray absorption near edge spectroscopy ( $\mu$ -XANES)

For these analyses, zebrafish were exposed to 40 and 25 nm at a concentration equal to the LC<sub>100</sub>, sacrificed and dissected as described above. The zebrafish were lyophilized prior to the measurements.

Cu-K edge  $\mu$ -XANES were recorded at the XRF beam line of the 1.37 GeV Brazilian Synchrotron Light Laboratory – LNLS, Campinas/SP. In this facility X-rays were provided by a bending magnet device, monochromatized by a double crystal Si(111), and the 20 x 25  $\mu\text{m}^2$  X-ray beam was focused on the sample by a KB mirror system. The detection was carried out in XRF mode using an element Si drift detector (KETEK GmbH, Germany). The  $\mu$ -XANES spectra were recorded in fluorescence mode from -80 to 250 eV relatively to the Cu K edge. At least six  $\mu$ -XANES spectra were recorded per sample. The energy step in the edge region was 0.5 eV. The spectra were subsequently merged to improve the signal-to-noise ratio.

$\mu$ -XRF 2D distribution of Cu intensity constructed previously helped to decide the appropriate regions of the zebrafish to be measured. The zebrafish were put on a sample holder and wrapped with a Kapton<sup>TM</sup> tape. Three biological replicate of each treatment were analyzed (Figure 2B, C) and the areas with the highest concentration of copper were evaluated.

Cu reference compounds were also measured (CuO bulk, nCuO 25 nm and 40 nm, Cu<sub>2</sub>O, CuSO<sub>4</sub>, Cu<sub>3</sub>PO<sub>4</sub>, Cu(OH)<sub>2</sub>, Cu(NO<sub>3</sub>)<sub>2</sub>, Cu(NH<sub>3</sub>)<sub>4</sub>, Cu-cysteine, Cu-histidine, Cu-glycine, Cu-glycose, Cu-malate). The Cu bound to organic molecules were obtained following the same procedure for Zn reported by Sarret et al. (2009). The  $\mu$ -XANES spectra were energy calibrated using a reference Cu foil. Data was normalized using the Athena software of the Demeter package (RAVEL; NEWVILLE, 2005).

## 4.3 Results and discussion

### 4.3.1 Characterization

#### 4.3.1.1 Nanoparticles and dispersion

The characterization of the nanoparticles by TEM, XRD and DLS and zeta potential in deionized water was previously reported in another study (SANTOS-RASERA et al., 2019). TEM images and histograms indicate that sizes of nCuO are close to the sizes reported by the supplier. nCuO 25 nm ( $26 \pm 8$  nm) is spherical shape, 40 nm ( $45 \pm 11$  nm) is elliptical shape and 80 nm ( $75 \pm 19$  nm) is quadratic shape (Figure 3 in the second chapter). Nevertheless, we decided to keep the nominal size reported by the supplier when. X-ray diffraction patterns of 40 and 80 nm nCuO are monoclinic CuO, the 25 nm nCuO contained a fraction of face centric cubic (*fcc*) metallic phase in addition to monoclinic CuO (Figure 2 in the second chapter).

Table 1 presents the zeta potential and hydrodynamic diameter of nCuO in culture medium of *D. rerio*. The zeta potential and hydrodynamic diameter of the nCuO in the *D. rerio* culture medium were different from those obtained in water (Table 3 in the second chapter). The hydrodynamic diameter of particles dispersed in deionized water showed lower values than particles dispersed in culture medium. This difference is partially explained by the lower values of zeta potential of particles dispersed in culture medium, which leads to lower electrical repulsion of the particles (LIU et al., 2009).



### 4.3.2 Acute assays

Figure 3 shows the dose-response curves of nCuO and CuSO<sub>4</sub> obtained during the acute assays. The LC<sub>50</sub> values, calculated from the percent mortality data, reveal that CuSO<sub>4</sub> is more toxic than any of the nCuO. The Probit software adopted the plateau linear model as the most representative model (SAKUMA, 1998). The parameters of the model curve and LC<sub>50</sub>s and LC<sub>10</sub>s are shown in the Table 5.

Figure 3. Dose-response curves for the acute toxicity of nCuO and CuSO<sub>4</sub> to *Danio rerio*

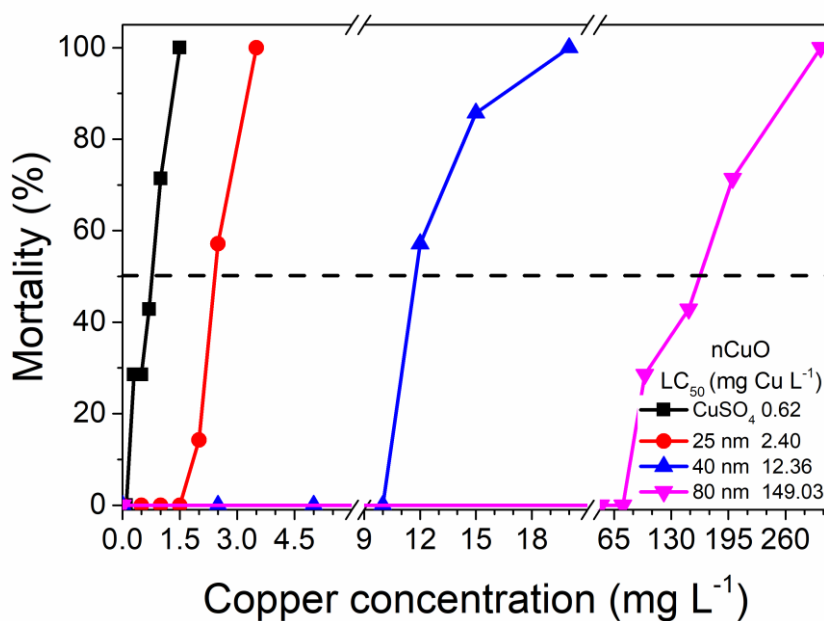


Table 5. Parameters of the plateau linear model ( $y = a + bx$ ) applied to the survival data of zebrafish exposed for 96 h to differently sized of nCuO particles and CuSO<sub>4</sub>. All parameters are given with corresponding standard error

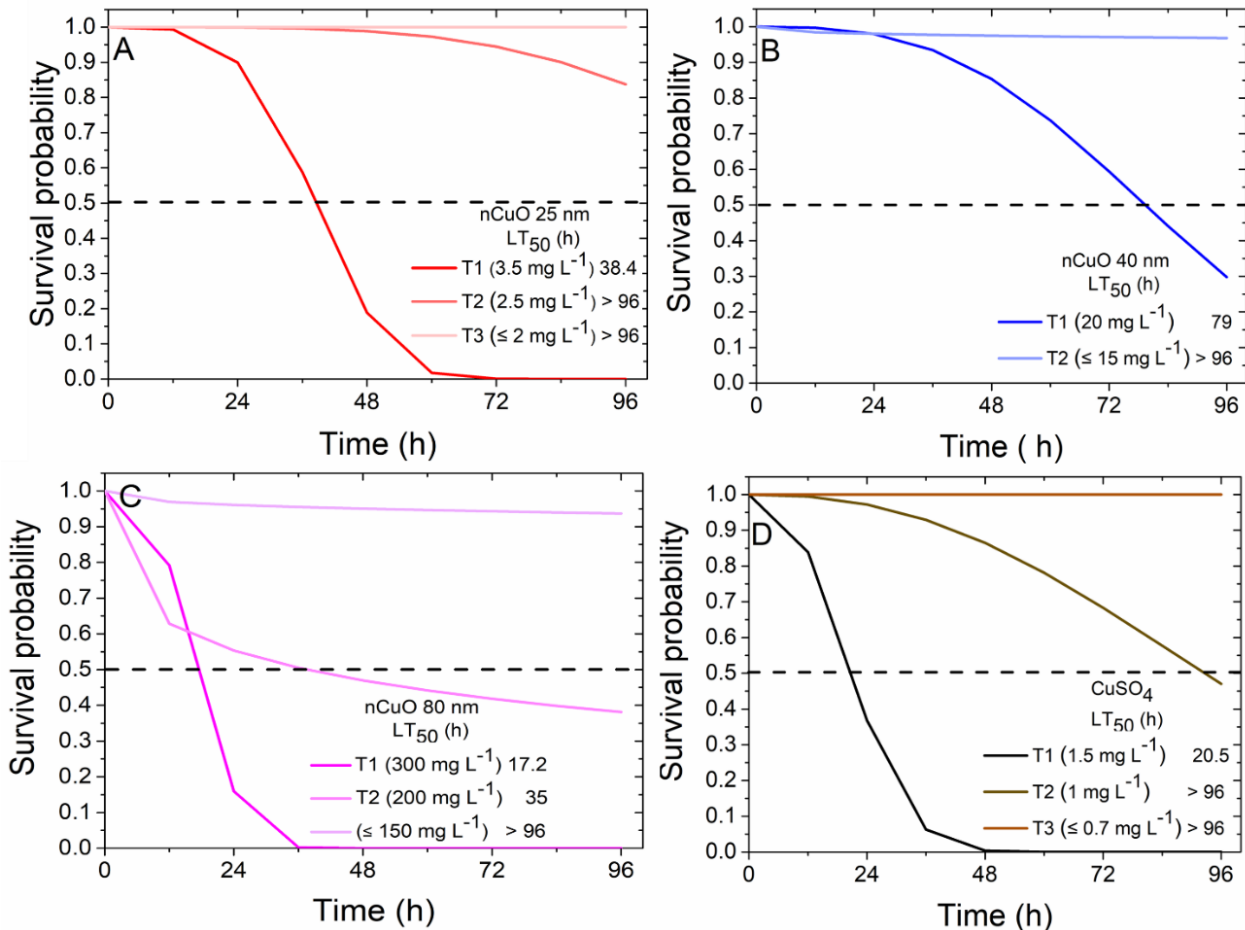
Treatment	a	b	LC <sub>50</sub>	LC <sub>10</sub>
nCuO 25 nm	5.63 ± 2.13	14.84 ± 5.73	2.39 ± 0.38	1.96 ± 0.30
nCuO 40 nm	-17.84 ± 6.04	16.33 ± 5.55	12.36 ± 1.09	10.32 ± 1.01
nCuO 80 nm	-12.82 ± 3.42	5.90 ± 1.58	149.03 ± 2.17	90.37 ± 1.95
CuSO <sub>4</sub>	0.67 ± 0.3	3.27 ± 1	0.62 ± 0.02	0.25 ± 0.06

On the other hand, zebrafish survival analyzes over time (Figure 4) show that there is significant difference for nCuO 25 nm ( $\chi^2 = 52.78$ ;  $df = 6$ ;  $p < 0.01$ ). The results indicate that, for nCuO 25 nm, only 70 h after the beginning of the experiment, 100% of T1 (3.5 mg Cu L<sup>-1</sup>) subjects were already dead. The second group - formed by T2 (2.5 mg Cu L<sup>-1</sup>) - presented

survival probability at the end of the experimental evaluation period of 0.83. The last group - consisting of treatments T3, T4, T5, T6, T7 ( $\leq 2 \text{ mg Cu L}^{-1}$ ) - had a survival probability of 1, after 96 h of the beginning of the trial. Van Den Belt et al. (2000) showed that the  $LT_{50}$  of zebrafish exposed to the 1000 and 2000  $\text{mg L}^{-1}$  of clay with cadmium for 144 h were 92 and 22 h, respectively.

The toxicity of metals is highly dependent on water quality parameters. The water pH can affect either the solubility and/or the speciation of metals (WITTERS, 1998). Boyle et al. (2020) investigated the toxicity of zebrafish embryos at acidic pH (5-7) exposed to copper oxide nanoparticles ( $< 90 \text{ nm}$ ). The authors concluded that the increase the toxicity is related to the amount of  $\text{Cu}^{2+}$  ions and that the acidic pH contributes to the dissolution of copper. However, in our study, the pH of the medium remained between 7.3 and 7.65 (Table 3) after the dispersion of the nCuO, which indicates that other mechanisms may be related to toxicity, such as the interaction between copper in culture medium.

Figure 4. Survival analyzes of *Danio rerio* over time subjected to nCuO, (A) 25 nm, (B) 40 nm, (C) 80 nm, and (D)  $\text{CuSO}_4$ , which  $-S(\text{time}) = \exp(-(\frac{\text{time}}{\delta}) \alpha)$ ,  $\delta =$  parameter of form;  $\alpha =$  scale parameter



The LC<sub>50</sub>s found in our study were  $2.40 \pm 0.38$  (25 nm),  $12.36 \pm 1.09$  (40 nm) and  $149.03 \pm 2.17$  (80 nm). The values found in the present study are higher than those reported by Griffitt et al. (2008) that found an LC<sub>50</sub> of  $0.94 \text{ mg L}^{-1}$  for adult fish exposed to CuO nanoparticles (15 - 45 nm) for 48 h. Another study presented LC<sub>50</sub> of  $1.5 \text{ mg L}^{-1}$  and  $0.25 \text{ mg L}^{-1}$  for 80 nm copper oxide and copper sulfate for 48 h, respectively (GRIFFITT et al., 2007).

Denluck et al. (2018) evaluated the effect of metallic copper and copper oxide nanoparticles (1.4 nm and < 50 nm, respectively) on embryonic zebrafish with and without the presence of chorion for 24 h and 120 h of exposition. The results showed that copper oxide nanoparticles is less toxic than copper nanoparticles regardless of chorion status and did not cause 100% mortality at even the highest exposure concentration ( $100 \text{ mg L}^{-1}$ ). However, the presence of the chorion inhibited Cu toxicity: the exposure without chorion to copper nanoparticles has an LC<sub>50</sub> of  $2.5 \pm 0.3 \text{ mg L}^{-1}$  compared to presence of chorion with LC<sub>50</sub> of  $13.7 \pm 0.8 \text{ mg L}^{-1}$ . Agglomerate size, zeta potential, and dissolved Cu did not sufficiently explain the differences in toxicity between copper nanoparticles and copper oxide nanoparticles; however, reactive oxygen species (ROS) generation did. Copper nanoparticles generated ROS in a concentration-dependent manner, while CuO nanoparticles did not and generated less than copper nanoparticles. The authors believe that the differences between the toxicities of copper nanoparticles and copper oxide nanoparticles are due in part to their ability to generate ROS, which could and should be a hazard consideration for risk assessments.

Thit et al. (2017) studied the effects of copper oxide nanoparticles (6 nm) using the parameters hatchability, zebrafish embryos mortality, and zebrafish fry mortality (4 days post-hatching) for 24 h exposure at 0 to 200  $\mu\text{M}$  concentration range. The LC<sub>50</sub>s for these parameters were  $0.5 \mu\text{M}$  ( $0.03175 \text{ mg Cu L}^{-1}$ ),  $10 \mu\text{M}$  ( $0.635 \text{ mg Cu L}^{-1}$ ), and  $> 200 \mu\text{M}$  ( $12.7 \text{ mg Cu L}^{-1}$ ), respectively. The authors concluded that the toxicity can be partially attributed to the dissolution of copper from nanoparticles.

Ganesan et al. (2016) investigated acute and sub-lethal effects in zebrafish embryos exposed to copper oxide nanoparticles (51 nm). The LC<sub>50</sub> is  $64 \text{ mg L}^{-1}$ , 48 h, and the sub lethal effects were evaluated at 40 and  $60 \text{ mg L}^{-1}$ . The results showed that embryos exposed to sub lethal dose accumulated (by atomic absorption spectroscopy)  $0.042$  and  $0.086 \mu\text{g Cu mg}^{-1}$ , respectively. Additionally, sub lethal effects consisted of heartbeat and hatching retarding, malformations of spinal cord and tail. These effects were more accentuated according to the increasing dose. The researchers suggested that the effects are

associated to the Cu dissolved in highest amount with the concentration. Kumari et al. (2017) showed that the LC<sub>50</sub> for embryos exposed to CuO nanoparticles (30 nm) for 72 h was 175 mg L<sup>-1</sup>.

Other authors have evaluated sub lethal effects on zebrafish embryos. Özel, Wallace and Andreescu (2014) explored the toxic effect of copper oxide (40 nm) in zebrafish embryos exposed at 1 to 100 ppm. At 50 to 100 ppm, 98% of the embryos fail to hatch and the effects of copper oxides nanoparticles on hatching rate are attributed to dissolved ions. Ions can pass through the chorion, increasing hatching interference.

Chang et al. (2015) studied the cell viability of zebrafish exposed at 1 to 100 µg Cu mL<sup>-1</sup> for 24 h from copper oxide nanoparticles 40 nm. The concentration of 100 µg Cu L<sup>-1</sup> reduced the cell viability to less than 80%. Sun et al. (2016), investigated the effects of CuO nanoparticles (50 - 60 nm) on zebra fish embryos, they were exposed to the treatments for 4 h after fertilization at concentrations of 1 to 50 mg L<sup>-1</sup> and evaluated after 24, 48 and 72 h. The results showed no malformation up to the concentration of 6.5 mg L<sup>-1</sup> in exposed embryos. Above 6.5 mg L<sup>-1</sup>, after 24 h, the embryos had not reached the primrose stage and the primary organs were hardly recognizable. After 48 h and 72 h, the embryos presented shorter body axis, reduced pigmentation, smaller eyes and noticeably larger calf sacs. As CuO NPs concentration increased, the more obvious abnormal phenotypes became. The hatching period was also evaluated and the hatching rates in the groups above 6.25 mg L<sup>-1</sup> were statistically lower than those exposed to the 1 mg L<sup>-1</sup> concentration.

Such differences were also noted in zebrafish embryos exposed to CuO nanoparticles (22-25 nm). After hatching, CuO NPs accumulated in the embryo's body, especially around the eyes and calf sacs which formed an exoskeleton structure around embryonic larvae, although no mortality was recorded. After 96 h, the hatching rate of embryos exposed to higher concentrations (2.6 mg L<sup>-1</sup>) was observed and extended to 120 h, however, the concentration did not affect hatching (HEINLAAN et al., 2016).

Xu et al. (2017) studied embryos exposed to CuO nanoparticles (500 nm) from 0.1 up to 50 mg L<sup>-1</sup> for 120 h. The results show that after hatching, the larvae exposed to 50 mg L<sup>-1</sup> presented shortened body length after 72, 96 and 120 h. The head and eyes decreased in size. The mortality of embryos exposed to 50 mg L<sup>-1</sup> was 60% at 24 h exposure and increased to approximately 80% at 120 h exposure. In the group exposed to 5 mg L<sup>-1</sup>, mortality increased to approximately 20% at 96 h and 40% at 120 h. Mortality in groups exposed to 0.1 and 0.5 mg L<sup>-1</sup> was below 20%. The authors suggested that mortality and larval size length due to dissolved copper are much more likely to be toxic than nanoparticles.

Likewise, Vicario-Parés et al. (2014) did not observe any significant decrease in survival of embryos exposed to 10 mg L<sup>-1</sup> CuO nanoparticles (> 100 nm). However, the LC<sub>50</sub> was 3.08 mg L<sup>-1</sup> for embryos exposed to ionic copper. Ionic copper also reduced the percentage of hatching at concentrations ranging from 0.1 to 10 mg L<sup>-1</sup>. At 0.1 mg Cu L<sup>-1</sup>, only about 40% of embryos could hatch, while at higher concentrations none of the surviving embryos were able to hatch. The study also suggested that ionic copper is related to malformations (edema and lesions on the tail of the yolk sac) caused at lower concentrations (0.1 mg Cu L<sup>-1</sup>) than other forms of copper and affected 100% of surviving embryos at concentrations of 1 and 5 mg Cu L<sup>-1</sup>.

As shown above, the release of ions seems to be the most acknowledged cause of toxicity by nanoparticles. Hence, nanoparticles act as a “Trojan horse” carrying the ions whose concentration increase end up harming the cells. In this sense, approaches that reduce the dissolution of nanomaterials could be a clever strategy to prevent toxic effects. Positively charged nanomaterials, due to their high attraction to negatively charged cell membranes, are more dangerous compared to negative charges. In addition to the intrinsic surface characteristics of nanomaterials, potential environmental discharge could lead to surface modifications by environmental molecules such as humic acids and organic matter. Such environmental modifications have been shown to alter the fate and transport of these nanomaterials and may lead to increased bioavailability and subsequent environmental toxicity in plants and aquatic organisms (LIN et al., 2018). Other researchers have indicated that copper nanoparticles are very highly reactive, and the toxic effects of nanocopper may result from this reactivity, possibly through metabolic alkalosis or intracellular dissolution of copper nanoparticles leading to high local ionic copper concentrations (GRIFFITT et al., 2008).

### **4.3.3 Total Cu inside zebrafish**

#### **4.3.3.1 Atomic absorption spectrophotometer**

Figure 5 shows the average concentration of copper found in the body of *D. rerio* exposed to LC<sub>50</sub> and LC<sub>100</sub> concentration of 25 nm, 40 nm, 80 nm nCuO and aqueous CuSO<sub>4</sub>. The regular concentration of copper in the body of the control group was 14.96 ± 4.42 mg Cu kg<sup>-1</sup>. A Pearson's correlation coefficient of 0.53 shows a weak positive correlation between the concentration of copper in the culture media and the concentration of copper found inside the organisms. However, if one considers only the groups control, CuSO<sub>4</sub> and 80 nm CuO the correlation coefficient increases to 0.73.

Figure 5. Average concentration of copper in the body of the *Danio rerio* (males and females are not distinguished) exposed to LC<sub>50</sub> and LC<sub>100</sub> of nCuO and CuSO<sub>4</sub> for acute assays. The asterisk indicates a significant difference in relation to the control Kruskal-Wallis  $p < 0.05$

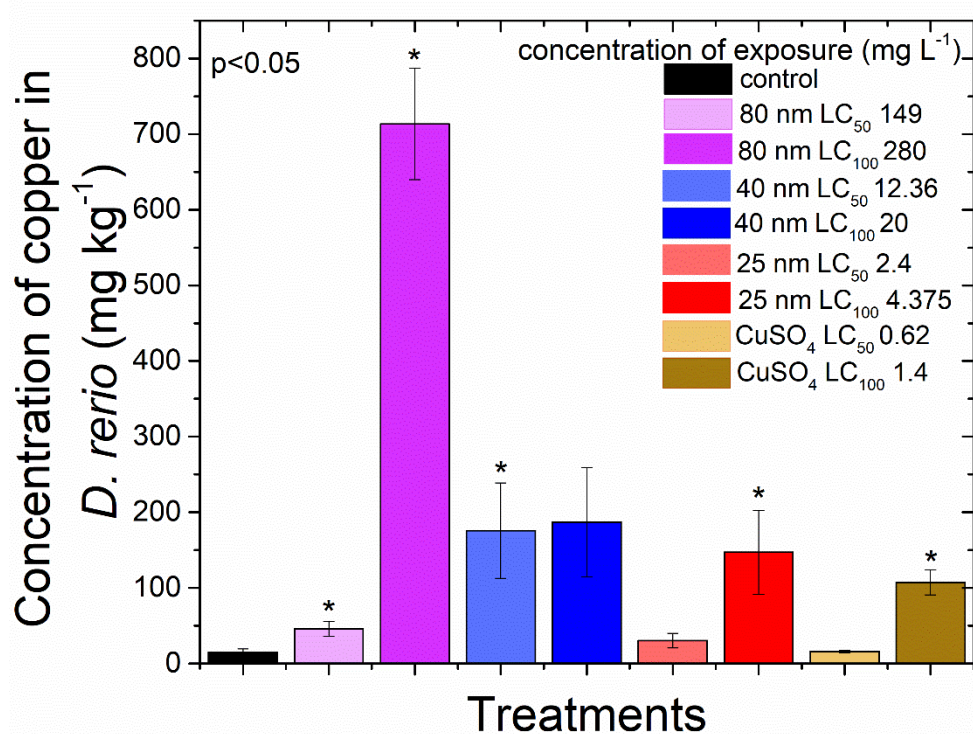
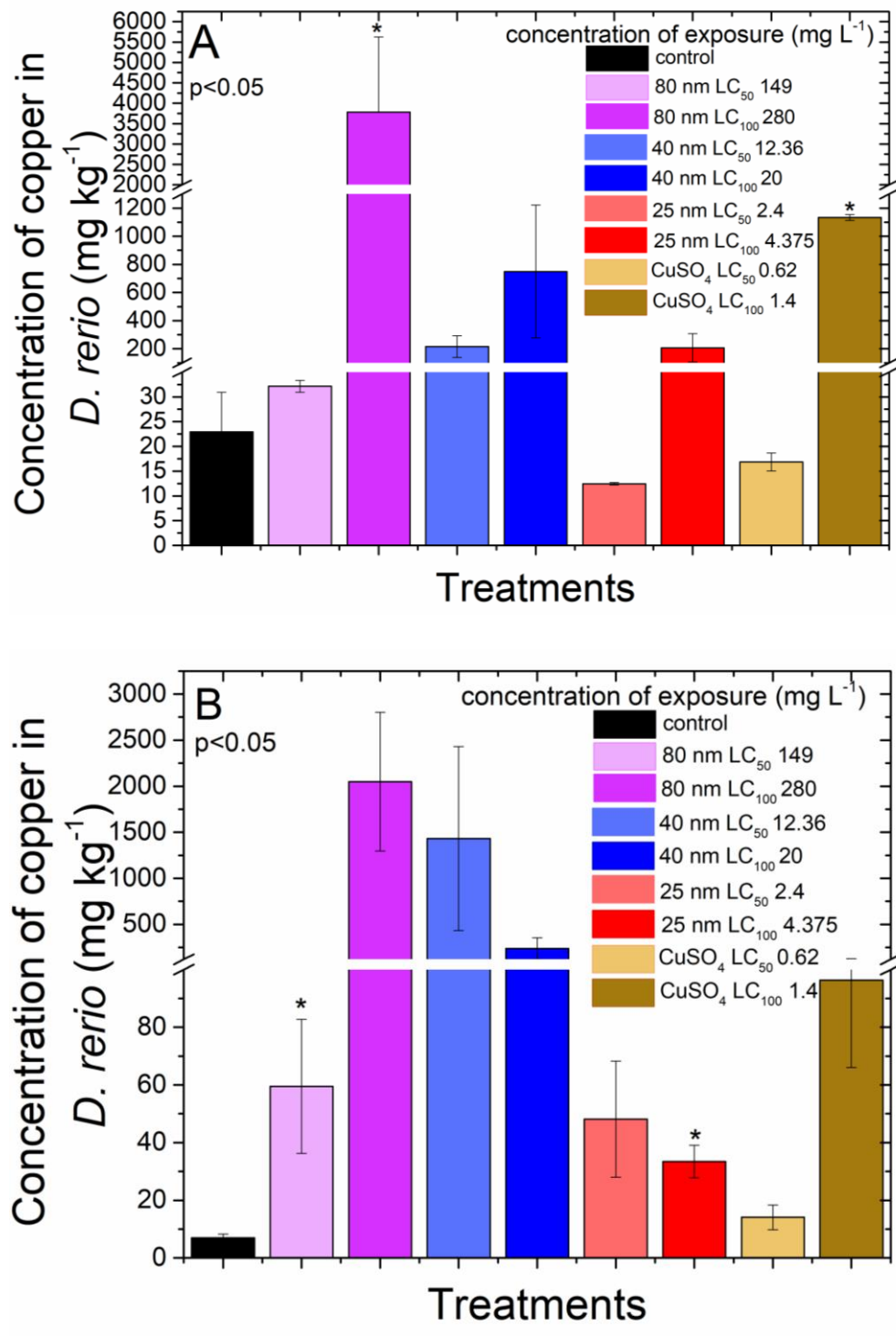


Figure 6 presents the concentration of copper found in the body of (A) males and (B) females *D. rerio*. Between males, there are statistical different in the 80 nm and CuSO<sub>4</sub> (both LC<sub>100</sub>) treatments to the control and between females, there are statistical different in the 80 nm LC<sub>50</sub> and 25 nm LC<sub>100</sub> to the control.

Figure 6. Average concentration of copper in the body of the *Danio rerio* (A) males and (B) females exposed to LC<sub>50</sub> and LC<sub>100</sub> of nCuO and CuSO<sub>4</sub> for acute assays. The asterisk indicates a significant difference in relation to the control Kruskal-Wallis  $p < 0.05$



The concentration copper in hepatocytes cells of zebrafish exposed to CuCl<sub>2</sub> for 24 h was determined by atomic absorption spectroscopy. Similar to our study, the hepatocytes with the highest copper concentration were those cells exposed to the highest concentrated treatment (30 mg Cu L<sup>-1</sup>); in this case the accumulation concentrations was 12.39 Cu ng 10<sup>6</sup> cells.

According to the these authors, hepatocytes cells are more resist to the copper than zebrafish embryos; this justified the exposure dose and the accumulation copper in the cells Sandrini et al. (2009).

Wang et al. (2014) also reported higher copper concentration in the liver of *Epinephelus coioides* (Pisces: Serranidae), exposed, for 25 days, to copper nanoparticles and CuSO<sub>4</sub>. The *E. coioides* juveniles were exposed to copper nanoparticles (10 – 30 nm) at 100 mg Cu L<sup>-1</sup> and the accumulation of copper was determined by ICP-OES. The results showed an approximate concentration of 15 mg Cu kg<sup>-1</sup> in liver, 10 mg Cu kg<sup>-1</sup> in stomach, 8 mg Cu kg<sup>-1</sup> in intestine, 2 mg Cu kg<sup>-1</sup> in muscle, 6 mg Cu kg<sup>-1</sup> in gills, 3 mg Cu kg<sup>-1</sup> in skin and 2.7 mg Cu kg<sup>-1</sup> the remaining tissues, for copper nanoparticles treatment. These figures are below the copper concentration range reported in the present study. The CuSO<sub>4</sub> treatment showed concentrations of 25 mg Cu kg<sup>-1</sup> in liver, 15 mg Cu kg<sup>-1</sup> in stomach, 7.8 mg Cu kg<sup>-1</sup> in intestine, 12 mg Cu kg<sup>-1</sup> in gills, 5.5 mg Cu kg<sup>-1</sup> in skin and 2.3 mg Cu kg<sup>-1</sup> in the remaining tissues (all the remaining parts of fish such as head, bone, fins, etc).

The study of plasma total of *Cyprinus carpio* (Pisces: Cyprinidae) exposed to CuSO<sub>4</sub> and copper nanoparticles (40 nm) for 14 days showed that the exposure of CuSO<sub>4</sub> and copper nanoparticles led to significant increase in total plasma copper levels. The values were of 110 µg Cu dL<sup>-1</sup> and 80 µg Cu dL<sup>-1</sup>, respectively, for 0.25 mg Cu L<sup>-1</sup> exposure dose (HEDAYATI; HOSEINI; HOSEINIFAR, 2016).

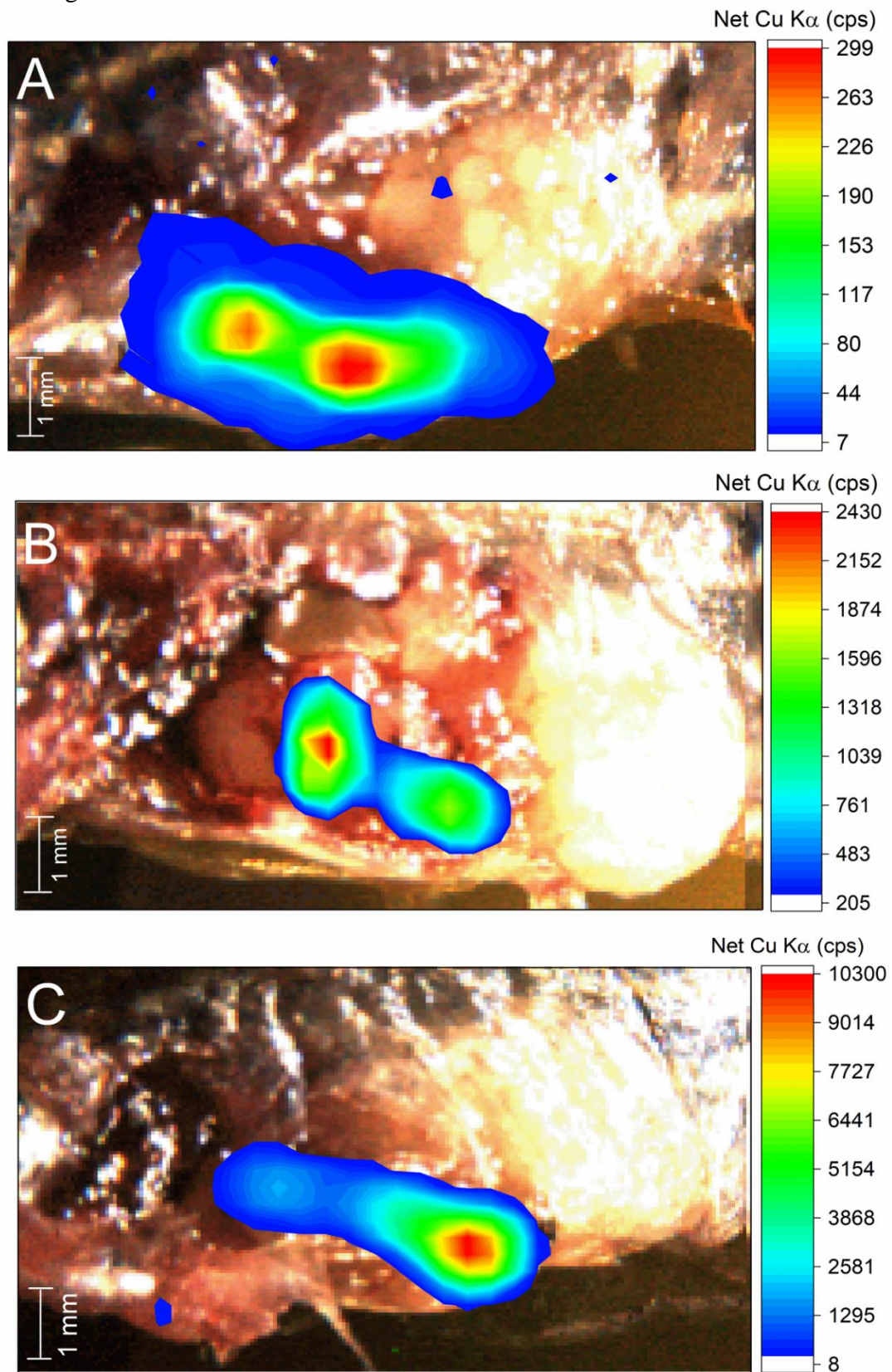
Mages et al. (2008) evaluated the inner concentration of embryos zebrafish exposed to Zn (3.3 g Zn kg wet sediment) for 48 h by TXRF. The results showed that the concentration inside embryos exposed to sediment + sand range of 125 to 5860 µg Zn g<sup>-1</sup> with median of 331 mg Zn kg<sup>-1</sup>.

#### **4.3.4 Spatial distribution of Cu inside *Danio rerio* X-ray fluorescence microanalysis (µ-XRF)**

Figure 7 shows copper spatial distribution within *D. rerio* exposed to nCuO at LC<sub>100</sub> for 96 h. The chemical images show that regardless the treatment, copper is mostly present at the gastric system (liver, spleen and stomach) and posterior gut. Copper accumulation in the liver is expected as this organ generally accumulates substances considered toxic.



Figure 7. X-ray fluorescence reveals the spatial distribution of copper inside zebrafish exposed to nCuO at LC<sub>100</sub>. (A) 25 nm nCuO, 3.5 mg L<sup>-1</sup>, (B) 40 nm nCuO 20 mg L<sup>-1</sup>, (C) 80 nm nCuO 280 mg L<sup>-1</sup>



Little is known about metal distribution and internalization in zebrafish. Histological analysis carried out by Griffitt et al. (2007) found, differently from the present study, copper accumulated in the gills of adult fish exposed to 80 nm copper oxide nanoparticles.

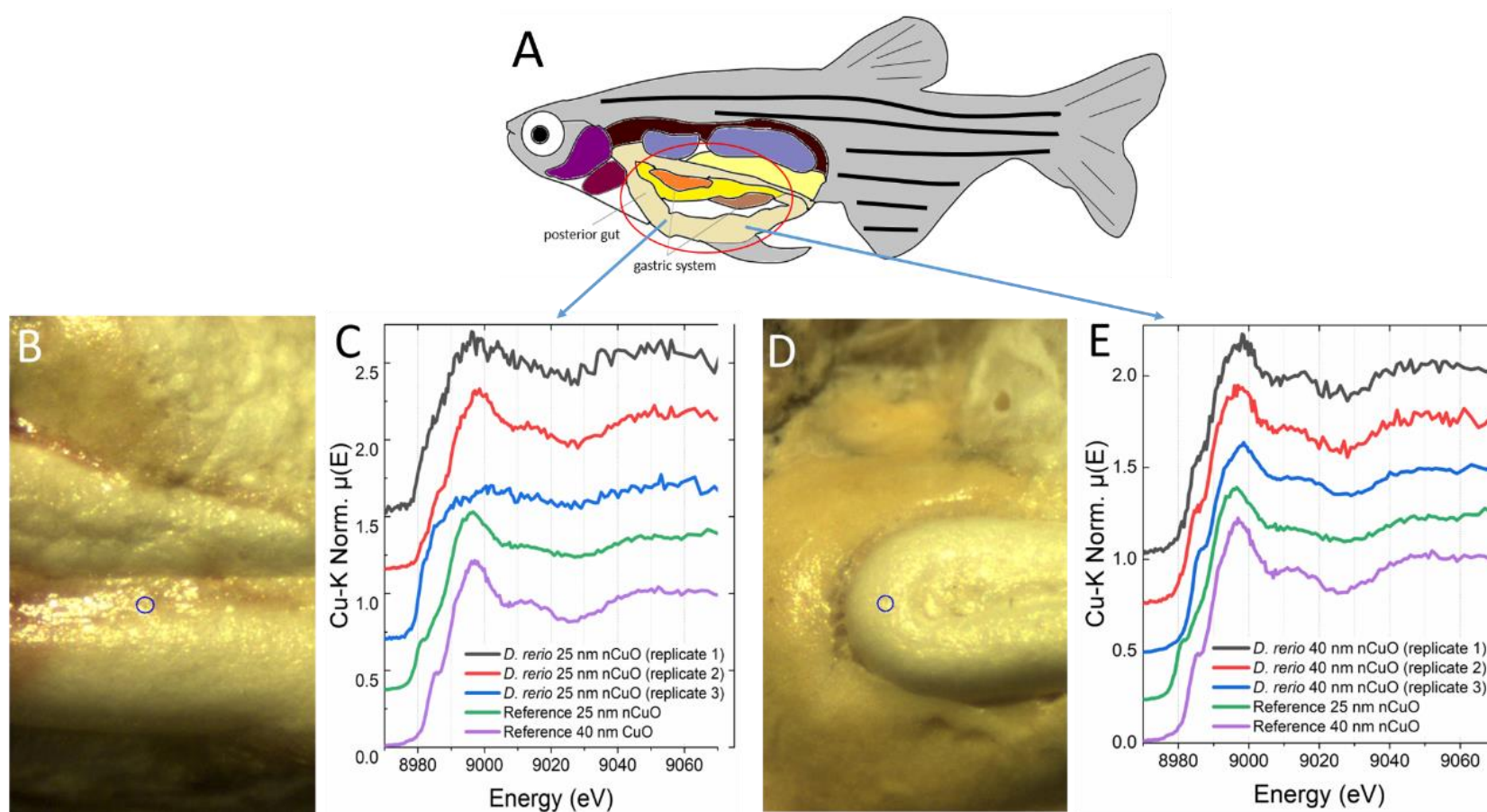
Other studies focus their research on zebrafish embryos, which is also widely used in ecotoxicological assays. Böhme et al. (2017) studied metal interactions and the uptake of different oxides metal-composed nanoparticles at different compartments in the zebrafish embryos. It was applying laser ablation ICP-MS and electron microscopy in the zebrafish embryos exposed to 60  $\mu\text{g}$  element per  $\text{L}^{-1}$  of nanoparticles. After exposure to nanoparticles, copper ( $132 \pm 2$  nm) was detected on the chorion and in the embryo. Denluck et al. (2018) evaluated the accumulation of copper in embryos zebrafish at the presence and absence of chorion by ICP-MS. The concentration of exposure at 10 mg Cu  $\text{L}^{-1}$  of copper oxide nanoparticles is  $0.18 \pm 0.01$   $\mu\text{g}$  Cu/fish compared to 2.4  $\mu\text{g}$  Cu/chorion. The exposure of presence of chorion at the same concentration is  $0.028 \pm 0.004$   $\mu\text{g}$ /fish which was not different to the control with  $0.0099 \pm 0.0006$   $\mu\text{g}$  Cu/fish. Similarly, Lin et al. (2011) studied hatching rate and CuO nanoparticles (18 nm) concentration inside and outside the chorion of zebrafish embryos by ICP-MS. Results showed that 50% decrease in hatching rate from 0.5 mg  $\text{L}^{-1}$  and after 1 h of exposure to 50 mg  $\text{L}^{-1}$ ,  $0.85 \pm 0.18$  mg  $\text{L}^{-1}$  was found inside the chorion and  $2.22 \pm 0.16$  mg  $\text{L}^{-1}$  outside the chorion; after 24 h  $9.99 \pm 0.24$  mg  $\text{L}^{-1}$  inside the chorion and  $3.77 \pm 0.37$  mg  $\text{L}^{-1}$  outside the chorion.

The distribution investigation of elements of embryos zebrafish exposed to a mixture of  $\text{CH}_3\text{Hg(II)}$ ,  $\text{As(III)}$ ,  $\text{Ag(I)}$  and  $\text{Cd(II)}$  by laser ablation. Images obtained showed  $\text{Cd(II)}$  and  $\text{CH}_3\text{Hg(II)}$  can be clearly seen and the distribution is homogeneous throughout the body, with hotspots in the area of the eye for  $\text{Cd(II)}$  and along the digestive tract for methylmercury, similarly to the present study Böhme et al. (2015).

#### **4.3.5 Microprobe X-ray absorption near edge spectroscopy ( $\mu$ -XANES) applied zebrafish**

The chemical speciation of the Cu taken up by the zebrafish was analyzed by measuring XANES on the Cu K edge. Figure 8 shows the spectra recorded for zebrafish exposed to 25 and 40 nCuO at  $\text{LC}_{100}$ . The spectra were measured at the concentration hotspots previously revealed by  $\mu$ -XRF. According to the spectra, zebrafish exposed to these treatments concentrated copper at the same form of nanoparticles (reference 25 nm and 40 nm nCuO). In the other words, there is not transformation of copper inside the zebrafish after 96 h of exposition.

Figure 8. (A) *Danio rerio* (zebrafish) inner scheme, (B, D) region XANES analysis of the zebrafish exposed to nCuO for 96 h and (C, E) spectra generated by XANES analysis of zebrafish exposed to 25 nm ( $3.5 \text{ mg L}^{-1}$ ) and 40 nm ( $20 \text{ mg L}^{-1}$ ) nCuO, per replicate, respectively



There are few reports on the chemical transformation of metals in fish, none studied on copper was found. The species most used in XAS analysis is the trout *Oncorhynchus mykiss* (Pisces, Salmonidae). Differently from the present study, some of them observed changes in the chemical species of metal and metalloids. Misra et al. (2012) evaluated the selenium chemical speciation in trout, the individuals were fed with Se-methionine ( $40 \text{ mg kg}^{-1}$ ) for two weeks through the diet. XANES determined that Se-methionine, Se-cystine and Se-cysteine were the predominant forms of selenium in all tissues; however, their relative proportion varied. Se-methionine was found in about 30 to 40% of all tissues analyzed. However, Se-cystine and Se-cysteine accumulated in about 25 to 60% and 10 to 20% of all tissues analyzed, respectively. Hence, the results showed that Se-methionine was metabolized inside trout.

Saibu et al. (2018) studied the distribution and chemical speciation in trout exposed to Zn salts by  $\mu$ -XRF and  $\mu$ -XANES, respectively. The fishes were exposed to Zn ( $1 \text{ mg L}^{-1}$ ); Zn ( $1 \text{ mg L}^{-1}$ ) + Cd ( $20 \text{ }\mu\text{g L}^{-1}$ ) and Zn ( $1 \text{ mg L}^{-1}$ ) + Cu ( $100 \text{ }\mu\text{g L}^{-1}$ ) through water by 24 h. In this study, the gills were the main spots of Zn accumulation. The  $\mu$ -XANES results recorded in this tissue showed the presence of Zn-phosphate, Zn-histidine, and Zn-cysteine.

Beauchemin et al. (2004) studied chemical speciation hepatic of trout exposed to Zn through diet by X-ray absorption spectroscopy (XAS). Juveniles trout were exposed to  $200 \text{ }\mu\text{g Zn L}^{-1}$  for 14 days, then  $370 \text{ }\mu\text{g Zn L}^{-1}$  for 23 days. The control consisted in trout exposed to  $10 \text{ }\mu\text{g Zn L}^{-1}$ . In the end of exposure, the spectra were recorded in the livers. The results showed that the concentration was larger in livers exposed to Zn treatment ( $22 \text{ mg Zn kg}^{-1}$ ) when compared to control (*ca.*  $14 \text{ mg Zn kg}^{-1}$ ). The chemical speciation was similar in both group that presented Zn-cysteine as predominant chemical species.

Kuwabara et al. (2007) evaluated fish from the Guadalupe Reservoir, California, and Lahontan Reservoir, Nevada, U.S.A.; both affected by the legacy of gold and silver mining in the Sierra Nevada during the nineteenth century. XANES clearly indicated that the accumulated mercury in these fish were in the form of methylmercury and mercury-cysteine complexes in the muscle tissues of piscivorous freshwater fish from two regions affected by reservoir mining. This result suggests that bioaccumulated mercury speciation at high trophic levels is consistent over a wide range of ionic forces and mercury sources.

Our results show that, under the described experimental conditions, no chemical transformation of copper was detected in the zebrafish. This fact may be related to some factors related to ecotoxicology such as exposure time, the source of copper, and the concentration of copper into zebrafish.

#### 4.4 Partial Conclusions

The various techniques and analyzes used in this study show that fish exposed to copper sources can absorb and accumulate copper in the gastric system as well as cause mortality.

This result can be explained by the characteristics of the copper sources used in the study. Among the copper sources evaluated, 25 nm nanoparticles and CuSO<sub>4</sub> showed higher toxicity for zebrafish which can be explained by the metal structure and the high reactivity and with the highest degree of dissolution, respectively.

The highest total copper concentration in fish occurred at the highest exposure concentrations. The total Cu concentration found in the body of individuals exposed to 80 nm nCuO was in the order hundreds of mg kg<sup>-1</sup>, however it presented the highest LC<sub>50</sub> value. XANES clearly showed it was not possible to detect any transformation from CuO to any other chemical form; nevertheless, one has to keep in mind that XANES sensitivity for the Cu-K edge would hardly detected fractions Cu species present below 5 wt%. Hence, in the present study, one can conclude that the toxic effects were more dependent on the chemical availability of Cu than on the total Cu concentration.

#### References

- ALPHANDÉRY, E. Natural metallic nanoparticles for application in nano-oncology. **International Journal of Molecular Sciences**, v. 21, n. 12, art. 4412, 2020.
- ANDREANI, T. et al. Ecotoxicity to freshwater organisms and cytotoxicity of nanomaterials: Are we generating sufficient data for their risk assessment? **Nanomaterials**, v. 11, n. 1, p. 1-25, 2021.
- BAEK, Y. W.; AN, Y. J. Microbial toxicity of metal oxide nanoparticles (CuO, NiO, ZnO, and Sb 2O 3) to Escherichia coli, Bacillus subtilis, and Streptococcus aureus. **Science of the Total Environment**, v. 409, p. 1603-1608, 2011.
- BEAUCHEMIN, S. et al. Speciation of Hepatic Zn in Trout Exposed to Elevated Waterborne Zn Using X-ray Absorption Spectroscopy. **Environmental Science and Technology**, v. 38, p. 1288-1295, 2004.
- BÖHME, S. et al. Exploring LA-ICP-MS as a quantitative imaging technique to study nanoparticle uptake in Daphnia magna and zebrafish (Danio rerio) embryos. **Analytical and Bioanalytical Chemistry**, v. 407, p. 5477-5485, 2015.
- BÖHME, S. et al. Metal uptake and distribution in the zebrafish (Danio rerio) embryo: Differences between nanoparticles and metal ions. **Environmental Science: Nano**, v. 4, p. 1005-1015, 2017.

BOYLE, D.; CLARK, N. J.; HANDY, R. D. Toxicities of copper oxide nanomaterial and copper sulphate in early life stage zebrafish: Effects of pH and intermittent pulse exposure. **Ecotoxicology and Environmental Safety**, v. 190, art. 109985, 2020.

BUFFET, P. E. et al. Behavioural and biochemical responses of two marine invertebrates *Scrobicularia plana* and *Hediste diversicolor* to copper oxide nanoparticles. **Chemosphere**, v. 84, p. 166-174, 2011.

BUFFET, P. E. et al. A mesocosm study of fate and effects of CuO nanoparticles on endobenthic species (*Scrobicularia plana*, *Hediste diversicolor*). **Environmental Science and Technology**, v. 47, p. 1620-1628, 2013.

CHANG, J. et al. Copper oxide nanoparticles reduce vasculogenesis in transgenic Zebrafish through down-regulation of vascular endothelial growth factor expression and induction of apoptosis. **Journal of Nanoscience and Nanotechnology**, v. 15, p. 2140-2147, 2015.

CHATTOPADHYAY, I. Application of nanoparticles in drug delivery. In: SIDDHARDHA, B.; DYAVAIHAH, M.; KASINATHAN, K. (Ed.). **Model organisms to study biological activities and toxicity of nanoparticles**. Singapore: Springer Singapore, 2020. p. 35–57.

DENLUCK, L. et al. Reactive oxygen species generation is likely a driver of copper based nanomaterial toxicity. **Environmental Science: Nano**, v. 5, p. 1473-1481, 2018.

DING, J. et al. Exposure of CuO nanoparticles and their metal counterpart leads to change in the gut microbiota and resistome of collembolans. **Chemosphere**, v. 258, art. 127347, 2020.

DONG, C. et al. The Coppery Age: Copper (Cu)-Involved Nanotheranostics. **Advanced Science**, v. 7, n. 21, art. 2001549, 2020.

GANESAN, S. et al. Acute and sub-lethal exposure to copper oxide nanoparticles causes oxidative stress and teratogenicity in zebrafish embryos. **Journal of Applied Toxicology**, v. 36, p. 554-567, 2016.

GHENO, E. M. et al. Zebrafish in Brazilian Science: Scientific Production, Impact, and Collaboration. **Zebrafish**, v. 13, p. 217-225, 2016.

GRIFFITT, R. J. et al. Exposure to copper nanoparticles causes gill injury and acute lethality in zebrafish (*Danio rerio*). **Environmental Science and Technology**, v. 41, p. 8178-8186, 2007.

GRIFFITT, R. J. et al. Effects of particle composition and species on toxicity of metallic nanomaterials in aquatic organisms. **Environmental Toxicology and Chemistry**, v. 9, p. 1972-1978, 2008.

HEDAYATI, A.; HOSEINI, S. M.; HOSEINIFAR, S. H. Response of plasma copper, ceruloplasmin, iron and ions in carp, *Cyprinus carpio* to waterborne copper ion and nanoparticle exposure. **Comparative Biochemistry and Physiology Part C: Toxicology and Pharmacology**, v. 179, p. 87-93, 2016.

HEINLAAN, M. et al. Toxicity of nanosized and bulk ZnO, CuO and TiO<sub>2</sub> to bacteria *Vibrio fischeri* and crustaceans *Daphnia magna* and *Thamnocephalus platyurus*. **Chemosphere**, v. 71, p. 1308–1316, 2008.

HEINLAAN, M. et al. Natural water as the test medium for Ag and CuO nanoparticle hazard evaluation: An interlaboratory case study. **Environmental Pollution**, v. 216, p. 689-699, 2016.

HEMMAT ESFE, M.; BAHIRAEI, M.; MIR, A. Application of conventional and hybrid nanofluids in different machining processes: A critical review. **Advances in Colloid and Interface Science**, v. 282, art.102199, 2020.

HOU, J. et al. Ecotoxicological effects and mechanism of CuO nanoparticles to individual organisms. **Environmental Pollution**, v. 221, p. 209–217, 2017.

JIA, H. R. et al. Nanomaterials meet zebrafish: Toxicity evaluation and drug delivery applications. **Journal of Controlled Release**, v. 311-312, p. 301-318, 2019.

KASEMETS, K. et al. Toxicity of nanoparticles of ZnO, CuO and TiO<sub>2</sub> to yeast *Saccharomyces cerevisiae*. **Toxicology in Vitro**, v. 23, p. 1116-1122, 2009.

KUMARI, P. et al. Mechanistic insight to ROS and Apoptosis regulated cytotoxicity inferred by Green synthesized CuO nanoparticles from *Calotropis gigantea* to Embryonic Zebrafish. **Scientific Reports**, v.7, art. 16284, 2017.

KUWABARA, J. S. et al. Mercury speciation in piscivorous fish from mining-impacted reservoirs. **Environmental Science and Technology**, v. 41, p. 2745-2749, 2007.

LIN, S. et al. High content screening in zebrafish speeds up hazard ranking of transition metal oxide nanoparticles. **ACS Nano**, v. 5, p. 7284-7295, 2011.

LIN, S. et al. Nanomaterials Safer-by-Design: An Environmental Safety Perspective. **Advanced Materials**, v. 30, n. 17, art. 1705691, 2018. Special issue.

LIPPARD, S. J.; BERG, J. M. **Principles of Bioinorganic Chemistry**. Mill Valley: University Science Books, 1994. p. 411: Physical Methods in Bioinorganic Chemistry.

LIU, P. C. et al. Dissolution of Cu nanoparticles and antibacterial behaviors of TaN-Cu nanocomposite thin films. **Thin Solid Films**, v. 517, n. 17, p. 4956–4960, 2009.

MAGES, M. et al. Zinc and cadmium accumulation in single zebrafish (*Danio rerio*) embryos - A total reflection X-ray fluorescence spectrometry application. **Spectrochimica Acta - Part B Atomic Spectroscopy**, v. 63, p. 1443-1449, 2008.

MILLER, G.; SENJEN, R. **Out of the laboratory and on to our plates: Nanotechnology in food & agriculture**. 2. ed. Collingwood, VIC, 2008. 68 p.

MISRA, S. et al. Tissue-specific accumulation and speciation of selenium in rainbow trout (*Oncorhynchus mykiss*) exposed to elevated dietary selenomethionine. **Comparative Biochemistry and Physiology - C Toxicology and Pharmacology**, v. 155, p. 560-565, 2012.

MORTIMER, M.; KASEMETS, K.; KAHRU, A. Toxicity of ZnO and CuO nanoparticles to ciliated protozoa *Tetrahymena thermophila*. **Toxicology**, v. 269, p. 182-189, 2010.

MOTELICA, L. et al. Smart food packaging designed by nanotechnological and drug delivery approaches. **Coatings**, v. 10, p. 806, 2020.

NNAMDI, A. H. et al. Antagonistic effects of sublethal concentrations of certain mixtures of metal oxide nanoparticles and the bulk (Al<sub>2</sub>O<sub>3</sub>, CuO, and SiO<sub>2</sub>) on gill histology in *clarias gariepinus*. **Journal of Nanotechnology**, v. 2019, art. 7686597, 2019.

ORGANISATION FOR ECONOMIC CO-OPERATION AND DEVELOPMENT - OECD. **Guidelines for Testing of Chemicals - OECD 203: Fish, Acute Toxicity Test**. Paris, 1992. 9 p.

ÖZEL, R. E.; WALLACE, K. N.; ANDREESCU, S. Alterations of intestinal serotonin following nanoparticle exposure in embryonic zebrafish. **Environmental Science: Nano**, v. 1, p. 27-36, 2014.

RAVEL, B.; NEWVILLE, M. ATHENA, ARTEMIS, HEPHAESTUS: Data analysis for X-ray absorption spectroscopy using IFEFFIT. **Journal of Synchrotron Radiation**, v. 12, p. 537–541, 2005.

RUSAKOVA, E. et al. Comparative evaluation of acute toxicity of nanoparticles of zinc, copper and their nanosystems using *Stylonychia mytilus*. **Oriental Journal of Chemistry**, v. 31, 2015. Special issue 1.13. Doi: <http://dx.doi.org/10.13005/ojc/31>.

SAGADEVAN, S. et al. Synthesis and evaluation of the structural, optical, and antibacterial properties of copper oxide nanoparticles. **Applied Physics A: Materials Science and Processing**, v. 125, art. 489, 2019.

SAIBU, Y. et al. Distribution and speciation of zinc in the gills of rainbow trout (*Oncorhynchus mykiss*) during acute waterborne zinc exposure: Interactions with cadmium or copper. **Comparative Biochemistry and Physiology Part - C: Toxicology and Pharmacology**, v. 206-207, p. 23-31, 2018.

SAKUMA, M. Probit analysis of preference data. **Applied Entomology and Zoology**, v. 33, n. 3, p. 339–347, 1998.

SANDRINI, J. Z. et al. Reactive oxygen species generation and expression of DNA repair-related genes after copper exposure in zebrafish (*Danio rerio*) ZFL cells. **Aquatic Toxicology**, v. 95, p. 285-291, 2009.

SANTOS-RASERA, J. R. et al. Toxicity, bioaccumulation and biotransformation of Cu oxide nanoparticles in *Daphnia magna*. **Environmental Science: Nano**, v. 6, p. 2897-2906, 2019.

SARRET, G. et al. Zinc distribution and speciation in *Arabidopsis halleri* × *Arabidopsis lyrata* progenies presenting various zinc accumulation capacities. **New Phytologist**, v. 184, n. 3, p. 581–595, 2009.



SHARMIN, E. et al. Linseed polyol-assisted, microwave-induced synthesis of nano CuO embedded in polyol-polyester matrix: antifungal behavior and coating properties. **Progress in Organic Coatings**, v. 105, p. 200-211, 2017.

SUN, Y. et al. Effects of copper oxide nanoparticles on developing zebrafish embryos and larvae. **International Journal of Nanomedicine**, v. 11, p. 905-918, 2016.

TAVARES, B.; SANTOS LOPES, S. The importance of Zebrafish in biomedical research. **Acta Medica Portuguesa**, v. 26, p. 583-592, 2013.

THAKUR, S. et al. Growth mechanism and characterization of CuO nanostructure as a potent Antimicrobial agent. **Surfaces and Interfaces**, v. 20, art. 100551, 2020.

THERNEAU, T. M.; LUMLEY, T. **R Package. Survival Analysis**. 2021. Available at: <https://cran.r-project.org/web/packages/survival/survival.pdf>.

THIT, A. et al. Effects of copper oxide nanoparticles and copper ions to zebrafish (*Danio rerio*) cells, embryos and fry. **Toxicology in Vitro**, v. 45, p. 89-100, 2017.

VAN DEN BELT, K.; VAN PUymbROECK, S.; WITTERS, H. Toxicity of cadmium-contaminated clay to the zebrafish *Danio rerio*. **Archives of Environmental Contamination and Toxicology**, v. 38, p. 191-196, 2000.

VICARIO-PARÉS, U. et al. Comparative toxicity of metal oxide nanoparticles (CuO, ZnO and TiO<sub>2</sub>) to developing zebrafish embryos. **Journal of Nanoparticle Research**, v. 16, art. 2550, 2014.

VOLLAND, M. et al. Synthesis methods influence characteristics, behaviour and toxicity of bare CuO NPs compared to bulk CuO and ionic Cu after in vitro exposure of *Ruditapes philippinarum* hemocytes. **Aquatic Toxicology**, v. 199, p. 285-295, 2018.

WANG, T. et al. The potential toxicity of copper nanoparticles and copper sulphate on juvenile *Epinephelus coioides*. **Aquatic Toxicology**, v. 152, p. 96-104, 2014.

WITTERS, H. E. Chemical speciation dynamics and toxicity assessment in aquatic systems. **Ecotoxicology and Environmental Safety**, v. 41, p. 90-95, 1998.

XU, J. et al. The effects of copper oxide nanoparticles on dorsoventral patterning, convergent extension, and neural and cardiac development of zebrafish. **Aquatic Toxicology**, v. 188, p. 130-137, 2017.



## 5 GENERAL CONCLUSIONS

The ecotoxicity of nanomaterials in aquatic model organisms proved to be a complex and provocative issue in the environmental area. The present study focused on X-ray fluorescence (XRF) and X-ray absorption (XAS) techniques - the latter never applied to daphnids and zebrafish - to understand part of this complexity - in addition to toxicity tests.

Regarding the hypotheses, the nanoparticles showed less toxicity than sulphate sources tested in this study. In comparison with other compounds present in industry, the toxicity is less than or equal to compounds of different chemical classes. Among nanomaterials, the toxicity of nCuO, both in daphnids and zebrafish, was higher in smaller nanoparticles. As for nZnO, toxicity was related to the presence of surfactant, being considered less toxic. This last result shows that probably the toxicity is related to the formation of aggregates that inhibited their availability and the surfactant can change the action of the nanoparticles to a less aggressive toxicity inside the organism. Thus, the presence of surfactants in these compounds is something to be considered. In summary, the nanomaterials and sulphate sources tested are toxic to aquatic organisms. Therefore, the concentration and exposure time of these compounds in the environment deserve more attention.

Daphnids exposed to copper sulphate showed morphological difference in the carapace (ruptures), which probably must have occurred due to the presence of soluble copper ions. Despite the differences in morphology, the spatial distribution of copper from nCuO in daphnids and zebrafish was similar. The copper remained in the region of the intestine and in the gastro intestinal tract, respectively. The distribution of zinc from nZnO in daphnids was also located in the intestine region, however no zinc clearance was observed. In daphnids and zebrafish, the absence of copper and zinc from nanoparticles in other tissues, indicates that these elements were absorbed by the intestine and the gastro intestinal tract, respectively, and there was no detectable transport to other parts of the organisms.

However, this absence may be due to the concentration of copper and zinc below the detection limits ( $8 \mu\text{g Zn cm}^{-2}$  and  $2.94 \text{ Cu } \mu\text{g cm}^{-2}$ ) by XRF technique. Lower limits of detection could be achieved by increasing the X-ray flux density, integration time, or detector solid angles. Further studies could be carried out at synchrotron facilities that could also offer nanosized beam that would allow mapping sections of the intestine. In addition, other XRF-derived techniques could be made, such as 3D measurements by tomography.

The chemical speciation of copper from nCuO inside daphnids and zebrafish, the after the toxicity assay, show that there was no change in the chemical environment; except for nCuO

25 nm in acute assay on *D. magna*, in which the chemical environment changed to  $\text{Cu}_3(\text{PO}_4)_2$ . Nevertheless, one shall keep in mind the relatively low sensitivity of XAS that would hardly detect compounds whose weigh fraction are below than 5%. Similar to the XRF technique, smaller beam size for XAS analysis, it can be an alternative for obtaining data more detailed information on the chemical environment of these organisms, especially in regions with lower concentration of the element of interest. Alternative sample preparation, eg samples under cryogenic conditions, could also be done with samples with low concentrations, in addition to measurements with organic compounds as a reference.

In general, the results presented in this study show that daphnids and zebrafish ingest nanoparticles present in the exposed medium in the form of agglomerates, accumulation occurs and they are not expelled for long hours. In daphnids, smaller nanoparticles can change the chemical speciation within the body after the exposure time, which may justify the greater toxicity of the smaller nanoparticles. Although this work has shown an innovative result, there are still gaps in this field that can perhaps be filled with enzymatic analysis and/or microscopy within the intestine inside organisms after exposure to find out how these compounds are in these tissues.

Finally, the use of multi-element techniques, such XRF and XAS in the aquatic ecotoxicology area is relatively new. This study was the first to use XAS in model aquatic organisms and discover its chemical environment after exposure to nanomaterials. In the field of aquatic ecotoxicology, based on the results presented from these techniques, the trend and the challenge is to focus on methods of analysis with a live model organism to know what the response is presented in real time. In this way, it will be possible to better understand the complexity of the mechanisms of toxicity and avoid/or reverse a possible scenario of aquatic environmental accident and to support the environmental agencies with information and measures to be adopted on nanomaterials.

As final considerations, after accessing a wide range of techniques and analyzes that show the interaction between compounds/organisms, the future of the environmental area and ecotoxicology is to show the conscious use of compounds containing nanomaterials. If used sparingly, they can be beneficial in several areas; otherwise, they can cause irreversible damage to species and the environment.

**ANNEXES**



## Annex A – Permission to reuse in Thesis

11/05/2021

Manage Account



Marketplace™

Special Requests &gt; Special Request Details

Review Cart

## Environmental Science : Nano

## GENERAL INFORMATION

Request ID	Request Date
600041432	02 May 2021
Request Status	Price
Accepted	0.00 USD  Special Terms

## ALL DETAILS

ISSN:	2051-8161
Type of Use:	Republish in a thesis/dissertation
Publisher:	Royal Society of Chemistry
Portion:	Chapter/article

## LICENSED CONTENT

Publication Title	Environmental Science : Nano	Country	United Kingdom of Great Britain and Northern Ireland
Author/Editor	Royal Society of Chemistry (Great Britain),	Rightholder	Royal Society of Chemistry
Date	01/01/2014	Publication Type	e-Journal
Language	English		

## REQUEST DETAILS

Portion Type	Chapter/article	Rights Requested	Main product and any product related to main product
Page range(s)	32	Distribution	Worldwide
Total number of pages	99	Translation	Original language of publication
Format (select all that apply)	Print, Electronic	Copies for the disabled?	No
Who will republish the content?	Author of requested content	Minor editing privileges?	No
Duration of Use	Life of current edition	Incidental promotional use?	No
Lifetime Unit Quantity	Up to 499		

[https://marketplace.copyright.com/rs-ui-web/manage\\_account/special-requests/details/a83c55fc-450e-4008-90e7-0d1e911f9269](https://marketplace.copyright.com/rs-ui-web/manage_account/special-requests/details/a83c55fc-450e-4008-90e7-0d1e911f9269)

1/3

11/05/2021

Manage Account

Currency

USD

## NEW WORK DETAILS

---

<b>Title</b>	TOXICITY, BIOACCUMULATION AND BIOTRANSFORMATION OF Cu OXIDE NANOPARTICLES IN Daphnia magna	<b>Institution name</b>	Universidade de São Paulo
<b>Instructor name</b>	Joyce Ribeiro Santos Rasera	<b>Expected presentation date</b>	2021-06-01

## ADDITIONAL DETAILS

---

The requesting person / organization to appear on the license thesis publication

## REUSE CONTENT DETAILS

---

<b>Title, description or numeric reference of the portion(s)</b>	TOXICITY, BIOACCUMULATION AND BIOTRANSFORMATION OF Cu OXIDE NANOPARTICLES IN Daphnia magna	<b>Title of the article/chapter the portion is from</b>	N/A
<b>Editor of portion(s)</b>	N/A	<b>Author of portion(s)</b>	Royal Society of Chemistry (Great Britain)
<b>Volume of serial or monograph</b>	N/A	<b>Publication date of portion</b>	2019-08-05
<b>Page or page range of portion</b>	10		

## COMMENTS

---

 [Add Comment / Attachment](#)

04 May 2021 6:55:18 AM, by Joyce Rasera

Yes, I want permission to reproduce the content of the article for my thesis. I am the main author and I am a PhD student by University of São Paulo/Brazil. The title of the thesis is: Evaluation of distribution,

04 May 2021 5:30:34 AM, by Gill Cockhead

Please confirm that you want to reproduce <https://doi.org/10.1039/C9EN00280D> in your thesis?



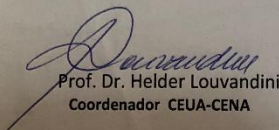
02 May 2021 8:42:36 PM, by Joyce Rasera

thesis publication

 [Review Cart](#)



**Annex B - Permission of the institutional Ethics Committee on the Use of Animals (CEUA - n° 008-2016)**

	UNIVERSIDADE DE SÃO PAULO Campus "Luiz de Queiroz" Centro de Energia Nuclear na Agricultura	
<p><b>Comissão de Ética no Uso de Animais – CEUA</b> Fone: (19) 3429-4683 www.cena.usp.br</p>		
<b><u>CERTIFICADO</u></b>		
<p>Certificamos que a proposta intitulada "Avaliação da distribuição, especiação química e efeitos tóxicos de nanopartículas de CuO e Fe<sub>3</sub>O<sub>4</sub> em <i>Daphnia magna</i> e <i>Danio rerio</i>", registrada com o n° 008-2016, sob a responsabilidade da Profa. Regina Teresa Rosim Monteiro - que envolve a produção, manutenção ou utilização de animais pertencentes ao filo Chordata, subfilo Vertebrata (exceto humanos), para fins de pesquisa científica - encontra-se de acordo com os preceitos da Lei n° 11.794, de 8 de outubro de 2008, do Decreto n° 6.899, de 15 de julho de 2009, e com as normas editadas pelo Conselho Nacional de Controle de Experimentação Animal (CONCEA), e foi aprovada pela COMISSÃO DE ÉTICA NO USO DE ANIMAIS (CEUA CENA) do CENTRO DE ENERGIA NUCLEAR NA AGRICULTURA/USP, em reunião de 17/08/2016.</p>		
Finalidade	( ) Ensino ( X ) Pesquisa Científica	
Vigência da autorização	01/03/2017 a 01/03/2018	
Espécie/linhagem/raça	Peixe/ <i>Danio rerio</i> (zebrafish)	
Nº de animais	160	
Peso/Idade	2 g/4 a 12 meses	
Sexo	Machos e Fêmeas	
Origem	Loja de comercialização de peixes	
 Prof. Dr. Helder Louvandini Coordenador CEUA-CENA		
Av. Centenário, 303, Bairro São Dimas - Caixa Postal 96 - CEP. 13400-970 - Piracicaba, SP, Brasil Fone: (19)3429-4600 - Fax (19) 3429-4610 - e-mail: diretoria@cena.usp.br - www.cena.usp.br		